Al-Mukhtar Journal of Basic Sciences

Volume 22
Issue 1
2024

eISSN:3006-8649

Published by OMU

Al-Mukhtar Journal of Basic Sciences

Peer-reviewed scientific journal, Volume Twenty-Two, Issue One, 2024

Published by Omar Al-Mukhtar University, Al-Bayda, Libya

A peer-reviewed journal published by Omar Al-Mukhtar University,

Al Bayda, Libya

Peer-reviewed scientific journal, Volume Twenty-Two, Issue One, 2024

Email: ljbs.sci@omu.edu.ly

EDITORS & STAFF

Al-Mukhtar Journal of Basic Sciences 22: (1), 2024

Papers	Pages
Preliminary Study on Ecto and Endoparasites of the Black Rats (*Rattus Rattus*) in Benghazi City Mahmoud Fadiel Doaa El senussi Anees Abdulwahid	**01-11**
The Possible Protective Role of N-acetylcysteine against Testicular Toxicity Induced by Paracetamol Overdose in Adult Male Rats. Fatma W Mohamed Farouzia I Moussa Horeya S Abd El-Gawad Salwa S Mahmoud	**12-29**
Isolation and characterization of lytic bacteriophage against common pathogenic bacteria Asma S. Alilesh Marwa S. Alwush Tasneem M. Alswehly Khawla A. Aween	**30-37**
The Effect of Wind Speed and Sea Surface Temperature on Chlorophyll –A Concentration in Sea Water Off the Libyan Coast Haifa M. Ben Miloud Maha A. Alssabri	**38-46**
Order Continuous Operators Manal A. Elzidani Hawa A. Eltaweel Abdusalam A. Emsimir	**47-54**
The Inhibition Effect of Alcoholic Extract of *Capsicum Annuum* (Chili Pepper) on The Growth of Barely Grains' Associated Fungi Species Fuzia E. Eltariki Mohamed M. Alsull	**55-63**
Performance Evaluation of Artificial Neural Networks for Estimating Reference Evapotranspiration in Shahat, Libya using limited climatic data Mohamed A. Momen Osama A. Abdelatty	**64-74**
Morphological and Histological Description of Spiny Dogfish shark Liver, *Squalusacanthais*(Linnaeus,1758), Elasmobranchii, Squaliformes Nagla A. Elfagi	**75-84**
On Menger Spaces in Generalized Topology Assakta K. Bashier	**85-91**
A Brief Comparison of Google Cloud and iCloud Services Faiza A. M. Mansour Najat A. Atbaiga	**92-102**

Al-Mukhtar Journal of Basic Sciences 22 (1): 01-11, 2024
Doi: https://doi.org/10.54172/gxg78671

Research Article

Open Access

Preliminary Study on Ecto and Endoparasites of the Black Rats (*Rattus Rattus*) in Benghazi City

Mahmoud Fadiel[1*], Doaa El senussi [2], Anees Abdulwahid[3]

***Corresponding author:**
Fmahmoud2010@gmail.com
Department of Zoology, Faculty of Science, University of Benghazi, Libya

Second Author:
Doaa.elsenussi@yahoo.com
Department of Zoology, Faculty of Science, University of Benghazi, Libya

Third Author:
anees.abdulwahid@uob.edu.ly
, Department of Zoology, Faculty of Science, University of Benghazi, Libya

Received:
09 January 2023

Accepted:
09 March 2024

Publish online:
30 April 2024

Abstract

Forty-five adult trapped black rats (*Rattus rattus*), 24 males and 21 females, were dissected and examined in this study for ecto and endoparasites. Three ectoparasites were detected, namely, the flea (*Xenopsallya cheopis*), mites (*Ornithonyssus bacoti*), and tick (*Ixodes spp*) with 48.9%, 13.3%, and 2.2% respectively. Meanwhile, many species of endoparasites were: *Entamoeba histolytica/dispar* (73.3%), *Entamoeba coli* (31.3%), *Blastocystis hominus* (8.9%), *Giardia lamblia* (15.6), *Chilomastix sp.* (4.4%), a *coccidia* sp. (13.3%), *Hymenolips nana* (2.2%), *Hymenolips diminuta* (44.4%), and *Taenia taeniaformis* (6.7%), and *Moniliformis moniliformis* (2.2%). Of all examined rats, 97.8 % (44/45) were found to harbor at least one parasite species with no significant differences between body weight, body length, and gender of the host with the prevalence of parasite species. Multiple infections occurred at six species per rat with different combinations of parasite infections. These results are the first records of the parasitic fauna of *R. rattus* in the Benghazi area.

Keywords: *Rattus Rattus*, Black Rat, Ectoparasites, Endoparasites, Libya.

INTRODUCTION

Rats are distributed worldwide and are one of the most common rodents found in cities and their surrounding areas. In tropical and subtropical regions, Black rats (*Rattus rattus*) and brown rats (*Norwegians rattus*) are highly common in human-inhabited areas. Their origin is derived from the Fareast and distributed globally through ship trades. The breeding of rats has increased rapidly in recent years due to the abundance of food resources and the lack of environmental hygiene in urban areas (Abdel-Aal & Abou-Eisha, 1997; Mohd-Qawiem et al., 2022). Rats impose economic damages and significantly increase costs on the public health system. They can destroy food stuff, electrical equipment, and buildings by gnawing or contaminating with excreta leading to significant economic losses (Coomansingh et al., 2009). They also act as hosts for several ectoparasites and endoparasites.

In Libya, the black rat (*R. rattus*) is widely prevalent and frequently encountered among the rodent population, especially in coastal regions such as Benghazi city. It has been seen in the streets, between buildings, markets, and houses. Although there are several reports of ectoparasitic and endoparasitic infections in *R. rattus* from different parts of the world (Becir et al., 2012; Claveria et al.,

2005; Daryani et al., 2023; Kataranovski et al., 2010; Menshawy et al., 2021; Ogunniyi et al., 2014; Porta et al., 2014; Shafiyyah et al., 2012; Sumangali et al., 2012), there were limited or no studies from Libya. Thus, this study aimed to conduct a preliminary survey of ectoparasites and endoparasites among the commonest rodent the black rat (*R. rattus*) in the city of Benghazi and to determine the risk of zoonotic parasites to humans.

MATERIALS AND METHODS

Study Area

This study was carried out in Benghazi city (32°10'N, 20°06'E), which is situated on the eastern southern coast of the Mediterranean Sea, north of Libya. It is the second-largest city in Libya, occupying an area of approximately 240 km². This city has a large port that serves general bulk cargoes and containers that imported from different parts of the world.

Samples Collection

All the rats were trapped alive using specially made wire box bait traps measuring 29 x 11 x 10.5 cm with a front spring door. Traps were distributed randomly indoors and outdoors of inhabited buildings just before sunset and collected by the following morning. The traps were cleaned with hot water and soap every time before reuse.

Anesthetization and killing of the study animals

The weight of each rat was obtained before anesthesia. Subsequently, each rat was placed individually in a glass flask and anesthetized using a cotton ball soaked in chloroform until it was euthanized. Additionally, the length of each rat was measured. The length of the rat was also measured.

Isolation and preservation of ectoparasites

The fur of each anesthetized rat was gently scraped and combed with a fine-tooth comb to dislodge any ectoparasite into a large white filter paper. Ectoparasites (mites, fleas, lice, and ticks) were then collected by forceps and transferred into 70% alcohol for preservation until used. A separate container was used for each animal. Preserved ectoparasites were transferred to10 % potassium hydroxide (KOH) for about 2-5 days until the exoskeleton dissolved, then washed with water to remove the excess of potassium hydroxide, transferred to serial grading of alcohol starting from 50% up to absolute alcohol, cleared in xylol, mounted with DPX on a glass slide, and examined under the microscope.

Animal dissection

In the post-mortem of rats, the skin was removed and the body cavity was slit open from the throat to the anus, revealing the esophagus, stomach, small intestine, large intestine, liver, and urinary bladder. The viscera were removed without damage, and dissected separately under the dissecting microscope and examined for helminths. All macro-parasites were washed with saline and fixed in warm 70% alcohol or 10% formalin. The contents of the small and large intestines were also examined carefully for microparasites (cysts, oocysts, trophozoites, and eggs) by direct wet mount smears and stained with 1% Lugol's iodine solution to be examined under the microscope.

Processing of cestode and acanthocephalan

Cestodes were collected individually in glass jars containing normal saline and washed many times to remove debris. The worm was then gently flattened between two glass slides that were held at the ends with rubber bands. It was then fixed in 10% formalin for 2-3 days. The specimen was dehydrated in an increasing series of alcohol starting from 30% to 100%, then transferred to carmine

stain for 24 hrs. The excessive stain was removed with clove oil. The stained specimen was washed with distilled water and dehydrated with ascending grades of alcohol (70%, 80%, 90%, 100%), cleared in xylol, and mounted in DPX (Paniker & Ghosh, 2017). According to Paniker and Ghosh (2017), Priyanto et al. (2014), and Service (1996), the identification of ectoparasites and endoparasites followed established procedures outlined in previous studies.

Statistical analysis

A statistical analysis was carried out to determine the incidence and significance of the data. The logistic regression was used to find the relationships between parasitic infection, sex, length, weight, regions, and the presence or absence of the parasites (Dowdy et al., 2004). Chi-square $\chi 2$ was employed to detect the significance or non-significance of the relationships between length, body weight, sex, and parasitic infection. The accepted level of $P < 0.05$ was considered significant. The statistical program (SPSS) was used to compute all analyses within the Windows environment.

RESULTS

The examination of 45 black rats (*Rattus rattus*) in this study revealed that these rodents were host to a diverse range of parasites. The detected parasites fell into two categories: ectoparasites and endoparasites. The ectoparasites include fleas, mites and ticks, while the endoparasites include many species of protozoa, cestodes, and one species of acanthocephalan.

The protozoa parasites are *Entamoeba histolytica*, *Entamoeba Coli*, *Blastocystis hominus*, *Giardia lamblia*, *Chilomastix spp*, and one species of coccidia. Three species of cestodes are *Hymenolips nana, Hymenolips diminuta* and *Taenia taeniaformis*. *Acanthocephalans* are represented by only one species which is *Moniliformis moniliformis*. The overall prevalence of ectoparasite and endoparasites among the examined male and female black rats (*Rattus rattus*) collected in this study was 97.8 % (44/45) (Table 1). The ectoparasites (fleas, mites and ticks) showed a prevalence rate of 64% while endoparasites have 86.6% (Table 1).

The most common ectoparasite that has detected was the flea with a 48.9% prevalence rate, followed by mites and ticks with 13.3% and 2.2% prevalence in rats respectively. The study findings indicated that male black rats (*R. rattus*) exhibited a slightly higher rate of parasitic infection (24%) compared to females (20%), although no statistically significant differences were observed.

Table: (1). The prevalence of ecto and endoparasites in examined black rat *Ratus ratus*.

Parasite types	Number of examined rats	Number of infected	Prevalence of Infection%
Ectoparasites	45	29	64
Endoparasites	45	39	86.6
Both	45	44	97.8

On the other hand, *Entamoeba histolytica/ dispar* and *Hymenolepis diminuta* were the most dominant endoparasites with 73.3% and 44.4% respectively (table 2).

Both male (n=24) and females (n=20) of examined black rats, *R. rattus*, were infected with one or more species of parasites. Thirty-six out of forty-four rats (81.8%) have mixed parasites, and only eight (18.2%) have a single infection. There were no significant differences ($P \geq 0.05$) between male and female prevalence rats with their types of infections (Figure1).

Table: (2). The prevalence of ecto and endoparasites in examined black rat Ratus ratus.

Types of parasites	Prevalence of examined rats %	Number of infected
Flea (Xenopsally cheopis)	48.9	22
Mites (Ornithonyssus bacoti)	13.3	6
Ticks (Ixodes spp)	2.2	1
Hymenolepis nana	2.2	1
Hymenolepis diminuta	44.4	20
Moniliformes moniliformes	2.2	1
Cysticercus fasciolaris, Taenia taeniaformes	6.7	3
Entamoeba histolytica/dispar	73.3	33
Entamoeba coli	31.1	14
Coccidia spp	13.3	6
Blastocystis hominis	8.9	4
Giardia lamblia	15.6	7
Chilomastix spp	4.4	2

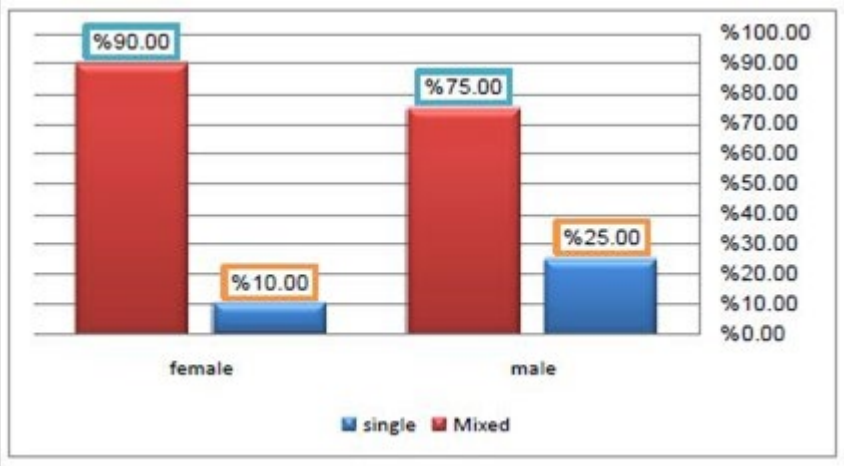

Figure: (1). Single and mixed parasitic infections among males and females of black rat (*R.rattus*).

The result also indicated that Twenty-five percent of examined rats (n = 11) were infected with three parasites, the highest level of infection, while some had more or fewer parasites. However, there were no significant differences between males (n = 24) and females (n = 20) about the intensity of parasites ($P \geq 0.05$). Male and female black rats were collected from urban (n = 33) and rural (n = 11) areas. This study showed there are no significant differences between parasitic infection rates ($P \geq 0.05$). In addition, the result showed no relationships between the examined rats' body weight, body length and parasitic infection.

DISCUSSION

In the present study, all the trapped rats belonged to only one species, which is the black rat (*R. rattus*). These rats are semi-domesticated and omnivorous and are often seen in streets, between buildings, in sewage channels, slaughterhouses, waste disposal sites, food storage, farms, and around houses in the city of Benghazi. The present investigation gives the first overview the ecto and endoparasitic infection of trapped black rats (*R. rattus*) in Benghazi, Libya of which 13 species of par-

asites were reported. These parasites are *Xenopslla cheopis, Orinthionyssus bacoti, Ioxodes sp, Hyminolepis nana, Hymenolepis diminuta, Cysticercus fasciolaris (Taenia taeniaformis), Acanthocephala, Entamoeba coli, Entamoeba histolytica/ dispar, Isospora sp, Blastocyst hominis, Giardia lamblia*, and *chilomastix sp*. All of them are zoonotic and have medical importance (Hernández et al., 2020; Paniker & Ghosh, 2017). The above parasites have been previously reported in black rats (*R. rattus*) from several parts of the world (Becir et al., 2012; Claveria et al., 2005; Kataranovski et al., 2010; Ogunniyi et al., 2014; Porta et al., 2014; Shafiyyah et al., 2012; Sumangali et al., 2012), and also many authors reported similar parasites in brown rats, *Rattus* norvegicus (Abu-Madi et al., 2001; Al-Bashan & Sabra, 2012; Coomansingh et al., 2009; Morsy et al., 2012; Pakdad et al., 2012; Porta et al., 2014; Priyanto et al., 2014; Stojcevic et al., 2004; Waugh et al., 2006).

The existence of rats, which act as reservoir hosts to different types of parasites in close association with human activities, may facilitate the transmission of zoonotic parasites (Amarasinghe & Premathilake, 2014; Guimarães et al., 2014; Sumangali et al., 2012). The results revealed a 97.8% overall prevalence rate of infected *R. rattus* with ectoparasites and endoparasites. Porta et al., 2014 recorded a lower incidence rate of 62.34 from the same species of rat in Brazil. Three ectoparasites were recorded on the trapped rats (*R. rattus*) with a prevalence rate of 64%. Solanki et al., 2013, reported a higher prevalence rate (67%) in black rats collected from India, while Kia et al., 2009, in Iran reported a lower prevalence rate (11.6%). The most abundant ectoparasites on trapped rats were fleas (*Xenopslla cheopis),* with an infection rate of 48.9%. This flea is the most important vector of plague, endemic typhus, and parasitic cestodes such as *H. diminuta* and *Dipylidium caninum* (Kia et al., 2009; Service, 1980). Many authors reported higher prevalence rates of fleas from different parts of the world (Becir et al., 2012; Zahedi et al., 1996), while others found lower infection rates (AL Hind & Abu-Haddaf, 2013; Ogunniyi et al., 2014; Porta et al., 2014; Sumangali et al., 2012). Tropical rat mites, *Ornithonyssus bacoti* were also collected from *R. rattus* in this study, with an incidence rate of 13.3%. This species is generally found on various animals, may temporarily also infest humans, and consequently, may be responsible for pruritic skin reactions (Baumstark et al., 2007). The same species of mites were reported from Iran (Daryani et al., 2023) and Hawaii (Yang et al., 2009) with, incidence rates of 73.9% and 14.7%, respectively. The third ectoparasite recorded in this study is a hard tick species (*Ioxodes spp.*) with an incident rate of 2.2%. Higher and lower infection rates of *R. rattus* with hard ticks were reported in different countries (Becir et al., 2012; Thanee et al., 2009; Zendehfili et al., 2015). Species of the hard tick may contribute to the spread of many viral, rickettsial, and bacterial diseases such as Russian spring-summer encephalitis, Rocky Mountain spotted fever, and Tularemia (Service, 1996).

The results of this study revealed that the overall prevalence rate of endoparasites in the examined rats was 86.6%. A high prevalence rate (58.5%) of endoparasitic infection was also recorded in black rats collected from Khan Younis and Jabalia in Palestine (AL Hind & Abu-Haddaf, 2013). The cestodes recorded in this study include *Hymenolepis nana*, *Hymenolepis diminuta*, and *cysticercus fasciolaris* (*Taenia taeniaformis*). *H. nana* is a common parasite of rodents as well as humans (Al-Bashan & Sabra, 2012). Infected persons are usually asymptomatic, but in massive infections, symptoms may include dizziness, abdominal pain, diarrhea, insomnia, and convulsions (Forbes et al., 2002). Only 2.2% of the total infected black rats (*R. rattus*) were infected with these parasites. Low prevalence rates of infection with *H. nana* were reported in rats from Ethiopia and Italy (Kassa & Assefa, 2000; Milazzo et al., 2010). On the other hand, Al-Bashan & Sabra, and Coello-Peralta two different studies, recorded a higher infection rate in black rats collected from Saudi Arabia Las, Pinas and Philippines (Al-Bashan & Sabra, 2012; Coello-Peralta et al., 2020). *Hymenolepis diminuta* is another intestinal cestode recovered from the examined black *R. rattus* with a high prevalence rate of 44.4%; this result is consistent with reports from Nigeria, Pakistan

and Brazil (Guimarães et al., 2014; Okoye & Obiezue, 2008; Ramesh et al., 2021). However, many other studies showed lower infection rates (Al-Bashan & Sabra, 2012; AL Hind & Abu-Haddaf, 2013; C Milazzo et al., 2010). *H.diminuta* is a common and cosmopolitan parasite of rats and mice and is an occasional parasite of humans, with most cases reported in children (Amin, 2019; Mohd-Qawiem et al., 2022; Tena et al., 1998). The most important intermediate hosts of this parasite are rat fleas (*Xenopsylla cheopis*) and flour beetles *(Tribolium confusatum*). Therefore, the results of this study showed high infection rates of *H. diminuta* which correlated with the presence of rat fleas (*Xenopsylla cheopis*). The third cestode recovered from the examined black rats, *R. rattus*, was *Cysticercus fascioliasis* (*Taenia taeniaformis*) with a prevalence rate of 6.7%. Similar results but with higher prevalence rates were reported in the same species of rats from India (Sharma et al., 2017), Seri Lanka (Sumangali et al., 2012), and Nigeria (Ogunniyi et al., 2014). Human cases of this parasite were also recorded (Ashford & Crewe, 1998). In the current study, *Moniliformis moniliformis* was the only acanthocephalan isolated from the black rats, *R. rattus*, with an incidence rate of 2.2%. A wide range of mammals, including rats, are susceptible to *M. monilifomis* (Hernández et al., 2020). Human cases of this parasite have been reported in many countries (Paniker & Ghosh, 2017; Salehabadi et al., 2008). The result of this study is in agreement with those of many authors (AL Hind & Abu-Haddaf, 2013; C Milazzo et al., 2010; Okoye & Obiezue, 2008). The most abundant parasitic protozoa in the examined black rats *(R. rattus*) in this study were *Entamoeba histolytica/ dispar* with an infection rate 73.3%. This result is higher than those reported by Al-Bashan & Sabra, 2012, AL Hind & Abu-Haddaf, 2013 from Saudi Arabia and Palestine respectively. Non-pathogenic *Entamoeba coli* were found with a prevalence rate of 31.1%. Lower incident rats of *Entamoeba coli* in *R. rattus* were recorded by Guimarães et al., 2014 in Brazil, and Ogunniyi et al., 2014, in Nigeria. Another protozoan recorded in this study was *Giardia lamblia* with a prevalence rate of 15.6%. A similar result was reported by AL Hind & Abu-Haddaf, 2013, in Palestine black rats *R. rattus* while Al-Bashan & Sabra, 2012 found a lower incident rate (10.7%) in Saudi Arabia. *Chilomastix* spp was also detected in the examined rats with an incidence rate (4.4%). Ogunniyi et al., 2014, recorded two species of *chilomastix* namely *Chilomastix bettencourti* and *Chilomastix intestinalis* in Nigerian black rats. The results of this study showed that 13.3% of the examined black rats were infected with oocysts of unidentified species of Coccidia. This result is in agreement with that reported by Raharivololona, Rakotondravao & Ganzhorn, 2007, from Madagascar. *Blastocyst hominis* has been detected with an incident rate of 8.9%. Isolates resembling *B. hominis* have been described in a variety of mammals, birds, reptiles, and even insects (Al & Hökelek, 2007). The significance of this parasite to human infection is uncertain, but it is still one of the most common parasites isolated from stool specimens in symptomatic and asymptomatic individuals (Paniker & Ghosh, 2017).

The presence of this parasite in black rats may play a role in its epidemiology. The present study showed that males had a higher parasitic infection rate (24%) than females (20%) in black rat's *R. rattus* although no significant differences were observed. This result is consistent with those recorded by (AL HIND & Abu-Haddaf, 2013; Kataranovski et al., 2010; Porta et al., 2014). The reason behind the above situation could be attributed to males being more active than females and haveing larger home territories which could increase their exposure to infection while reproductive females show a stronger site-specific organization and also the male hormone testosterone harms the immune function (Grossman, 1989).

CONCLUSION

In conclusion, a lot of tension should be made to the role of black rats and other rodents in spreading parasitic diseases in Libya. So far, most of the recorded endoparasites in this study from black rats have been reported in humans from the city of Benghazi. Moreover, the increased population of

rats in the city may increase the risk of infection with plague disease because they act as a reservoir host. Scattered foci of enzootic plague exist across the country. The last outbreak of plague was reported in the Mediterranean coastal town of Tobruk. To avoid unpleasant situations, a full program of rodent control should be implemented in the city of Benghazi and other parts of the country.

ACKNOWLEDGEMENT

We would like to thank our colleagues and friends who provided assistance and constructive feedback during various stages of this research journey. Their input and discussions have greatly enriched the quality of this work.

ETHICS

Ethical approval was not sought for the present study because the number of forty-five animals was very low according to the huge amounts of rodents in the Libyan environment. The scientific procedures for killing animals were completely followed by the researchers during this research.

Duality of interest: There are no conflicts of interest regarding this research. We have no financial or non-financial relationships or affiliations with any organization or entity that could be perceived as a conflict of interest in connection with this work.

Author contributions: All authors contributed equally to this research project. They collectively conceptualized the study, designed the methodology, conducted data collection and analysis, interpreted the results, and jointly wrote and reviewed the manuscript. All authors have read and approved the final version of the manuscript.

Funding: This research did not receive any external funding. The study was self-funded by the authors.

REFERENCES

Abdel-Aal, A. A., & Abou-Eisha, A. M. (1997). The role of rats as reservoir of some internal parasites with possible public health implications in the Suez Canal area. *Assiut University Faculty Of Veterinary Medicine*, *37*, 174–185.

Abu-Madi, M. A., Lewis, J. W., Mikhail, M., El-Nagger, M. E., & Behnke, J. M. (2001). Monospecific helminth and arthropod infections in an urban population of brown rats from Doha, Qatar. *Journal of Helminthology*, *75*(4), 313.

Al-Bashan, M. M., & Sabra, S. M. (2012). Prevalence of some enteric parasites in rats at Taif governorate with special reference to associated pathogenic bacteria. *African Journal of Microbiology Research*, *6*(14), 3431–3439.

Al, F. D., & Hökelek, M. (2007). Is Blastocystis hominis an opportunist agent? *Turkiye Parazitolojii Dergisi*, *31*(1), 28–36.

AL HIND, A. I., & Abu-Haddaf, E. (2013). Gastrointestinal parasites and ectoparasites biodiversity of Rattus rattus trapped from Khan Younis and Jabalia in Gaza strip, Palestine. *Journal of the Egyptian Society of Parasitology*, *43*(1), 259–268.

Amarasinghe, L. D., & Premathilake, E. (2014). Parasites of domestic animals and their possible

zoonoses-a study from selected sites of western province, Sri Lanka. *Journal of Experimental Biology and Agricultural Sciences*, *2*(2), 182–187.

Amin, O. (2019). *Intestinal and Ectoparasites of black rats (Rattus rattus) in Garmian, Kurdistan region of Iraq*. *6*, 623–629. https://doi.org/10.24271/garmian.1050

Ashford, R. W., & Crewe, W. (1998). The parasites of homo sapiens Liverpool school of tropical medicine. *El-Sevier Science Ltd, 15(12): 51*.

Baumstark, J., Beck, W., & Hofmann, H. (2007). Outbreak of tropical rat mite (Ornithonyssus bacoti) dermatitis in a home for disabled persons. *Dermatology*, *215*(1), 66–68.

Becir, F., Bitam, I., Hannachi, H., & Bouslama, Z. (2012). Rattus rattus parasites of El-kala national park (Algeria). *Chapters*.

Claveria, F. G., Causapin, J., De Guzman, M. A., Toledo, M. G., & Salibay, C. (2005). Parasite biodiversity in Rattus spp caught in wet markets. *Southeast Asian Journal of Tropical Medicine and Public Health*, *36*, 146.

Coello-Peralta, R. D., Martínez-Cepeda, G. E., Pinela-Castro, D., Reyes-Echeverria, E. O., Rodríguez-Burnham, E. X., Salazar Mazamba, M. de L., Pazmiño-Gómez, B., Ramírez-Tigrero, A., Bernstein, M., & Cedeno-Reyes, P. (2020). Presence of Hymenolepis nana and diminuta in rodents of the Las Pinas citadel, in Milagro, Ecuador, and its risk for public health. *Revista Mexicana de Ciencias Pecuarias*, *11*(4), 961–970.

Coomansingh, C., Pinckney, R. D., Bhaiyat, M. I., Chikweto, A., Bitner, S., Baffa, A., & Sharma, R. (2009). Prevalence of endoparasites in wild rats in Grenada. *West Indian Veterinary Journal*, *9*(1), 17–21.

Daryani, A., Amouei, A., Pagheh, A. S., Sharif, M., Sarvi, S., Rahimi, M. T., & Rezaei, F. (2023). Prevalence of Ecto and Gastrointestinal Parasites of Rattus rattus in Mazandaran Province, North of Iran. *Turkiye Parazitolojii Dergisi*, *47*(1), 53–58. https://doi.org/10.4274/tpd.galenos.2022.85570

Dowdy, S., Wearden, S., & Chilko, D. (2004). Statistics for Research, A John Wiley & Sons. *Inc. Publication. 204e210*.

Forbes, B., Sham, D., & Weissfeld, A. (2002). *Bailly and scottŝ diagnostic microbiology. Eleventh Edition,*. Thirteenth edition. St. Louis, Missouri : Elsevier, [2014]. https://search.library.wisc.edu/catalog/9910155738802121

Grossman, C. (1989). Possible underlying mechanisms of sexual dimorphism in the immune response, fact and hypothesis. *Journal of Steroid Biochemistry*, *34*(1–6), 241–251.

Guimarães, A. O., Valença, F. M., Sousa, J. B. S., Souza, S. A., Madi, R. R., & de Melo, C. M. (2014). Parasitic and fungal infections in synanthropic rodents in an area of urban expansion, Aracaju, Sergipe State, Brazil. *Acta Scientiarum. Biological Sciences*, *36*(1), 113–120.

Hernández, W. C., Morán, D., Villatoro, F., Rodríguez, M., & Álvarez, D. (2020). Zoonotic Gastrointestinal Helminths in Rodent Communities in Southern Guatemala. *Journal of*

Parasitology, *106*(3), 341–345.

Kassa, M., & Assefa, T. (2000). Prevalence of intestinal helminthic infections among household rats in Addis Ababa. *SINET: Ethiopian Journal of Science*, *23*(1), 115–120.

Kataranovski, D., Kataranovski, M., & Deljanin, I. (2010). Helminth fauna of Rattus norvegicus Berkenhout, 1769 from the Belgrade area, Serbia. *Archives of Biological Sciences*, *62*(4), 1091–1100.

Kia, E. B., Moghddas-Sani, H., Hassanpoor, H., Vatandoost, H., Zahabiun, F., Akhavan, A. A., Hanafi-Bojd, A. A., & Telmadarraiy, Z. (2009). Ectoparasites of rodents captured in Bandar Abbas, southern Iran. *Iranian Journal of Arthropod-Borne Diseases*, *3*(2), 44.

Menshawy, S., Mahmoud, S., & Aboulaila, M. (2021). Study on Parasites Infecting Black Rats (Rattus rattus) in Some Districts At Western Region of Nile Delta, Egypt. *Alexandria Journal of Veterinary Sciences*, *71*, 29–35. https://doi.org/10.5455/ajvs.125754

Milazzo, C., Cagnin, M., Bella, C. D. I., Geraci, F., & Ribas, A. (2010). Helminth fauna of commensal rodents, Mus musculus (Linnaeus, 1758) and Rattus rattus (Linnaeus, 1758)(Rodentia, Muridae) in Sicily (Italy). *Revista Ibero-Latinoamericana de Parasitología*, *69*(2), 194–198.

Mohd-Qawiem, F., Nur-Fazila, S. H., Ain-Fatin, R., Yong, Q. H., Nur-Mahiza, M. I., & Yasmin, A. R. (2022). Detection of zoonotic-borne parasites in Rattus spp. in Klang Valley, Malaysia. *Veterinary World*, *15*(4), 1006–1014. https://doi.org/10.14202/vetworld.2022.1006-1014

Morsy, K., Ramadan, N., Al Hashimi, S., Ali, M., & Bashtar, A.-R. (2012). First description of the adult stages of Postorchigenes sp.(Trematoda: Lecithodendriidae) and Malagashitrema sp.(Trematoda: Homalometridae) infecting the common chameleon Chamaeleo chamaeleon (Reptilia: Chamaeleonidae) in Egypt. *Life Science Journal*, *4*, 9.

Ogunniyi, T., Balogun, H., & Shasanya, B. (2014). Ectoparasites and endoparasites of peridomestic house-rats in Ile-Ife, Nigeria and implication on human health. *Iranian Journal of Parasitology*, *9*(1), 134.

Okoye, I. C., & Obiezue, R. N. N. (2008). A survey of the gut parasites of rodents in Nsukka ecological zone. *Animal Research International*, *5*(2).

Pakdad, K., Ahmadi, N. A., Aminalroaya, R., Piazak, N., & Shahmehri, M. (2012). *A study on rodent ectoparasites in the North district of Tehran, Iran during 2007-2009*.

Paniker, C. K. J., & Ghosh, S. (2017). *Paniker's textbook of medical parasitology*. JP Medical Ltd.

Porta, D., Gonçalves, D. D., Gerônimo, E., Dias, E. H., Martins, L. A., Ribeiro, L. V. P., Otutumi, L. K., Messa, V., & Gerbasi, A. V. (2014). Parasites in synanthropic rodents in municipality of the Northwest region of the State of Paraná, Brazil. *Afr. J. Microbiol. Res*, *8*(16), 1684–1689.

Priyanto, D., Rahmawati, R., & Ningsih, D. P. (2014). Identification of endoparasites in rats of various habitats. *Health Science Journal of Indonesia*, *5*(1), 49–53.

Raharivololona, B. M., & Rakotondravao & Ganzhorn, J. U. (2007). Gastrointestinal parasites of

small mammals in the littoral forest of Mandena. *Biodiversity, Ecology, and Conservation of Littoral Ecosystems in the Region of Tolagnaro (Fort Dauphin), Southeastern Madagascar, JU Ganzhorn, SM Goodman & M. Vincelette (Eds.)*, 247–258.

Ramesh, M. R., Birmani, N. A., & Naz, S. (2021). Hymenolepis diminuta rudolphi, 1819 (hymenolepipidae: cyclophyllidea) from house rat rattus rattus linnaeus, 1758 (rodentia: muridae) from hyderabad, sindh, pakistan. *Pakistan J. Parasitol*, *71*, 19–22.

Salehabadi, A., Mowlavi, G., & Sadjjadi, S. M. (2008). Human infection with Moniliformis moniliformis (Bremser 1811)(Travassos 1915) in Iran: another case report after three decades. *Vector-Borne and Zoonotic Diseases*, *8*(1), 101–104.

Service, M. W. (1980). *Guide to Medical Entomology*. Macmillan Press.

Service, M. W. (1996). *Medical entomology for students*.

Shafiyyah, C. O. S., Jamaiah, I., Rohela, M., Lau, Y. L., & Aminah, F. S. (2012). Prevalence of intestinal and blood parasites among wild rats in Kuala Lumpur, Malaysia. *Tropical Biomedicine*, *29*(4), 544–550.

Sharma, R., Tiwari, K., Birmingham, K., Armstrong, E., Montanez, A., Guy, R., Sepulveda, Y., Mapp-Alexander, V., & DeAllie, C. (2017). *Cysticercus fasciolaris* in Brown Rats *(Rattus norvegicus)* in Grenada, West Indies. *Journal of Parasitology Research*, *2017*, 1723406. https://doi.org/10.1155/2017/1723406

Solanki, S. K., Chauhan, R., Rahman, A., & Solanki, K. (2013). Original research article prevalence of ectoparasites in commensal rats in Dehradun, India. *Int. J. Current Microbiol. Appl. Sci*, *24*, 38–41.

Stojcevic, D., Mihaljevic, Z., & Marinculic, A. (2004). Parasitological survey of rats in rural regions of Croatia. *Veterinarni Medicina-UZPI (Czech Republic)*.

Sumangali, K., Rajapakse, R., & Rajakaruna, R. S. (2012). Urban rodents as potential reservoirs of zoonoses: a parasitic survey in two selected areas in Kandy district. *Ceylon Journal of Science (Biological Sciences)*, *41*(1).

Tena, D., Simón, M. P., Gimeno, C., Pomata, M. T. P., Illescas, S., Amondarain, I., González, A., Domínguez, J., & Bisquert, J. (1998). Human infection with Hymenolepis diminuta: case report from Spain. *Journal of Clinical Microbiology*, *36*(8), 2375–2376.

Thanee, N., Kupittayanant, S., & Pinmongkholgul, S. (2009). Prevalence of ectoparasites and blood parasites in small mammals at Sakaerat Environmental Research Station, Thailand. *Thai Journal of Agricultural Science*, *42*(3), 149–158.

Waugh, C. A., Lindo, J. F., Foronda, P., Ángeles-Santana, M., Lorenzo-Morales, J., & Robinson, R. D. (2006). Population distribution and zoonotic potential of gastrointestinal helminths of wild rats Rattus rattus and R. norvegicus from Jamaica. *Journal of Parasitology*, *92*(5), 1014–1018.

Yang, P., Oshiro, S., & Warashina, W. (2009). *Ectoparasitic arthropods occurring on Rattus norvegicus and Rattus rattus collected from two properties on the island of Oahu, Hawaii*

(Acarina, Siphonaptera, and Anoplura).

Zahedi, M., Jeffery, J., Krishnasamy, M., & Bharat, V. (1996). Ectoparasites of Rattus rattus diardii from Kuala lumpur city Malaysia. *Proc 2nd Int Conf Urban Pest*, *1996*, 437–439.

Zendehfili, H., Zahirnia, A. H., Maghsood, A. H., Khanjani, M., & Fallah, M. (2015). Ectoparasites of rodents captured in Hamedan, Western Iran. *Journal of Arthropod-Borne Diseases*, *9*(2), 267.

Al-Mukhtar Journal of Basic Sciences 22 (1): 11-29, 2024
Doi: https://doi.org/10.54172/hsh5mn09

Research Article

Open Access

The Possible Protective Role of N-acetylcysteine against Testicular Toxicity Induced by Paracetamol Overdose in Adult Male Rats

Fatma W Mohamed[1*], Farouzia I Moussa[2], Horeya S Abd El-Gawad[2] and Salwa S Mahmoud[2]

***Corresponding author:** fatma.wanis@uob.edu.ly Department of Zoology (Physiology), Faculty of Art and Science, University of Benghazi, Libya

Second Author: Department of Zoology, Faculty of Science, University of Alexandria, Egypt

Third Author: Department of Zoology, Faculty of Science, University of Alexandria, Egypt

Fourth Author: Department of Zoology, Faculty of Science, University of Alexandria, Egypt

Received:
20 February 2023

Accepted:
17 April 2024

Publish online:
30 April 2024

Abstract

Many substances, even medicines with proven therapeutic benefits, can harm cells by metabolically activating them into extremely reactive substances. Paracetamol is one of the most widely used over-the-counter analgesics. This study examines the harmful effects of paracetamol on the lipid peroxidation process in testes homogenates as well as enzymatic and non-enzymatic antioxidant activities. Also, examine the effects on male hormones and sperm count. The study also assesses if N-acetylcysteine protects against testicular damage induced by paracetamol excess. Forty mature male albino rats were created. Group 1 as a control, Group 2 paracetamol (650 mg/kg), Group 3 NAC (150 mg/kg), and Group 4 both paracetamol and NAC. Samples of blood and testicles were taken after 15 days to measure sperm and testicular biochemistry. Testicular tissues had considerably higher amounts of MDA and H2O2. SOD, GSH, and CAT levels significantly decreased. FSH and LH rise. On the other hand, testosterone levels decrease following paracetamol exposure. The administration of NAC generated changes in testosterone levels, FSH, LH, and antioxidant enzymes. The sperm morphology showed an increase in abnormalities but a significant decrease in motility and count. NAC effectively lowers the toxicity of paracetamol to the testicles while restoring biomarkers associated with normal testicular function.

Keywords: Sperms, Paracetamol, Testis, Albino Rats, N-Acetylcysteine.

INTRODUCTIO

Many substances, even medicines with proven therapeutic benefits, can harm cells by metabolically activating them into extremely reactive substances. Paracetmol is one of the most widely used over-the-counter analgesics. Called chemically N acetyl p aminophenol, paracetamol (PCM), also referred to as acetaminophen, is a moderate analgesic medication. It is frequently used to treat mild aches and pains, including headaches. It is also a key component of many cold and flu medicines. When combined with opioid analgesics, paracetamol is used to treat more severe pain, such as pain following surgery, and to give palliative care to patients with advanced cancer (Olaniyi and Agunbiade, 2018).

Paracetamol was introduced by Merring. (1893) as a potential analgesic drug. However, its effectiveness as a therapeutic drug was only realized in the 1960s. Its use has increased with time leading to its use as a combination in many other drugs. Even though paracetamol is used to

treat inflammatory pain, its limited antiinflammatory activity prevents it from being considered a nonsteroidal anti-inflammatory medicine (NSAID). (Jóźwiak-Bebenista and Nowak, 2014).

When paracetamol is taken therapeutically, the liver is mainly responsible for its metabolis this process produces metabolites that are easily eliminated through the kidney and do not cause any harm (El-Maddawy and El-Sayed, 2018). Hepatic cytochrome P450 isoenzymes bioactivate a part of paracetamol to form the hepatotoxic reactive metabolite N-acetyl-para-benzoquinone imine (NAPQI). (Koling *et al.,* 2007). The conjugation of hepatic glutathione (GSH), which is likewise safely eliminated by bile, quickly quenches NAPQI. However, due to insufficient glucuronidation and sulfation, high doses overwhelm the paracetamol detoxication pathways (Adil *et al*., 2016).

90% of the drug's administered dose (the therapeutic dose) is metabolized in the liver where it is conjugated in glucuronide and sulphate. The remaining drug is then hydroxylated to form N-Acetyl P Benzoquineime (NAPQI) (5-10%), a highly reactive oxidative product that conjugates with glutathione and GSH to form mercpturicacid, which is excreted in urine (Grahame-Smith and Aronson, 2002). Overdosing paracetamol alters reproductive parameters and produces harmful substances in the organs, such as hepatotoxicity, renal toxin, and testicular toxin (Radosavljevic *et al*., 2010). Elevted dosages of paracetamol seem to impact the masculine reproductive system, altering the quality of semen, namely the morphology of sperm and consequently their capacity to fertilize (Khayyat, 2021).

Early in the 1960s, N-acetylcysteine (NAC) was shown to have therapeutic value. Natural sources do not include this medication (Larsson *et al*., 2015). Furthermore, it is recognized as an antioxidant that directly benefits hepatic tissue by raising intracellular GSH (Ribeiro *et al*., 2011). It has an ideal thiol redox state, which is crucial for maximizing the cell's capacity to fend against inflammation and oxidative stress (OS). The amino acid N-acetyl cysteine has a thiol group. Because of its dual roles as a sulfhydryl (-SH) donor and a nucleophile, NAC has a protective effect against the toxicity of chemicals (Wang *et al*., 2013 and Mokhtari *et al*., 2017). When taken orally, NAC is absorbed in the stomach and intestines before traveling through the portal vein to the liver.NAC rapidly integrates peptides in the liver to produce a variety of metabolites and proteins (Lasram *et al*., 2015).

NAC exists in plasma in both reduced and different oxidized forms. Furthermore, it underwent oxidation to produce diacetylcystine, a disulfide. It has the potential to react with other low molecular mass thiols, such as glutathione and cysteine, to generate mixed disulfides. Furthermore, NAC may undergo oxidation through redox interactions with the plasma proteins' thiol groups. When given orally to rats, NAC is absorbed; just 3% of NAC is expelled in the feces. (Dodd *et al*., 2008).

De Andrade et al. (2015) state that cysteine is released and taken up by amino acid transporters into cells as a result of extracellular deacetylation of NAC. It is hypothesized that the production of GSH requires free cysteine. NAC prevents apoptosis and oxygen related genotoxicity in endothelial cells, which in turn increases intracellular glutathione levels and decreases mitochondrial membrane depolarization (Amin *et al* ., 2008; Elgindy *et al*., 2010).

Because it is a precursor to glutathione, one of the most significant naturally occurring antioxidants, NAC has antioxidant properties. N-acetylcysteine has a variety of pharmacological potentials for prophylaxis and therapy, including anti-inflammatory (Uraz *et al*., 2013) and antiox-

idant (Ahmed *et al*., 2011) effects. By scavenging free radicals and raising cellular GSH, they exercise their strong antioxidant properties and guard against lipid peroxidation (Dhouib *et al*., 2016). According to İçer *et al*. (2016), N-acetylcysteine has protective properties against hepatotoxicity induced by paracetamol.

According to El-Maddawy and El-Sayed (2018), it successfully maintained and restored liver, kidney, and testicular functions while preventing oxidative damage caused by paracetamol. According to Nencini *et al*. (2007), oxidative stress is caused by an imbalance between free radicals that can cause protein oxidation, DNA fragmentation, and lipid peroxidation, and reactive oxygen and nitrogen species (ROS and RNS) that are produced and scavenged. Protein structural and functional alterations, gene mutations, and a loss of membrane integrity are the outcomes of these damages (Reddy *et al*., 2009).

According to Sharma *et al*. (2011), oxidative stress plays a crucial role in several illnesses. Because the liver is the primary organ engaged in the body's detoxification of several medications and xenobiotics, it plays a critical role in the regulation of numerous physiological processes. Additionally, extra-hepatic organ damage such as brain impairment, kidney failure, and testicular failure can result from systemic oxidative stress that escalates with liver disease (Palma *et al*., 2014).

MATERIALS AND METHODS

Experimental animals

40 mature male albino rats weighing between 150 and 200 grams were acquired from the Animal House, Alexandria University, Egypt's Medical Technology Center and Research Institute. Before beginning the experiments, the animals were kept in plastic cages in an environmentally controlled room with a 12-hour light/dark cycle and a constant temperature of 2527°C. They were fed a standard rat diet consisting of 24% protein, 5% fat, 4% fiber, 55% carbohydrates, 0.6% calcium, 10% moisture, and 9% ash for ten days.

Chemicals

Sigma Chemical Co., St. Louis, MO, USA, provided the N-acetylcysteine (C5H9NO3S) 2-Acetamido-3-sulfanylpropanoic acid that was purchased. The supplier of paracetamol (C8H9NO2) was GlaxoSmithKline, Dungarvan Ltd. in Ireland. The highest purity and analytical grade were possessed by all other substances and solvents needed for the biochemical tests.

Experimental design

This study was carried out on 40 male rats, who were randomly divided into 4 equal groups (10 rats each) as follows: Group 1 (control group): Rats were administrated 1 ml distilled water by esophageal gastric syringe daily. Group 2 (Paracetamol group): Rats were administrated with 650mg/kg.b.w Paracetamol dissolved in 1ml distilled water by esophageal gastric syringe daily. Group 3 (N-acetylcysteine group): Rats were administrated 150mg/kg.b.w NAC dissolved in 1ml distilled water daily by esophageal gastric syringe. Group 4 (paracetamol + N-acetylcysteine): Rats were administrated (650mg/kg) Paracetamol daily after one hour followed by a dose of NAC (150mg/kg) by as in groups 2, 3. Two weeks passed during the experiment. The animals in the experiment were monitored for signs of death. The amounts of N-acetylcysteine and paracetamol were as per (Yousef *et al*., 2010).

Determination of antioxidant enzymes and oxidative stress in testes tissues

Testicular whole tissues were acquired through dissection, followed by a physiological saline wash and weighing. Next, a part of each rat's testicular tissue was kept in storage at 20°C. The piece to be

remembered was chopped and mixed thoroughly in 510 milliliters of cold buffer (potassium phosphate, 50 mM, pH 7.4, and ethylene diamine tetraacetic acid (EDTA). According to Goldberg and Spooner (1983), homogenates were centrifuged at 10,000×g for 20 minutes at 4°C. The clear supernatants were then utilized for MDA, glutathione peroxidase, superoxide dismutase, hydrogen peroxide, and catalase analyses.

Determination of serum testosterone level

The competitive inhibition enzyme immunoassay method is used in this assay. On a microplate, a monoclonal antibody that is specific to rat T has been pre-coated. Using the pre-coated rat T-specific antibody, a competitive inhibitory response is initiated between biotin-labeled rat T and unlabeled rat T (Calibrators or samples). The unbound conjugate is removed after incubation. Each microplate well is then filled with avidin conjugated to horseradish peroxidase (HRP), and the mixture is incubated. The concentration of T in the sample is inversely proportional to the amount of bound HRP conjugate. Following the addition of the substrate solution, the color created has an inverse relationship with the sample's T concentration.

Determination of serum Follicle stimulating level

Monoclonal anti-FSH antibody-coated wells are used to incubate biotin-conjugated anti-FSH and standard or sample in the Rat FSH ELISA Kit. Horseradish peroxidase (HRP) conjugated avidin is added and incubated for 30 minutes after washing and incubating for 15 to 18 hours. After washing, the HRP complex that was left in the wells reacted for 20 minutes with a chromogenic substrate (TMB). The reaction was then stopped by adding an acidic solution, and the absorbance of the yellow result was measured using spectrophotometry at 450 nm (the sub-wavelength is 620 nm). The absorbance and FSH concentration are almost directly correlated. Plotting absorbance versus standard FSH concentrations creates the standard curve. Using this standard curve, the FSH concentrations in unknown samples are ascertained.

Determination of serum luteinizing level

To detect LH in Shibayagi's Rat LH ELISA Kit, wells coated with monoclonal anti-LH antibody are treated with standards or samples. The biotin-labeled anti-LH antibodies is added and incubated for an additional hour to bind with captured LH after two hours of incubation and washing. Following washing, avidin labeled with horse radish peroxidase (HRP) is applied and incubated for half an hour. Following washing, the HRP complex that was left in the wells reacted for 20 minutes with a chromogenic substrate (TMB). The reaction was then stopped by adding an acidic solution, and the absorbance of the yellow result was measured at 450 nm using spectrophotometry. The absorbance and LH concentration are proportionate. Plotting absorbance versus standard LH values creates the standard curve. This standard curve is used to calculate the LH concentrations in unknown samples.

Quantitative and qualitative analysis of sperms

Collection of epididymis sperm and sperm function test: When the experiment concluded, all of the animals were given dimethyl ether without authorization, and their epididymis was removed right away. The caudal epididymis was utilized for sperm analysis. In short, Gray *et al*. (1989) described the process of collecting epididymis sperm by slicing the caudal epididymis. After cutting the epididymis with a sharp razor blade in 5 milliliters of physiological solution, it was incubated for 5 minutes at 35 degrees Celsius. Sperm obtained in the medium were used to measure sperm motility, count, and abnormalities after multiple washings. Sperm Vision TM CASA System (Eclipse E-200 Nikon Co., Japan) computer-aided semen analysis was used to measure these parameters. Krause (CASA). (1995).

Sperm motility, count and abnormalities

An Eclipse E-200 phase contrast microscope from Nikon Co., Japan, with a heat plate and Sperm Class Analyzer® software (SCA, full research version 5.1 from Microptic Co., Barcelona, Spain) comprised the CASA system. A video camera (Basler Vision, A312FC, Technologies' Co., Ahrensburg, Germany) with an X = 20 magnification was used to record the images at 50 frames per second. Within five minutes of the sperm suspension's separation from the epididymis, it was analyzed for this purpose. A 4 microliter sample of the sperm suspension was obtained and pipetted into a 10 Microliter makler counting chamber (Sefi-Medical Instruments, Germany). Before analysis, the loaded chamber was heated to 37°C on the microscope plate for three minutes. Next, a Nikon microscope was used to examine each sample. The following criteria were assessed for each rat: the proportion of motile and abnormalities, the sperm count expressed as (million/ml) under the last ten distinct and randomly selected fields.

Sperm morphology

Study of the morphology of sperm to assess the sperm morphological anomalies, smears were prepared using a portion of the sperm suspension. By Rezvanfar *et al*. (2008), a single drop of sperm suspension was added to an equivalent volume of 1% eosin-y 5% nigrosin, mixed, and smears were formed on clean glass slides and air-dried. The spermatozoa's abnormalities were assessed using a light microscope with an X= 400 magnification. Any deviation from the normal in the head, tail, or both morphology and structure was regarded as aberrant.

Statistical analysis

The mean ± SE is used to express the values. One-way analysis of variance was used in the statistical computation of the results using the statistical package for social sciences (SPSS software package, version 15). To compare groups, post hoc analysis of variance (ANOVA) testing was done. Regarding the LSD use. Significant differences were defined as $P<0.05$ (Howell, 1995).

RESULTS

Enzymatic and non-enzymatic antioxidants activities in the testis

Effects of paracetamol on both non-enzymatic and enzymatic antioxidants testis tissue levels of glutathione reduced (GSH), superoxide dismutase (SOD), and catalase (CAT) were displayed in Table 1 and Figures 1-3. There was a notable reduction in the activities of CAT, SOD, and GSH in the testes of rats administered PCM in comparison to the control group. A significant drop was obtained in CAT, SOD and GSH levels in rats treated with PCM. Treatment with NAC in combination with PCM significantly increased the activities of CAT, SOD and GSH levels ($P<0.05$) as compared with the PCM group.

Table: (1). Effect of N-acetylcysteine, paracetamol and their combination on enzymatic and non-enzymatic antioxidants in the testes of rats.

Parameters	Experimental groups			
	Control	PCM	PCM+ NAC	NAC
Catalase(CAT) (u/mg)	36.40±4.77	13.40±4.16[a]	26.80±6.65[ab]	37.60±5.90
Superoxide Dismutase (SOD) (u/mg)	64.40±6.58	22.40±7.50[a]	50.40±6.11[ab]	61.20±10.03
Glutathione reduced (GSH) (u/mg)	36.80±5.54	11.80±2.59[a]	33.40±5.22[b]	36.00±6.60

* Noteworthy at the 0.05 level. The values show the mean (± SE) of seven samples. (a) Means show a significant difference ($P<0.05$) from the control group. (b) Means show a significant difference ($P<0.05$) from the paracetamol group.

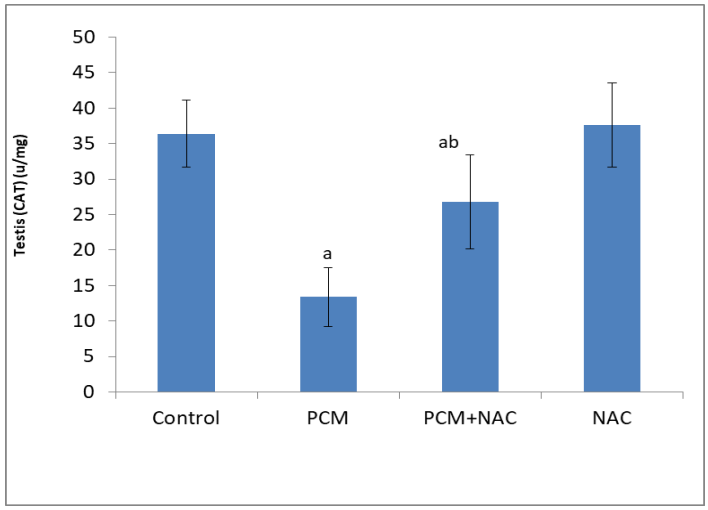

Figure: (1). Effect of NAC on testis homogenate's Catalase (CAT) level in rats given paracetamol in experimental groups.

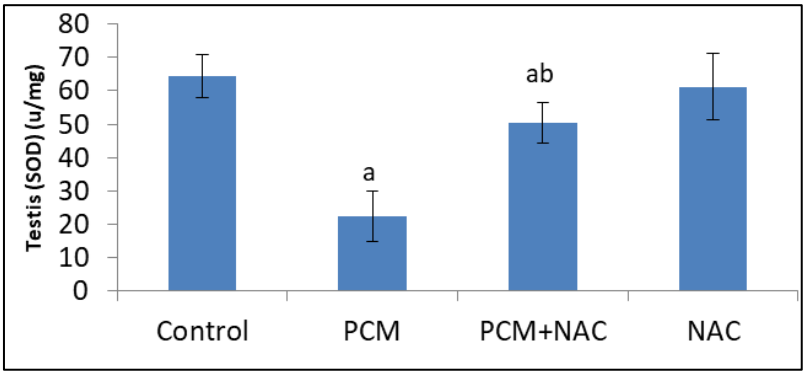

Figure: (2). Effect of NAC on testis homogenate glutathione reduced (GSH) levels in rats given paracetamol in experimental groups.

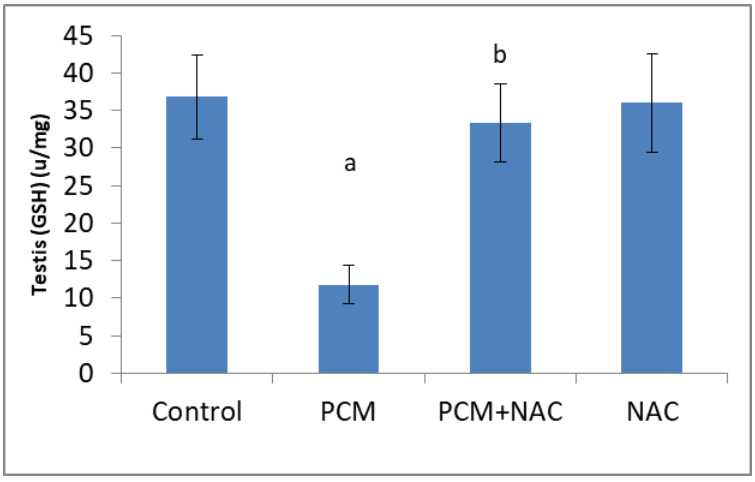

Figure: (3). Effect of NAC on testis homogenate levels of Superoxide Dismutase (SOD) in rats given paracetamol in experimental groups.

Measurement of hydrogen peroxide (H2O2) and malondialdhyde (MDA):

As a sign of free radical-mediated damage in testis tissue, the amount of hydrogen peroxide (H2O2) and lipid peroxidation end product (MDA) in the homogenate of the testes was measured. When compared to the control group, the PCM treated group showed a substantial rise in MDA and

H2O2. When compared to the group that received paracetamol, those who received NAC in addition to PCM demonstrated a partial recovery. (Figures 4,5), Tables 2.

Table: (2). Effect of N-acetylcysteine, paracetamol and their combination on lipid peroxidation tests in the testes of rats.

Parameters	Experimental groups			
	Control	PCM	PCM+ NAC	NAC
(MDA) testis tissue (nmol/g)	11.40±3.05	33.20±6.72[a]	21.00±3.16[ab]	9.20±3.11
H2O2(mM/g)	16.36±6.36	30.02±8.06[a]	20.20±4.76[b]	8.28±1.38

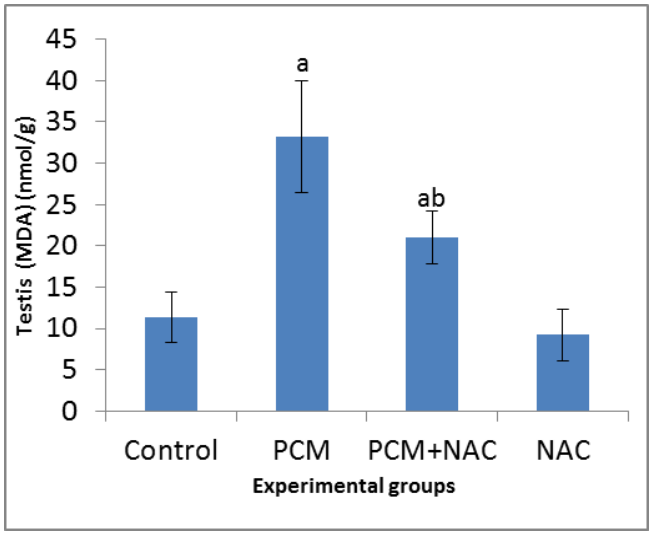

Figure: (4). Effect of NAC on testis homogenate levels of malondialdehyde (MDA) in rats given paracetamol in experimental groups

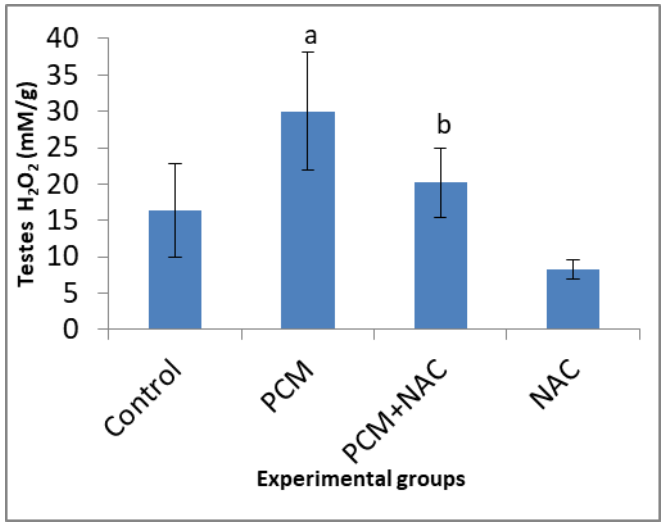

Figure: (5). Effect of NAC on Hydrogen peroxide (H2O2) level of testis homogenate in experimental groups of rats treated with paracetamol.

Determination of sex hormones

Rats receiving PCM showed a significant ($P < 0.05$) drop in testosterone levels when compared to the control group. The drop in testosterone levels was regulated by the combination of PCM and NAC therapy. Rats treated with APAP showed a significant ($P < 0.05$) rise in FSH levels when compared to the control group. When PCM and NAC were used together, the FSH level somewhat

recovered. The results of this investigation showed that the LH value increased significantly (P≤ 0.05) when treated with paracetamol in comparison to the control value. The LH value of rats given oral PCM+NAC therapy improved somewhat. Figures (6-8) and Table (3).

Table: (3). Effect of N-acetylcysteine, paracetamol and their combination on hormones tests in the testes of rats.

Parameters	Experimental groups			
	Control	PCM	PCM+ NAC	NAC
Testosterone(pg/ml)	4.86±0.76	1.32±0.52[a]	2.92±0.94[ab]	4.32±0.78
FSH(ng/ml)	0.37±0.07	0.78±0.10[a]	0.52±0.05[ab]	0.28±0.06
LH(ng/ml)	0.83±0.13	1.35±0.23[a]	0.90±0.13[b]	0.68±0.09

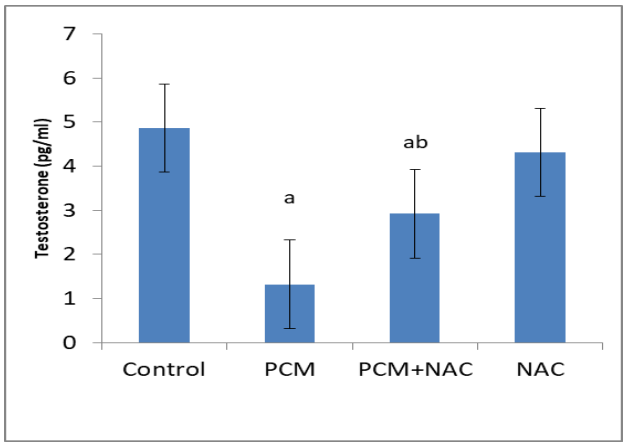

Figure: (6). Effect of NAC on testosterone hormone levels in experimental groups of rats treated with paracetamol.

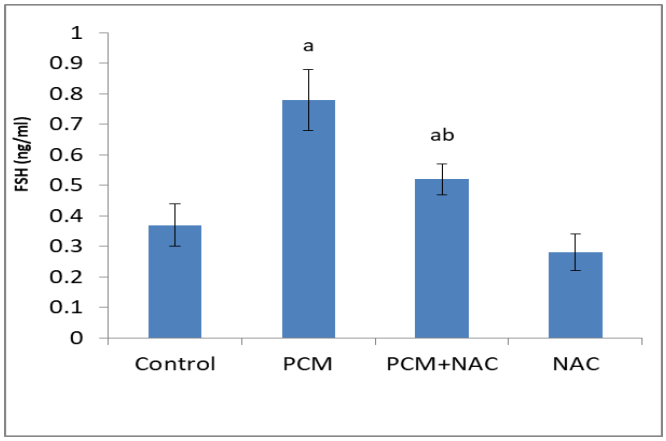

Figure: (7). Effect of NAC on the level of follicle-stimulating hormone (FSH) in rats given paracetamol in experimental groups.

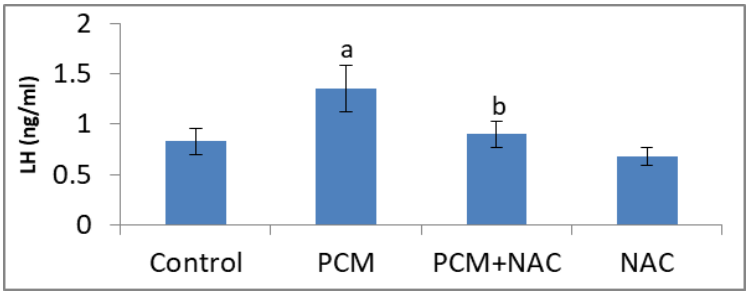

Figure: (8). Effect of NAC on levels of luteinizing hormone (LH) in rats given paracetamol in experimental groups.

Quantitative analysis and qualitative analysis of sperms

The sperm count, motility, and abnormalities treated with paracetamol, N-acetylcysteine, and their combination are displayed in Table (4) and Figures (9-12). Sperm count significantly decreased ($P < 0.05$) in male rats treated with PCM. When combined with PCM, NAC therapy significantly increased the number of sperm. When compared to the control group, the sperms' motility significantly decreased following the injection of paracetamol. Sperm motility was significantly reduced by administering NAC in addition to PCM. According to the current study, there was a significant increase ($P < 0.05$) in sperm abnormalities in the PCM-treated group as compared to the control group. The abnormality level was significantly reduced ($P < 0.05$) when (NAC) and (PCM) were administered together.

Table: (4). Effect of N-acetylcysteine paracetamol and their combination on sperm characteristics in the testes of rats.

Parameters	Experimental groups			
CASA	Control	PCM	PCM+NAC	NAC
Sperm Count (million/ml)	86.60±6.11	17.60±4.04[a]	61.40±7.77[ab]	83.60±16.1
Sperm Motility (%)	84.00±5.48	16.80±2.49[a]	52.40±14.60[ab]	82.40±8.44
Sperm Abnormality (%)	12.20±2.39	54.60±3.78[a]	34.40±7.02[ab]	10.80±5.40

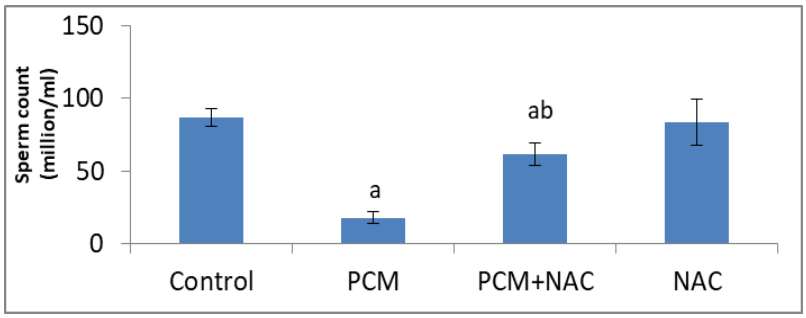

Figure: (9). Effect of NAC on sperm count in rats receiving paracetamol in an experimental setting.

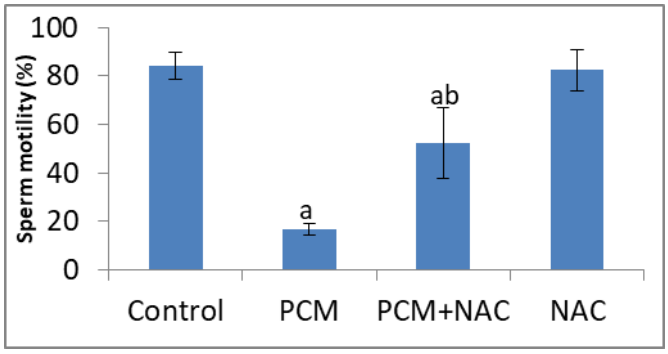

Figure: (10). Effect of NAC on motility of sperms in experimental groups of rats treated with paracetamol.

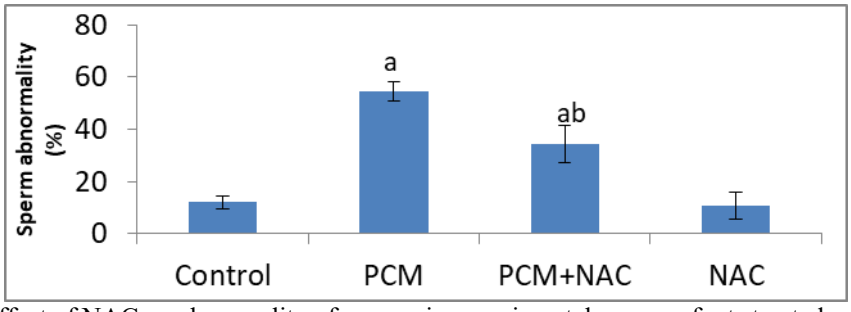

Figure: (11). Effect of NAC on abnormality of sperms in experimental groups of rats treated with paracetamol.

DISCUSSION

Important antioxidant markers are the CAT, GSH, and SOD. The body's antioxidant capacity shields the body against harm brought on by oxidative stress (Canayakin *et al*., 2016). Two crucial components of the toxicity process are the heightened production of reactive oxygen species and oxidative stress (Hinson *et al*., 2010). Lipid peroxidation (LPO) increases when oxidative stress increases due to the antioxidant enzymes' depletion, which scavenges harmful superoxide and hydrogen peroxide radicals (Kisaoglu *et al*., 2014).

Key antioxidant defense system enzymes, SOD and GSH, help detoxify reactive chemicals or repair the damage they cause to cells (Whidden *et al*., 2011). Lipid peroxidation is slowed down by natural antioxidants like SOD and CAT, according to Kisaoglu *et al*. (2014). While CAT directly neutralizes the increased H2O2 during oxidative stress, it also shields cells from the damaging effects of superoxide radicals. Where there is a large concentration of H2O2, catalase functions more efficiently.

The current study's findings showed that, in comparison to the control group, oral paracetamol administration was linked to a decrease in the activity of antioxidant enzymes (CAT, GSH, SOD) and an increase in MDA and H2O2 in testis tissues. However, when compared to the paracetamol group, these data showed a considerable improvement in the rats treated with PCM+NAC. These findings concurred with those of Mohammed & Sabry (2020); Kisaoglu *et al*. (2014), and Yousef *et al*. (2010). Testicular injury resulted from an increase in lipid peroxidation (Morsy *et al*., 2012; Lonare *et al*., 2016).

Yayla *et al.* (2014), indicated that an increase in antioxidant enzymes was accompanied by a significant reduction in the GSH levels. According to Karakus *et al*. (2013), oxidative stress and the loss of glutathione, coupled with an increase in the production of reactive oxygen species (ROS) and high doses of paracetamol, are crucial components of the toxicity process. Additionally, N-Acetyl P Benzo-quinine (NAPQI) causes the testis' intracellular GSH levels to decrease (EI-maddawy and EI-sayed, 2018).

Conversely, the testes are the site of the paracetamol toxicity mechanisms through metabolizing enzyme activity. According to Saito *et al.* (2010), the testes have lower relative levels of P450 against glutathione transferase and glutathione than the liver. Reactive metabolites produced in the liver are therefore unlikely to be transferred to the testicular cells. Ravinder Singh *et al*. (2011) discovered that glutathione was depleted in the testes as a result of paracetamol exposure, which is consistent with this theory. Furthermore, testicular toxicity was found to be generated by a mechanism other than the production of a reactive metabolite (Morakinyo *et al*., 2010). According to Heard (2008) and Olaleye and Rocha (2008), long-term or excessive usage of paracetamol can have negative consequences, such as altered testicular anatomy and decreased capacity for reproduction.

The testis antioxidant levels of CAT, GSH, and SOD were significantly elevated when NAC was administered, while testis MDA and H2O2 levels were significantly decreased. This indicated that the rats receiving PCM were better able to fend off the oxidative stress caused by paracetamol. These findings are in line with those of Morsy *et al*. (2012), Kisaoglu *et al*. (2014), and Lonare *et al*. (2016), who reported that because NAC possesses antioxidant and free radical scavenging properties, it can prevent testicular dysfunction and encourage the regeneration of injured cells.

Numerous investigations demonstrated that NAC might lower lipid peroxidation and restore a reduced level of antioxidant ability. In the current investigation, NAC stopped antioxidant enzyme depletion, including GSH. Additionally, this outcome agrees with Rushworth and Megson's work.

(2014). De Andrade *et al*. (2015) investigated that, the medication NAC's possible therapeutic applications as well as its capacity to fend off the toxicity brought on by a paracetamol overdose.

Luteinizing hormone (LH) and follicle stimulating hormone (FSH) are crucial for reproduction and sperm production by stimulating testosterone hormone release. Positive and negative regulatory mechanisms govern the activity of LH and FSH. Gonadotropin-releasing hormone (GnRH) is secreted by hypothalamic neurons. This hormone binds to gonadotroph receptors in the pituitary and stimulates gonadal secretion of LH and FSH. This, in turn, causes the testes gland to synthesize and release testosterone hormone, which in turn stimulates the gonadal secretion of the sex hormone testosterone (Tilbrook and Clarke, 2001).

In mammals and other vertebrates, the primary male sex hormone is testosterone, which is produced in the testes Leydig cells. According to Jensen *et al*. (2010), the primary functions of testosterone are to promote spermatogenesis and the secretion of the accessory sex glands. Numerous studies have demonstrated that testosterone withdrawal from the rat testes causes increased germ cell death, which in turn leads to diminished reproductive capabilities. Adult mammalian spermatogenesis is a testosterone-dependent process (El-Sharaky *et al*., 2010).

According to the current research, serum levels of luteinizing hormone (LH) and follicle-stimulating hormone (FSH) have significantly increased, but a drop in testosterone levels following the use of paracetamol. This is consistent with the findings of Mohammed & Sabry (2020) and Albert *et al*. (2013), who found that paracetamol exposure dramatically, reduced testosterone secretion.

According to Hassan (2013), male rabbits given large doses of paracetamol for an extended period experienced a significant drop in blood testosterone levels. The paracetamol toxicity mechanism, which is demonstrated by a significant elevation in the lipid peroxidation biomarker (MDA) and a reduction in the antioxidant molecules (CAT and GSH) in the testicles, is the cause of the decreased testosterone production caused by increased testicular oxidative stress. (Kheradpezhouh *et al*., 2010; Karthivashan *et al.,* 2016; Olaniyi and Agunbiade ., 2018).

Olaniyi and Agunbiade (2018) proposed a further explanation for the decrease in testosterone levels, stating that it can be brought on by an increase in gonadotropic hormones (FSH and LH) through a negative feedback process that affects the pituitary and hypothalamus.

According to research by Jensen *et al*. (2010); Kristensen *et al*. (2010, 2012), Snijder *et al*. (2012); Lind *et al*. (2013), and Mazaud-Guittot *et al*. (2013), paracetamol may be regarded as an endocrine disruptor that affects the development of the male reproductive system and the generation of testicular hormones.

According to Garu *et al*. (2011), LH and FSH activity depends on both the quantity of these hormones and the number of certain receptors in the testes. The manufacture and secretion of androgens, which are essential for male development and reproductive function, are carried out by the Leydig cells of the testes. Boekelheide (2005) stated that a decrease in the number of Leydig cells results in a fall in testosterone levels. Leydig and Sertoli cells, as well as the germ cells themselves, are the three primary target cells in the testes for toxicants that impair spermatogenesis.

In opposition to Olaniyi and Agunbiade (2018), there is another study found that the use of paracetamol increased levels of testosterone, luteinizing hormone (LH), and follicular stimulating hormone (FSH). They found that testicular dysfunction was brought on by paracetamol's altered oxidative stress.

Follicle stimulating-hormone (FSH), luteinizing hormone (LH), and testosterone levels improved in the PCM+NAC-treated group of rats as compared to the PCM-only group, according to the current study. Because NAC possesses antioxidant and free radical scavenging potentials, similar results were observed by Morsy *et al*. (2012) and Lonare *et al*. (2016), confirming the ability of NAC to prevent testicular dysfunction and accelerate the regeneration of damaged cells. NAC also aids in increasing testosterone levels.

According to Zafarullah *et al*. (2003), NAC lowers lipid peroxidation in cell membranes and shields the cell from reactive oxygen species-induced oxidative stress. Additionally, as a defense against ROS-induced damage, cell growth and survival rates rose, which led to growth arrest and apoptosis.

It has been demonstrated by Kanter *et al*. (2010) and Del Vento *et al*. (2018) that supplementing the medium with N-acetylcysteine in vitro culture decreased the apoptosis of germ cells. According to El-Kirdasy *et al*. (2014), NAC has a crucial role in testicular protection as well as anti-apoptotic and anti-inflammatory effects on testicular function. Many different types of cells are protected by NAC.

According to the results of the current investigation, taking paracetamol damaged testicles. Toxicology from paracetamol has a negative impact on sperm count and motility. These findings concur with those of Oyedeji *et al*. (2013); Aksu *et al*. (2016), and Mohammed & Sabry (2020), who hypothesized that paracetamol would cross the blood-testis barrier and change the seminiferous tubule microenvironment as a result.

Olaniyi and Agunbiade (2018) claim that chemical agents' capacity to pass across the blood-testis barrier and produce a distinct microenvironment in the inner section of the seminiferous tubule wall is what caused the decrease in sperm motility. The effects of paracetamol on the testes and epididymis may be the cause of the effect (Oyedeji *et al*., 2013).

Additionally, the spermatozoa of rats given paracetamol showed a markedly higher incidence of anomalies related to sperm in the current investigation. Our findings are consistent with those of Morakinyo *et al*. (2010), who found that giving male rats paracetamol increased the occurrence of sperm. High doses of paracetamol have been linked to abnormalities in sperm.

According to studies by Ratnasooriya & Jayakody (2000) and Mohammed & Sabry (2020), paracetamol reduces sperm motility and quantity while also causing sperm cell death, which reduces testicular size and suggests the presence of mild testicular toxicity. Furthermore, excessive paracetamol dosages may result in lipid peroxidation, which may harm sperm fertilization potential by preventing glycolysis and reducing ATP supply, both of which aid in sperm motility. In a similar vein, Olaniyi and Agunbiade (2018) demonstrated that gonadotropic hormones (LH and FSH) and increased testicular oxidative stress caused sperm count, motility, and normal morphology to decline upon paracetamol (500 mg/kg b. w).

Numerous studies have shown that giving paracetamol can enhance oxidative stress by activating cytochrome P450, which can lead to an increase in reactive oxygen species (ROS). The body's built-in antioxidant resistance mechanisms are weakened by an excess of reactive oxygen species (ROS), which leads to oxidative stress and subsequent cellular damage. ROS takes two actions. It first weakens the sperm membrane and reduces its motility. Second, ROS has the ability to change sperm DNA, leading to a genetic abnormality (Wahyudi *et al*., 2015).

Rats given NAC+PCM in this study demonstrated a noteworthy improvement in sperm parameters (count, motility, and morphology) as compared to the group given paracetamol. Furthermore, NAC improved the characteristics of sperm. According to Samuni *et al*. (2013); Kumar *et al*. (2013) and

Takemura *et al*. (2014), these findings are consistent. It was believed that these advantages of NAC were related to the decrease in ROS, which enhanced sperm motility.

According to a study by Prasad *et al*. (2016), NAC improves sperm quality measures. Additionally, because of its antioxidant properties, it is useful against harmful substances that impair the quality of sperm. By enhancing the glutathione antioxidant mechanism, which is necessary for ideal sperm activities, NAC enhances male reproductive capabilities.

CONCLUSION

The results of this study showed that NAC, an antioxidant, improves most testis function biomarkers and causes improvement in sperm parameters and hormone levels in rats given paracetamol. Therefore, during oxidative stress, NAC can correct the imbalance between pro-oxidant and antioxidant systems. The high incidence of infertility in countries where paracetamol is consumed can be explained by the negative effects of excessive paracetamol usage on male fertility. To determine the proper dose of N-acetylcysteine in cases of paracetamol toxicity in humans, more research has to be done.

ACKNOWLEDGEMENT

Authors declare there are no financial supports or relationships that may pose a conflict of interest in the covering letter submitted with the manuscript.

ETHICS

The authors address no any ethical issues that may arise after the publication of this manuscript.

Duality of interest: The authors declare that there are no conflicts of interest.

Author contributions: All Authors contributed equally to this manuscript.

Funding: A funding statement indicates there are no funding for the work reported in their manuscript.

REFERENCES

Adil, M., Kandhare, A. D., Ghosh, P., Venkata, S., Raygude, K. S., & Bodhankar, S. L. (2016). Ameliorative effect of naringin in acetaminophen-induced hepatic and renal toxicity in laboratory rats: role of FXR and KIM-1. *Renal failure, 38*(6), 1007-1020.

Ahmed, T., Pathak, R., Mustafa, M. D., Kar, R., Tripathi, A. K., Ahmed, R. S., & Banerjee, B. D. (2011). Ameliorating effect of N-acetylcysteine and curcumin on pesticide-induced oxidative DNA damage in human peripheral blood mononuclear cells. *Environmental monitoring and assessment, 179*(1-4), 293-299.

Aksu, E. H., Özkaraca, M., Kandemir, F. M., Ömür, A. D., Eldutar, E., Küçükler, S., & Comaklı, S. (2016). Mitigation of paracetamol-induced reproductive damage by chrysin in male rats via reducing oxidative stress. *Andrologia, 48*(10), 1145-1154.

Albert, O., Desdoits-Lethimonier, C., Lesné, L., Legrand, A., Guillé, F., Bensalah, K., ... & Jégou, B. (2013). Paracetamol, aspirin and indomethacin display endocrine disrupting properties in the adult human testis in vitro. *Human reproduction, 28*(7), 1890-1898.

Amin, A. F., Shaaban, O. M., & Bediawy, M. A. (2008). N-acetyl cysteine for treatment of recurrent unexplained pregnancy loss. *Reproductive biomedicine online, 17*(5), 722-726.

Boekelheide, K. (2005). Mechanisms of toxic damage to spermatogenesis. JNCI Monographs, 2005(34), 6-8.

Canayakin, D., Bayir, Y., Kilic Baygutalp, N., Sezen Karaoglan, E., Atmaca, H. T., Kocak Ozgeris, F. B., ... & Halici, Z. (2016). Paracetamol-induced nephrotoxicity and oxidative stress in rats: the protective role of Nigella sativa. *Pharmaceutical biology, 54*(10), 2082-2091.

de Andrade, K. Q., Moura, F. A., dos Santos, J. M., de Araújo, O. R. P., de Farias Santos, J. C., & Goulart, M. O. F. (2015). Oxidative stress and inflammation in hepatic diseases: therapeutic possibilities of N-acetylcysteine. *International journal of molecular sciences, 16*(12), 30269-30308.

Del Vento, F., Vermeulen, M., de Michele, F., Giudice, M. G., Poels, J., des Rieux, A., & Wyns, C. (2018). Tissue Engineering to Improve Immature Testicular Tissue and Cell Transplantation Outcomes: One Step Closer to Fertility Restoration for Prepubertal Boys Exposed to Gonadotoxic Treatments. *International journal of molecular sciences, 19*(1), 286.

Dhouib, I. E., Jallouli, M., Annabi, A., Gharbi, N., Elfazaa, S., & Lasram, M. M. (2016). A minireview on N-acetylcysteine: an old drug with new approaches. *Life sciences, 151*, 359-363.

Dodd, S., Dean, O., Copolov, D. L., Malhi, G. S., & Berk, M. (2008). N-acetylcysteine for antioxidant therapy: pharmacology and clinical utility. *Expert opinion on biological therapy, 8*(12), 1955-1962.

Elgindy, E. A., El-Huseiny, A. M., Mostafa, M. I., Gaballah, A. M., & Ahmed, T. A. (2010). N-acetyl cysteine: could it be an effective adjuvant therapy in ICSI cycles? A preliminary study. *Reproductive biomedicine online, 20*(6), 789-796.

El-Kirdasy, A. F., Nassan, M. A., Baiomy, A. A. A., Ismail, T. A., Soliman, M. M., & Attia, H. F. (2014). Potential ameliorative role of n-acetylcysteine against testicular dysfunction induced by titanium dioxide in male albino rats. *American Journal of Pharmacology and Toxicology, 9*(1), 29.

El-Maddawy, Z. K., & El-Sayed, Y. S. (2018). Comparative analysis of the protective effects of curcumin and N-acetyl cysteine against paracetamol-induced hepatic, renal, and testicular toxicity in Wistar rats. *Environmental Science and Pollution Research, 25*(4), 3468-3479.

El-Sharaky, A. S., Newairy, A. A., Elguindy, N. M., & Elwafa, A. A. (2010). Spermatotoxicity, biochemical changes and histological alteration induced by gossypol in testicular and hepatic tissues of male rats. *Food and Chemical Toxicology, 48*(12), 3354-3361.

Garu, U., Sharma, R., & Barber, I. (2011). Effect of lead toxicity on developing testis of mice. *International Journal of Pharmaceutical Sciences and Research, 2*(9), 2403.

Gray, J. L., Ostby, J., Ferrell, J., Sigmon, R., Cooper, R., Linder, R., ... & Laskey, J. (1989). Correlation of sperm and endocrine measures with reproductive success in rodents. *Progress in clinical and biological research, 302*, 193-206.

Hassan, N. A. (2013). Toxic effects of paracetamol on male reproductive system of adult rabbits. *International Journal of Pharma and Bio Sciences, 4*(1), 806-821.

Heard, K. J. (2008). Acetylcysteine for acetaminophen poisoning. *New England Journal of Medicine, 359*(3), 285-292.

Hinson, J. A., Roberts, D. W., & James, L. P. (2010). Mechanisms of acetaminophen-induced liver necrosis. *In Adverse drug reactions* (pp. 369-405). Springer, Berlin, Heidelberg.

Howell, D.C. (1995): Fundamental statistics for the behavioral sciences. 3rd ed. *An imprint of Wads Worth publishing company Belmont*. California: Duxbury press; 163-166.

İçer, M., Zengin, Y., Gunduz, E., Dursun, R., Durgun, H. M., Turkcu, G., ... & Guloglu, C. (2016). Is montelukast as effective as N-acetylcysteine in hepatic injury due to acetaminophen intoxication in rats?. *Experimental and Toxicologic Pathology, 68*(1), 55-59.

Jensen, M. S., Rebordosa, C., Thulstrup, A. M., Toft, G., Sørensen, H. T., Bonde, J. P., ... & Olsen, J. (2010). Maternal use of acetaminophen, ibuprofen, and acetylsalicylic acid during pregnancy and risk of cryptorchidism. *Epidemiology, 21*(6), 779-785.

Jóźwiak-Bebenista, M., & Nowak, J. Z. (2014). Paracetamol: mechanism of action, applications and safety concern. *Acta poloniae pharmaceutica, 71*(1), 11-23.

Kanter, M., Topcu-Tarladacalisir, Y., & Parlar, S. (2010). Antiapoptotic effect of L-carnitine on testicular irradiation in rats. *Journal of molecular histology, 41*(2-3), 121-128.

Karakus, E., Halici, Z., Albayrak, A., Polat, B., Bayir, Y., Kiki, I., ... & Aksak, S. (2013). Agomelatine: an antidepressant with new potent hepatoprotective effects on paracetamol-induced liver damage in rats. *Human & experimental toxicology, 32*(8), 846-857.

Karthivashan, G., Kura, A. U., Arulselvan, P., Isa, N. M., & Fakurazi, S. (2016). The modulatory effect of Moringa oleifera leaf extract on endogenous antioxidant systems and inflammatory markers in an acetaminophen-induced nephrotoxic mice model. *PeerJ, 4*, e2127.

Kheradpezhouh, E., Panjehshahin, M. R., Miri, R., Javidnia, K., Noorafshan, A., Monabati, A., & Dehpour, A. R. (2010). Curcumin protects rats against acetaminophen-induced hepatorenal damages and shows synergistic activity with N-acetyl cysteine. *European journal of pharmacology, 628*(1-3), 274-281.

Kisaoglu, A., Ozogul, B., Turan, M. I., Yilmaz, I., Demiryilmaz, I., Atamanalp, S. S., ... & Suleyman, H. (2014). Damage induced by paracetamol compared with N-acetylcysteine. *Journal of the Chinese Medical Association, 77*(9), 463-468.

Kristensen, D. M., Hass, U., Lesné, L., Lottrup, G., Jacobsen, P. R., Desdoits-Lethimonier, C., ... & Brunak, S. (2010). Intrauterine exposure to mild analgesics is a risk factor for development of male reproductive disorders in human and rat. *Human Reproduction, 26*(1), 235-244.

Kristensen, D. M., Lesné, L., Le Fol, V., Desdoits-Lethimonier, C., Dejucq-Rainsford, N., Leffers, H., & Jégou, B. (2012). Paracetamol (acetaminophen), aspirin (acetylsalicylic acid) and

indomethacin are anti-androgenic in the rat foetal testis. *International journal of andrology, 35*(3), 377-384.

Kumar, B. A., Reddy, A. G., Kumar, P. R., Reddy, Y. R., Rao, T. M., & Haritha, C. (2013). Protective role of N-Acetyl L-Cysteine against reproductive toxicity due to interaction of lead and cadmium in male Wistar rats. *Journal of natural science, biology, and medicine, 4*(2), 414.

Larsson, S. C., Håkansson, N., & Wolk, A. (2015). Dietary cysteine and other amino acids and stroke incidence in women. *Stroke, 46*(4), 922-926.

Lasram, M. M., Dhouib, I. B., Annabi, A., El Fazaa, S., & Gharbi, N. (2015). A review on the possible molecular mechanism of action of N-acetylcysteine against insulin resistance and type-2 diabetes development. *Clinical biochemistry, 48*(16-17), 1200-1208.

Lind, J. N., Tinker, S. C., Broussard, C. S., Reefhuis, J., Carmichael, S. L., Honein, M. A., ... & National Birth Defects Prevention Study. (2013). Maternal medication and herbal use and risk for hypospadias: data from the National Birth Defects Prevention Study, 19972007. *Pharmacoepidemiology and drug safety, 22*(7), 783-793.

Lonare, M., Kumar, M., Raut, S., More, A., Doltade, S., Badgujar, P., & Telang, A. (2016). Evaluation of ameliorative effect of curcumin on imidacloprid-induced male reproductive toxicity in wistar rats. *Environmental toxicology, 31*(10), 1250-1263.

Mazaud-Guittot, S., Nicolaz, C. N., Desdoits-Lethimonier, C., Coiffec, I., Maamar, M. B., Balaguer, P., ... & Dejucq-Rainsford, N. (2013). Paracetamol, aspirin, and indomethacin induce endocrine disturbances in the human fetal testis capable of interfering with testicular descent. *The Journal of Clinical Endocrinology & Metabolism, 98*(11), E1757-E1767.

Mohammed, H.O & Sabry, R.M (2020). The Possible Role of Curcumin against Changes Caused by Paracetamol in Testis of Adult Albino Rats (Histological, Immunohistochemical and Biochemical Study). *Egyptian Journal of Histology, 43* (3), 819-834.

Mokhtari, V., Afsharian, P., Shahhoseini, M., Kalantar, S. M., & Moini, A. (2017). A Review on Various Uses of N-Acetyl Cysteine. *Cell Journal (Yakhteh), 19*(1), 11.

Morakinyo, A. O., Achema, P. U., & Adegoke, O. A. (2010). Effect of Zingiber officinale (Ginger) on sodium arsenite-induced reproductive toxicity in male rats. *African Journal of Biomedical Research, 13*(1), 39-45.

Morsy, M. A., Abdalla, A. M., Mahmoud, A. M., Abdelwahab, S. A., & Mahmoud, M. E. (2012). Protective effects of curcumin, α-lipoic acid, and N-acetylcysteine against carbon tetrachloride-induced liver fibrosis in rats. *Journal of physiology and biochemistry, 68*(1), 29-35.

Nencini, C., Giorgi, G., & Micheli, L. (2007). Protective effect of silymarin on oxidative stress in rat brain. *Phytomedicine, 14*(2-3), 129-135.

Olaleye, M. T., & Rocha, B. J. (2008). Acetaminophen-induced liver damage in mice: effects of some medicinal plants on the oxidative defense system. *Experimental and Toxicologic Pa-*

thology, 59(5), 319-327.

Olaniyi, K. S., & Agunbiade, T. B. (2018). α-tocopherol attenuates acetaminophen-induced testicular dysfunction in adult male rats. *International Journal of Health & Allied Sciences, 7*(1), 6.

Oyedeji, K. O., Bolarinwa, A. F., & Ojeniran, S. S. (2013). Effect of paracetamol (acetaminophen) on haematological and reproductive parameters in male albino rats. *IOSR Journal of Pharmacy and Biological Sciences (IOSR-JPBS), 4*(6), 1-6.

Palma, H. E., Wolkmer, P., Gallio, M., Corrêa, M. M., Schmatz, R., Thomé, G. R., ... & de Oliveira, L. S. (2014). Oxidative stress parameters in blood, liver, and kidney of diabetic rats treated with curcumin and/or insulin. *Molecular and cellular biochemistry, 386*(1-2), 199-210.

Prasad, S. V., Ghongane, B. B., & Nayak, B. B. (2016). Journal of Chemical and Pharmaceutical Research, 2016, 8 (5): 845-851. *Journal of Chemical and Pharmaceutical Research, 8*(5), 845-851.

Ravinder Singh, C., R. Nelson P.Muthu Krishnan and K. Mahesh (2011). Hepatoprotective and anti-oxidant effect of root and root callus extract of premna serratifolia l. in paracetamol induced liver damage in male albino rats. *International Journal of Pharma and Bio Sciences, 2*(1), 0975-6299.

Reddy, B. V., Sundari, J. S., Balamurugan, E., & Menon, V. P. (2009). Prevention of nicotine and streptozotocin treatment induced circulatory oxidative stress by bis-1, 7-(2-hydroxyphenyl)-hepta-1, 6-diene-3, 5-dione in diabetic rats. *Molecular and cellular biochemistry, 331*(1-2), 127.

Rezvanfar, M. A., Sadrkhanlou, R. A., Ahmadi, A., Shojaei-Sadee, H., Rezvanfar, M. A., Mohammadirad, A., ... & Abdollahi, M. (2008). Protection of cyclophosphamide-induced toxicity in reproductive tract histology, sperm characteristics, and DNA damage by an herbal source; evidence for role of free-radical toxic stress. *Human & experimental toxicology, 27*(12), 901-910.

Ribeiro, G., Roehrs, M., Bairros, A., Moro, A., Charão, M., Araújo, F., ... & Leal, M. (2011). N-acetylcysteine on oxidative damage in diabetic rats. *Drug and chemical toxicology, 34*(4), 467-474.

Rushworth, G. F., & Megson, I. L. (2014). Existing and potential therapeutic uses for N-acetylcysteine: the need for conversion to intracellular glutathione for antioxidant benefits. *Pharmacology & therapeutics, 141*(2), 150-159.

Saito, C., Zwingmann, C., & Jaeschke, H. (2010). Novel mechanisms of protection against acetaminophen hepatotoxicity in mice by glutathione and N-acetylcysteine. *Hepatology, 51*(1), 246-254.

Samuni, Y., Goldstein, S., Dean, O. M., & Berk, M. (2013). The chemistry and biological activities of N-acetylcysteine. *Biochimica et Biophysica Acta (BBA)-General Subjects, 1830*(8), 4117-4129.

Sharma, S. K., Arogya, S. M., Bhaskarmurthy, D. H., Agarwal, A., & Velusami, C. C. (2011). Hepatoprotective activity of the Phyllanthus species on tert-butyl hydroperoxide (t-BH)-induced cytotoxicity in HepG2 cells. *Pharmacognosy magazine, 7*(27), 229.

Snijder, C. A., Kortenkamp, A., Steegers, E. A., Jaddoe, V. W., Hofman, A., Hass, U., & Burdorf, A. (2012). Intrauterine exposure to mild analgesics during pregnancy and the occurrence of cryptorchidism and hypospadia in the offspring: the Generation R Study. *Human Reproduction, 27*(4), 1191-1201.

Takemura, S., Ichikawa, H., Naito, Y., Takagi, T., Yoshikawa, T., & Minamiyama, Y. (2014). S-allyl cysteine ameliorates the quality of sperm and provides protection from age-related sperm dysfunction and oxidative stress in rats. *Journal of clinical biochemistry and nutrition, 55*(3), 155-

Tilbrook, A. J., & Clarke, I. J. (2001). Negative feedback regulation of the secretion and actions of gonadotropin-releasing hormone in males. *Biology of reproduction, 64*(3), 735-742.

Uraz, S., Tahan, G., Aytekin, H., & Tahan, V. (2013). N-acetylcysteine expresses powerful anti-inflammatory and antioxidant activities resulting in complete improvement of acetic acid-induced colitis in rats. *Scandinavian journal of clinical and laboratory investigation, 73*(1), 61-66.

Wahyudi, S., Ekowati, R. R., & Rinaldi, A. (2015). Effect of Dates (Phoenix Dactilyfera L) on male infertility. *Althea Medical Journal, 2*(1), 82-85.

Wang, Q., Hou, Y., Yi, D., Wang, L., Ding, B., Chen, X., ... & Wu, G. (2013). Protective effects of N-acetylcysteine on acetic acid-induced colitis in a porcine model. *BMC gastroenterology, 13*(1), 133.

Whidden, M. A., Kirichenko, N., Halici, Z., Erdos, B., Foster, T. C., & Tümer, N. (2011). Life-long caloric restriction prevents age-induced oxidative stress in the sympathoadrenal system of Fischer 344 x Brown Norway rats. *Biochemical and biophysical research communications, 408*(3), 454-458.

Yayla, M., Halici, Z., Unal, B., Bayir, Y., Akpinar, E., & Gocer, F. (2014). Protective effect of Et-1 receptor antagonist bosentan on paracetamol induced acute liver toxicity in rats. *European journal of pharmacology, 726*, 87-95.

Yousef, M. I., Omar, S. A., El-Guendi, M. I., & Abdelmegid, L. A. (2010). Potential protective effects of quercetin and curcumin on paracetamol-induced histological changes, oxidative stress, impaired liver and kidney functions and haematotoxicity in rat. *Food and Chemical Toxicology, 48*(11), 3246-3261.

Zafarullah, M., Li, W. Q., Sylvester, J., & Ahmad, M. (2003). Molecular mechanisms of N-acetylcysteine actions. *Cellular and Molecular Life Sciences CMLS, 60*(1),6-20.

Al-Mukhtar Journal of Basic Sciences 22 (1): 30-37, 2024
Doi: https://doi.org/10.54172/21srcz92

Research Article

Open Access

Isolation and characterization of lytic bacteriophage against common pathogenic bacteria

Asma S. Alilesh*, Marwa E. Alwush, Tasneem M. Alswehly and Khawla A. Aween

***Corresponding author:** micro-gene86@gmail.com Department of Genetics and Biotechnology, Faculty of Science, University of Misurata, Libya.

Second Author: Department of Genetics and Biotechnology, Faculty of Science, University of Misurata, Libya.

Third Author: Department of Genetics and Biotechnology, Faculty of Science, University of Misurata, Libya.

Fourth Author: Department of Genetics and Biotechnology, Faculty of Science, University of Misurata, Libya.

Received:
02 August 2023

Accepted:
17 April 2024

Publish online:
30 April 2024

Abstract

Regarding their specificity, bacteriophages have been widely investigated to combat bacterial infections. Phage therapy is proposed as a promising alternative antibacterial agent. The present study was conducted to isolate and characterize bacteriophages against clinical bacterial isolates from sewage water. Recovery of phage was high from the processed sewage water (66%) against tested bacterial hosts. Plaque assay revealed four different plaques morphology against *Escherichia coli* with high lytic activity. In contrast, one small morphology plaques were appeared against *Staphylococcus aureus* with low lytic activity. The mean phage titer of phage isolates was $7.7x10^9$ and $2.9x10^{11}$ plaque forming unit/ml for *S. aureus* and *E. coli* respectively. The isolated phages showed a narrow host range when tested against 19 different bacterial isolates. The electron microscopy revealed that EC1 Phage has the typical morphology of the family Podoviridae, order Caudovirales. The isolated bacteriophages need to be further characterized at the molecular level and tested in vivo to be used in one of the bacteriophage applications.

Keywords: Bacteriophages, Sewage Water, *Escherichia* Coli, *Staphylococcus Aureus*, Antibacterial Agent.

INTRODUCTION

The emergence of multi-drug resistance (MDR) bacteria strains, which are posing a global health threat, has developed the interest of scientists to use alternative strategies to control pathogenic bacteria (Ullah et al., 2021). Lytic bacteriophages or phage therapy, were suggested to be an attractive alternative to antibiotics for the biological control of bacterial disease (Yu et al., 2013).

Phages are widely distributed in soil, sewage, animal wastes and their secretions. Determination of their host range is very important for their use in phage therapy, while there are two types of host range, some phages can only infect one or a few bacterial strains so they have a narrow host range, while other phages can infect many species from different genera and this called broad host rang (Ross et al., 2016).

Unlike antibiotics, phages kill target bacteria specifically and do not destroy the normal flora of the host, so the application of phage therapy could be a natural and non-toxic method to reduce and

control the growth of human pathogenic bacteria (Masoud et al., 2020); The efficacy of phages to control bacterial growth had been extensively investigated, Shende and his colleagues isolated and characterized phages from dairy farm waste disposal using *E. coli* and *Bacillus subtilis* as the host system. The recovered phage had a broad host range (Shende et al., 2017). Other investigations succeeded in the isolation highly virulent phages with high specificity to their host even MDR strains like methicillin resistant *S. aureus, Acinetobacter baumanni,* and *E. coli* 0157:H7 (Esmael et al., 2021; Rasool et al., 2016; Sjahriani et al., 2021).

There is considerable attention on using phages to treat bacterial infections (Al-Anany et al., 2023); Le and his colleagues employed intravenous administration of phage in place of antibiotics to successfully treat a recurrent UTI caused by *Klepsiella pneumoniae* (Le et al., 2023). Some identified and isolated phages, however, have a very limited host range and are unable to infect distinct bacterial strains within the same species. This restriction might be overcome by preparing phage libraries, which would enable researchers to choose the best phage cocktail for a given infection (Duarte et al., 2024).

The present study aims to isolate and characterize bacteriophage from sewage water against common pathogenic bacteria, and this will be the first report on the isolation of a bacteriophage in Misurata city.

MATERIALS AND METHODS

Sample collection

Sewage water sample from the Wastewater Treatment Station in Misurata was collected in January 2022 in sterile container, brought to the lab and processed by centrifugation at 4000 r.p.m for 10 min to remove any large debris. Then the supernatant was filtered using 0.22μm syringe filter unit in an attempt to obtain phage containing water sample (Rasool et al., 2016).

Bacterial primary host

In this study, four-gram negative bacteria (2 *Acinetobacter sp., Pseudomonas aeruginosa*, and *Escherichia coli*) and two *Staphylococcus aureus* isolates were used as host strains for bacteriophage isolation. These clinical isolates were obtained from Misurata Reference Laboratory and Misurata Central Laboratory. Most of these isolates revealed a remarkable elevation of resistance to antibiotics.

Amplification and preliminary screening of bacteriophage

Phage contents in filtrated sewage water against each bacterial isolate were propagated by culture-enrichment method according to the Sambrook et al. protocol with minor modifications (Sambrook et al., 1989). Briefly: 15ml filtrate sewage sample and 25ml sterile nutrient broth were mixed with 10ml overnight culture of host stain and incubated at 37 C^0 for 48h. After that bacteria were removed by centrifugation at 4000 r.p.m for 10min then filtration of the supernatant via 0.22μm syringe filter unit.

To test the presence of lytic phages in filtrates, spot assay and turbidity reduction assay were used. In the spot method; 100μl of filtrate was spot inoculated on the surface of counterpart log phase bacterial lawn on Mullar Hinton Agar plates. After 24h incubation period, plates were examined for the presence of lytic zones on bacterial lawns (Masoud et al., 2020; Rasool et al., 2016).

The test was repeated twice and two high lytic positive filtrates were selected for further experiments. Whereas in the turbidity reduction technique, 3ml log phase bacterial culture was inoculated

with 0.5ml from filtrate, OD of enriched culture is measured at 600nm wavelength with respect to control (bacterial culture only) via spectrophotometer at zero time, after 24h and after 48h, incubation period at 37 C^0 (Qamar et al. 2019). The two methods were repeated thrice before judgment the results.

Bacteriophage morphology

In order to determine the plaque morphology, double agar layer (DAL) method was conducted (Shende et al., 2017). Briefly: a mixture of serially diluted phage filtrates with their log phase host culture was added to 3ml molten soft agar and poured quickly onto solidified Mullar Hinton agar plates. The plague morphology was noted and counted after incubating the plates overnight at 37 C^0. The phage titer was expressed as plaque forming unit per 1 milliliter (PFU/ml) and determined by the following formula: (PFU/ml = (number of plaques X dilution factor) / volume of phage plated in ml) (Qamar et al., 2019).

E. coli Phage morphology was determined using a transmition electron microscope (TEM) with the same protocol described by Chen et al. (Chen et al., 2018). The phage filtrate was negatively stained with 2% unaryl acetate on carbon coated grids and examined under TEM (Zeiss EM10CR, Germany). The size and morphology of the phage were determined from three identical phage particles.

Host range

Spot assay was carried out as described previously to determine the host range of the two isolated phages. The primary bacterial host along with 19 different MDR bacteria stains were tested (2 *Acinetobacter sp., Pseudomonas aeruginosa, 2 Staphylococcus aureus, Enterococcus sp., 6 Escherichia coli, 3 Klebsiella sp., 2 Citrobacter koseri*).

RESULTS AND DISCUSSION

Efficacy of sewage water for bacteriophage isolation:

Bacteriophages are obligate bacterial parasites that infect and kill bacteria in a specific manner. Considering of emergence of bacterial resistance to broad-spectrum antibiotics; phage therapy is proposed as a promising alternative antibacterial agent. Besides this, they are ubiquitous in nature and they have been estimated to be more abundant in aquatic systems especially, in sewage water (10^8-10^{10} / ml), compared to seawater and soil (Ullah et al., 2021).

In the present study, an untreated sewage water sample was processed for phage isolation against six different clinical pathogens. The final filtrate obtained after the enrichment step with each host was separately assessed against the coordinate host through spot assay.

Recovery of phage was high (66%); The tested sewage sample showed positive lytic spots against all the tested hosts except for two (figure1), which is in accordance with previous studies reporting the high recovery (72% - 93%) of bacteriophage in sewage water against *S. aureus, E. coli, B. subtilis and A. baumannii* [5, 6, 13](Alsaffar,2019; Rasool et al., 2016; Shende et al., 2017).

Lytic activity of processed sewage filtrates

In order to confirm the presence of bacteriophages in *E. coli* and *S. aureus* filtrates which revealed clear lytic zones in spot assay; each filtrate was added to both cultures of counterpart bacteria and monitored for cell lysis as indicated by reduction of culture turbidity comparing with control.

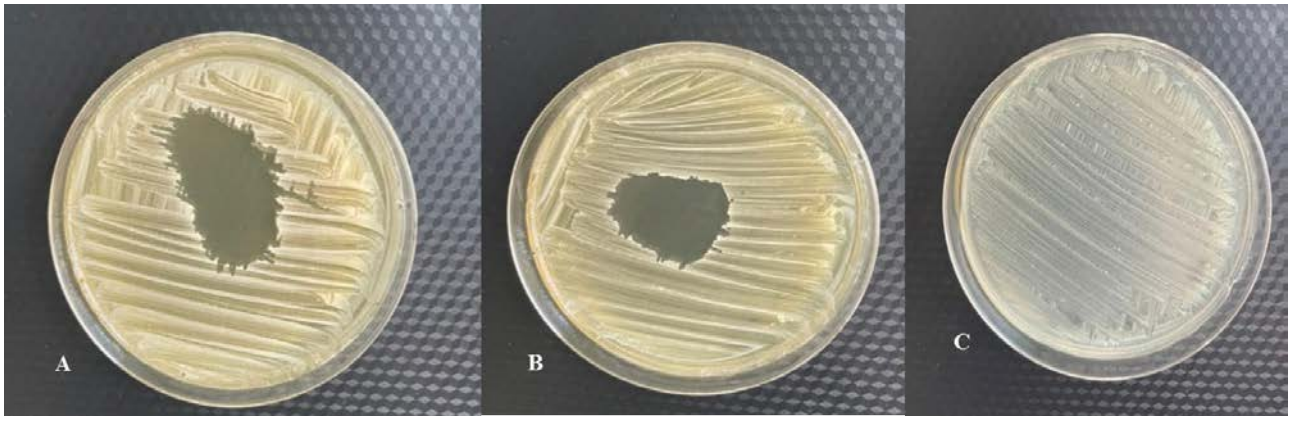

Figure (1). Spot assay for lytic bacteriophage screening is sewage water filtrates. A: The lytic activity of filtrates *on E. coli S1* (clear zone), B: Lytic activity of filtrates on *S. aureus* (clear zone). C: No lytic activity of filtrates on *Acineto-bacter sp* .

OD600nm of filtrate treated *E. coli* was recorded as 0.141 and 0.066 after 24h and 48h incubation period respectively. The reduction in the turbidity compared with the control indicates to presence of bacteriophages, which lyse the bacteria. The high reduction in the turbidity (0.066) compared with turbidity at zero time (0.559), suggests that phage in *E. coli* filtrate has high lytic activity. Whereas turbidity assay of *S. aureus* filtrate indicates to presence of phage with low lytic activity since it revealed a slight reduction in the turbidity between the zero time (0.315) and 48h (0.263) incubation period.

Characterization of phage plaque and determination of phage titer

Plaque assay by using the double agar layer (DAL) method was used to isolate and characterize the suspected phages in positive filtrates in this study. Under optimal conditions; plaque morphology can be a consistent feature of the bacteriophage. Except for T7, most phage plaques acquire a certain size, appearance and edges after a period of incubation. Therefore, it is assumed that a change in plaque morphology during the study may have resulted from a mutation in viral strain (Spanakis & Horne, 1987). Additionally, Shende suggests that variation in the plaque morphology may related to the differences in phage strain, agar strength and addition of cations (Shende et al., 2017).

Generally, more virulent phages have less lysis time and produce larger clear plaques with high plaque productivity (Galle et al., 2011). Depending on the morphology of plaques; four different lytic phage morph-type were observed against *E. coli* (figure2). In this study infection of *E. coli* S1 by these phages exhibited clear, circular plaques with infinitive edges and depending on differences in the size these morph-type recorded as: Large (3.5mm), medium (1.5-2mm), small (=1mm) and very small which referred to as phage EC1, phage EC2, phage EC3 and Phage EC4 respectively.

Electron microscopy of phage EC1 showed that the appearance of PhageEC1 was composed of an isometric polyhedral head approximately 43nm in diameter and a short tail approximately 12nm in length (figure 3). Based on these morphological characteristics and according to the International Committee on Taxonomy of Viruses (ICTV) classification; PhageEC1 was determined as a member of the family Podoviridae and the order Caudovirales (Chen et al., 2017). bacteriophage effective against *E. coli* belonging to the Podoviridae family was reported previously (Vera-Mansilla et al., 2022).

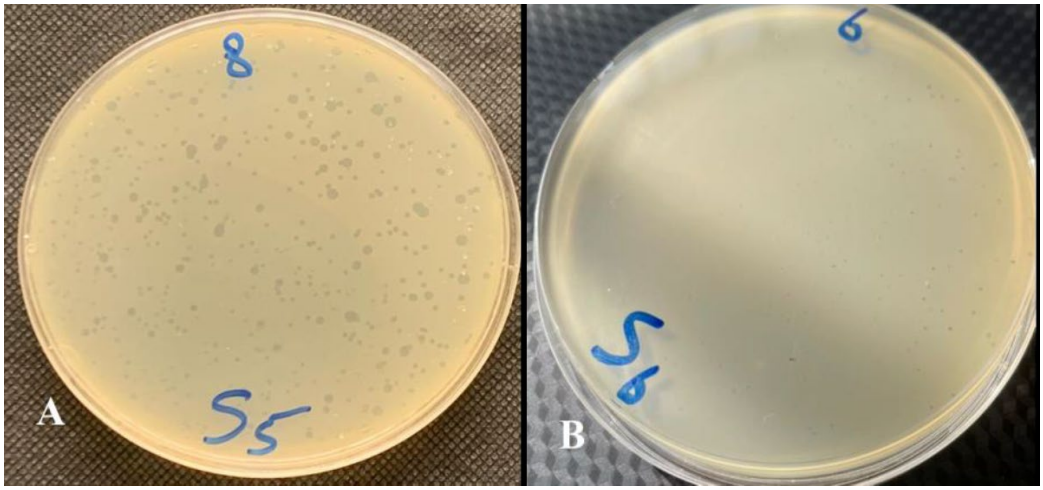

Figure (2). Plaques morphology. A: DLA plate of 10-8 dilution of *E. coli* S1 phages shows different morph-type plaques. B: DLA plate of 10-6 dilution of *S. aureus* S1 phages with one morph-type plaques.

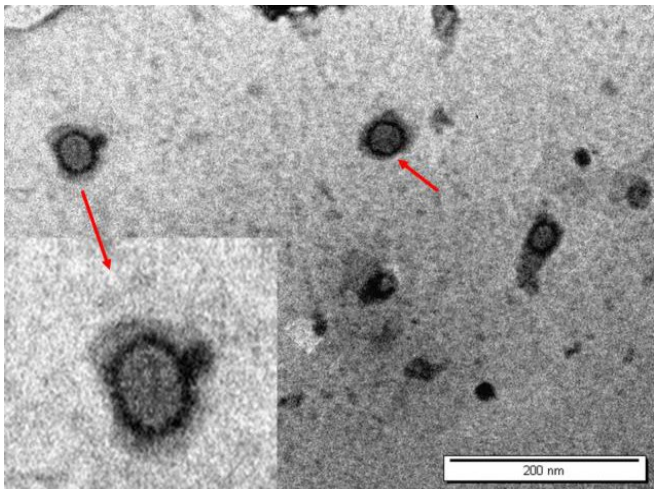

Figure (3). Transmission electron micrograph of phage EC1(marked with red arrows).

For the determination of phage titer, 10^{-8} and 10^{-9} dilution plates having 198 and 58 plaques were selected (falling in the recommended range of 30 - 300). The total *E. coli* plague titer was high in the used sewage water sample ($2.9x10^{11}$ PFU/ml.). the present findings are in accordance with earlier reports of Shende et al., who isolated three different phage morph-types against *E.coli* with mean phage titer ranging between $3x10^{10}$ and $5x10^{12}$ PFU/ml (Shende et al.,2017). Qamar and his colleagues found 5 different lytic coli-phage with (10^{2}-10^{7} PFU/ml) titer in sewage water (Qamar et al., 2019). However, other studied showed low coli-phage plaque assay results (21-86 PFU/ml) (Megha et al., 2017).

Infection of MDR S. aureus isolates by phage produced one morph-type clear tiny plaques on the surface of the double layer agar plate with a mean titer of $7.7x10^{9}$ PFU/ml (Figure 2), the isolated phage against *S. aureus* S1 strain designated as phage SA. The tiny clear plaques were previously reported for *S. aureus* phages (Kaur et al., 2012; Rasool et al., 2016).

Host range of isolated phages

The isolated phages were tested against a variety of multi drug resistance clinical bacterial isolates. Among the nineteen strains, none of the bacteria was found sensitive to phage SA except its prima-

ry hosts. Besides their respective hosts, phage ECs showed lytic activity against two MDR isolates: *Acinetobacter sp*. and *Staph. aureus*.

Likewise present study, various investigations revealed that host specific bacteriophages against human MDR pathogen are prevalent and can be readily isolated from sewage samples (Kaur et al., 2012; Rasool et al., 2016; Shende et al., 2017).

The narrow host range reported during this study conforms to the reports of Carey-Smith et al., Shende et al., Qamar *e*t al., and Othman et al., who had isolated narrow host range phages restricted to respected host only or to maximum of two bacterial species (Carey-Smith et al., 2006; Othman et al., 2015., Qamar et al., 2019; Shende et al., 2017). The Specificity of phages is due to the fact that the virion of the virus interacts with specific receptors on its host's surface and this interaction cannot be achieved if a slight change happens in the structure of the receptor. Therefore, highly specific phages have applications in phage typing methods for the identification of bacteria at the sub species level (Megha et al., 2017). In contrast, broad host range phages are more useful in some applications of bacteriophages, mainly, phage therapy since a broad host range phage would be equivalent to broad-spectrum antibiotics. Noteworthy, narrow host range phages against MDR bacteria are effective for personalized phage therapy (Mattila et al., 2015).

CONCLUSION

Specific bacteriophage against multidrug resistance bacteria could be isolated from sewage water that was positive for 66% of tested MDR bacteria hosts in the present study. High titers of five different morph-type phages were isolated; four against *E. coli* with high lytic activity and one against *S. aureus* isolate. The isolated phages showed a narrow host range mainly specific to the respective host or a maximum three different species. This preliminary study needs to be extended to include more sewage water samples and more different hosts. Additionally, the isolated bacteriophages need to be further purified and characterized to evaluate it is lytic efficacy at the vivo level.

ACKNOWLEDGEMENT

The authors express their gratitude towards the Pathology and Transmission Electron Microscope Unit lab staff at Jordan University/ Amman/ Jordan for providing technical assistance.

ETHICS

There are no ethical issues that may arise after the publication of this manuscript.

Duality of interest: The authors declare that they have no duality of interest associated with this manuscript.

Author contributions: Asma Alilesh and Marwa Al-wash designed the research work and carried out the major experiments. Asma Alilesh performed the scientific discussion and wrote the manuscript. Tasneem M. Alswehly1and Khawla A. Aween assissted in experiments.

Funding: No specific funding was received for this work.

REFERENCES

Al-Anany, A. M., Hooey, P. B., Cook, J. D., Burrows, L. L., Martyniuk, J., Hynes, A. P., & German, G. J. 2023. Phage Therapy in the Management of Urinary Tract Infections: A Compre-

hensive Systematic Review. PHAGE (New Rochelle, N.Y.), 4(3),112–127. https://doi.org/10.1089/phage.2023.0024

Al-Saffar, M. 2019. Isolation and characterization of lytic bacteriophages infecting Acinetobacter Baunannii from sewage water in babylon province, Iraq. *Biochem. Cell. Arch*., 19(1): 1881-1888.

Carey-Smith, G. V., Billington, C., Cornelius, A. J., Hudson, J. A., & Heinemann, J. A. 2006. Isolation and characterization of bacteriophages infecting Salmonella spp. *FEMS microbiology letters*, 258(2),182–186. https://doi.org/10.1111/j.15746968.2006.00217.x

Chen, Y., Sun, E., Song, J., Yang, L., & Wu, B. 2018. Complete Genome Sequence of a Novel T7-Like Bacteriophage from a Pasteurella multocida Capsular Type A Isolate. *Current microbiology*, 75(5),574–579. https://doi.org/10.1007/s00284-017-1419-3

Duarte, J., Máximo, C., Costa, P., Oliveira, V., Gomes, N.C.M., Romalde, J.L., Pereira, C., & Almeida, A. 2024. Potential of an Isolated Bacteriophage to Inactivate *Klebsiella pneumoniae*: Preliminary Studies to Control Urinary Tract Infections. *Antibiotics* .13(2), 195. https://doi.org/10.3390/antibiotics13020195

Esmael, A., Azab, E., Gobouri, A. A., Nasr-Eldin, M. A., Moustafa, M. M. A., Mohamed, S. A., Badr, O. A. M., & Abdelatty, A. M. 2021. Isolation and Characterization of Two Lytic Bacteriophages Infecting a Multi-Drug Resistant Salmonella Typhimurium and Their Efficacy to Combat Salmonellosis in Ready-to-Use Foods. *Microorganisms*, 9(2),423. https://doi.org/10.3390/microorganisms9020423

Gallet, R., Kannoly, S., & Wang, I. N. 2011. Effects of bacteriophage traits on plaque-formation. *BMC Microbiology*, 11,181. https://doi.org/10.1186/1471-2180-11-181.

Kaur, S., Harjai, K., & Chhibber, S. 2012. Methicillin-resistant Staphylococcus aureus phage plaque size enhancement using sublethal concentrations of antibiotics. *Applied and environmental microbiology*, 78(23), 8227–8233. https://doi.org/10.1128/AEM.02371-12

Le, T., Nang, S. C., Zhao, J., Yu, H. H., Li, J., Gill, J. J., Liu, M., & Aslam, S. 2023. Therapeutic Potential of Intravenous Phage as Standalone Therapy for Recurrent Drug-Resistant Urinary Tract Infections. Antimicrobial agents and chemotherapy, 67(4), e0003723. https://doi.org/10.1128/aac.00037-23

Masoud, S., Refat, H., Sayed, N., Abd-El Aal, M., Dosocky, A., Mohammed, Z., Abdel-Wahab, M., Mekawy, D., Ali, A., Atya, B., Welliam, K., Abd El-Baky, R. and Hashem, Z. 2020. Application of bacteriophages isolated from sewage to control urinary O157:H7 Escherichia coli and several bacterial uropathogens. *Novel research in microbiology journal*, 4(5): 1005-1014.

Mattila, S., Ruotsalainen, P., & Jalasvuori, M. 2015. On-Demand Isolation of Bacteriophages Against Drug-Resistant Bacteria for Personalized Phage Therapy. *Frontiers in microbiology*, 6,1271. https://doi.org/10.3389/fmicb.2015.01271.

Megha, P.S., Murugan S. and Harikumar, P.S. 2017. Isolation and Characterization of Lytic Coliphages from Sewage Water. *Journal of pure applied microbiology*, 11(1): 559-565. http://dx.doi.org/10.22207/JPAM.11.1.73

Othman, B. A., Askora, A., & Abo-Senna, A. S. 2015. Isolation and characterization of a Siphoviridae phage infecting Bacillus megaterium from a heavily trafficked holy site in Saudi Arabia. *Folia Microbiologica*, 60(4), 289–295. https://doi.org/10.1007/s12223-015-0375-1.

Qamar, H., Owais, M., Chauhan, D. and Rehman, S.2019. Isolation of bacteriophages from untreated sewage water against multi-drug resistant E. coli - An initiative to fight against drug resistance .*Research square*,10(21203): 1-15

Rasool, M. H., Yousaf, R., Siddique, A. B., Saqalein, M., & Khurshid, M. 2016. Isolation, Characterization, and Antibacterial Activity of Bacteriophages Against Methicillin-Resistant Staphylococcus aureus in Pakistan. *Jundishapur journal of microbiology*, 9(10),e36135. https://doi.org/10.5812/jjm.36135

Ross, A., Ward, S., & Hyman, P. 2016. More Is Better: Selecting for Broad Host Range Bacteriophages. *Frontiers in microbiology*, *7,1352.* https://doi.org/10.3389/fmicb.2016.01352

Sambrook, J., Fritsch, E. R., & Maniatis, T. (1989). Molecular Cloning: A Laboratory Manual (2nd ed.). Cold Spring Harbor, NY: Cold Spring Harbor Laboratory Press.

Shende, R. K., Hirpurkar, S. D., Sannat, C., Rawat, N., & Pandey, V. 2017. Isolation and characterization of bacteriophages with lytic activity against common bacterial pathogens. *Veterinary world*, 10(8), 973–978. https://doi.org/10.14202/vetworld.2017.973-978

Sjahriani, T., Wasito, E. B., & Tyasningsih, W. 2021. Isolation and Identification of Escherichia coli O157:H7 Lytic Bacteriophage from Environment Sewage. *International journal of food science*, 2021,7383121. https://doi.org/10.1155/2021/7383121

Spanakis, E., & Horne, M. T. 1987. Co-adaptation of Escherichia coli and coliphage lambda vir in continuous culture. *Journal of general microbiology*, 133(2), 353–360. https://doi.org/10.1099/00221287-133-2-353

Ullah, A., Qamash, T., Khan, F. A., Sultan, A., Ahmad, S., Abbas, M., Khattak, M. A. K., Begum, N., Din, S. U., Jamil, J., & Kalsoom 2021. Characterization of a Coliphage AS1 isolated from sewage effluent in Pakistan. *Brazilian journal of biology - Revista brasleira de biologia*, 82, e240943. https://doi.org/10.1590/1519-6984.240943

Vera-Mansilla, J., Sánchez, P., Silva-Valenzuela, C. A., & Molina-Quiroz, R. C. 2022. Isolation and Characterization of Novel Lytic Phages Infecting Multidrug-Resistant *Escherichia coli*. *Microbiology spectrum*, 10(1), e0167821. https://doi.org/10.1128/spectrum.01678-21

Yu, Y. P., Gong, T., Jost, G., Liu, W. H., Ye, D. Z., & Luo, Z. H. 2013. Isolation and characterization of five lytic bacteriophages infecting a Vibrio strain closely related to Vibrio Owensii. *FEMS microbiology letters*, 348(2),112–119. https://doi.org/10.1111/1574-6968.12277

Al-Mukhtar Journal of Basic Sciences 22 (1): 37-46, 2024
Doi: https://doi.org/10.54172/whj12t15

Research Article

Open Access

The Effect of Wind Speed and Sea Surface Temperature on Chlorophyll –A Concentration in Sea Water Off the Libyan Coast

Haifa M. Ben Miloud[1] and Maha A. Alssabri[2]

***Corresponding author:** regcm00@yahoo.com Department of Atmospheric Science, Faculty of Science, University of Tripoli, Libya.

Second Author: m.alssabri@uot.edu.ly Department of Botany, Faculty of Science, University of Tripoli, Libya

Received:
05 August 2023

Accepted:
14 April 2024

Publish online:
30 April 2024

Abstract

The effect of winds and sea surface temperature on the concentration of chlorophyll-a, which is the primary source for phytoplankton to produce carbon through photosynthesis, is one of the climatic changes formed in the atmosphere and oceans that are the focus of current global studies. The study found a strong correlation between the concentration of chlorophyll-a and wind speed. The concentration of chlorophyll-a rises with increasing wind speed and reaches 0.85. Conversely, the relationship between sea surface temperatures and chlorophyll-a concentration is inverse, meaning that the higher the sea surface temperatures, the lower the concentration of chlorophyll-a. The inverse relationship approaches -0.798 in seawater. The intensity of chlorophyll-a concentration at sea and its relationship with wind speed and sea surface temperature explain why the percentage of the effect of variable wind speed and sea surface temperature on the concentration of chlorophyll-a is affected by (73.6%, 63.8%) on the concentration of chlorophyll-a, respectively.

Keywords: Libya, Climate change, Sea Surface Temperature, Wind speed, Chlorophyll-a.

INTRODUCTION

The Mediterranean region, which lies between two latitudes 30-40 N0, has mild, wet winters and warm to hot, dry summers (Lionello et al., 2006). The Mediterranean Sea's limited nutrient availability for phytoplankton growth which is enhanced from west to east makes it an oligotrophic marine environment (Kotta & Kitsiou, 2019; Turley et al., 2000). The Eastern Mediterranean Sea exhibits non-blooming traits, such as gradual increases in chlorophyll concentrations from summertime lows to wintertime highs (Kotta & Kitsiou, 2019).

Because phytoplankton form the base of the marine food web and account for half of the planet's primary production, they play a crucial role in Earth's system (Kotta & Kitsiou, 2019). Additionally, climate change has a significant impact on marine environment microorganisms. The composition of microorganisms in the ocean is impacted by temperature rises, and this causes changes in the distribution of these organisms. It also has an impact on chlorophyll concentrations, which are markers of phytoplankton abundance and their critical role in the global carbon cycle, influencing changes in production (Gregg et al., 2003; Hays et al., 2005).
Chlorophyll is impacted by heat, and wind currents, which carry water from the deep ocean to

the surface. Nutrient-rich water rises to the surface through a process known as spring and autumn inversion (Feng et al., 2015; Kahru et al., 2010; Katara et al., 2008), and this is one of the main dynamic factors that can drive nutrients from deep water to the surface, which can create wind-driven upward and enhance vertical mixing. Therefore, it can control the production of phytoplankton during the stratified season (Hopkins et al., 2021). However, the relationship between wind and phytoplankton biomass varies by region and is dependent on factors such as water depth, latitude, and other environmental factors. Consequently, further research is required to properly comprehend how wind affects phytoplankton, particularly in coastal oceans with complex environments (Lin et al., 2023). Rushing to the sea's surface is the process of moving a large body of water from the deep water column to the surface. This rise results in a decrease in sea surface temperatures and an increase in chlorophyll-a concentration, which boosts fishery productivity. The fishing season can be identified by two indicators: temperature and chlorophyll-a (Wirasatriya et al., 2018).

Libya is characterized by a long coastline, so some scholars have a major role in conducting some research on the Libyan coast. Statistical analyses show that the theoretical and experimental distributions of chlorophyll concentration for phytoplankton abundances obtained by the model in chlorophyll concentrations and compared with field data collected in twelve marine sites along the Cape Passero (Sicily)-Misurata (Libya) transect agree well. As a result, satellite remote sensing has emerged as a promising technique for large-scale ocean studies because of the wide spatial coverage offered by portable observation platforms in space (Valenti et al., 2017).

Study objectives

Find the effect of wind speed and sea surface temperature on chlorophyll-a, and know the strength of the correlation between the increase or decrease of chlorophyll in the Libyan coast with these factors.

MATERIALS AND METHOD

Area study and data sources

The search area is situated in Libyan waters across from the Mediterranean Sea, with latitudes of 30.36^0 to 35.54^0 and longitudes of 11.46^0 to 23.75^0 ,figure 1, From January 2003 through April 2023, the study used the Merrra-2 model for wind speed and the Aqua model for chlorophyll-a concentration and sea surface temperature. The data was obtained from Goddard Space Flight Center.

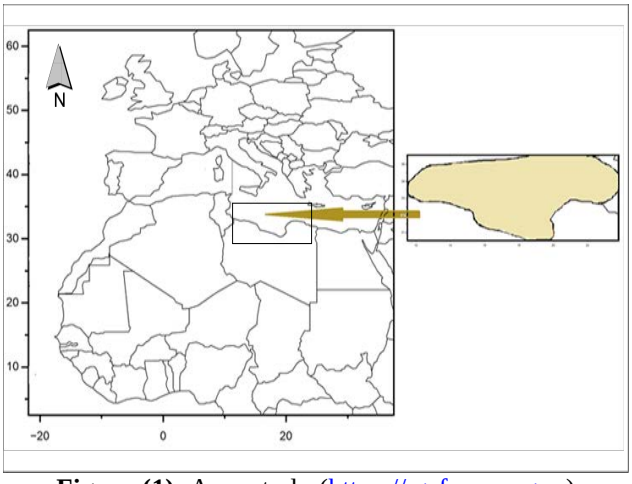

Figure (1): Area study (https:// gsfc.nasa.gov)

Climate data analysis

It is well known that the Mediterranean Sea has relatively low levels of chlorophyll, with levels rising in the west and falling in the east. By examining the concentration of chlorophyll-a, wind speed, and sea temperature from January 2003 to April 2023 and calculating the yearly average as presented in Figure 1, the Libyan shores are highly susceptible to temperature variations, as evidenced by the annual average temperature of the Mediterranean, which rises in the middle opposite the Libyan coast by approximately 22.5 C^0 and falls in the east by approximately 22 C^0 (see Figure 2,c). This is in contrast to the decrease in chlorophyll-a quantities in the middle opposite the Libyan coast by approximately 0.1 mg.m-^{3}, increases as we head west and reaches 0.25 mg.m-^{3}, and decreases to the east by a value of 0.13 mg.m-^{3}a look at Figures (2,a) and (2,b), where the wind speed measured in meters per second (m/s) increases by approximately 6.4–7 m/s, indicating a drop in temperature and an increase in levels of chlorophyll-a, and then drops to 6 m/s, indicating a rise in temperature and a decrease in chlorophyll-a.

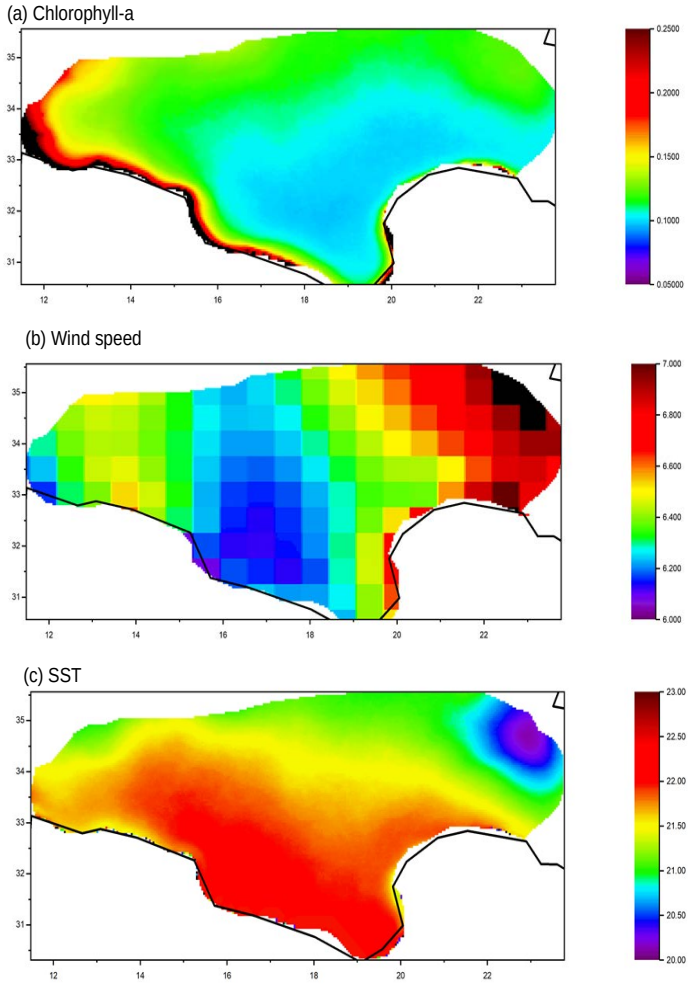

Figure (2): The annually average for (a) sea surface temperature (C^0), (b) wind speed (m.s^{-1}), and (c) chlorophyll-a concentration (mg.m^{-3}) from January 2003 to April 2023.

Statistical analysis of data and discussion

For clarification, statistical techniques were applied in the current study. To ascertain the kind and degree of correlation between the two variables wind speed (m.s^{-1}) and sea surface temperature (C^0) and the variable chlorophyll-a concentration (gm.m^{-3}) in the Mediterranean Sea close

to Libya's coast. Table 1 displays the Pearson correlation coefficient that was used in this study. There is a strong direct relationship of approximately 0.858 between wind speed and chlorophyll-a, and a strong inverse correlation of approximately -0.799 between sea temperature and chlorophyll-a.

Table (1). Statistics

	Chlorophyll-a	
	Wind speed	Sea surface Temperature
Number of Points	244	244
Degrees of Freedom	242	242
Residual Sum of Squares	0.18706	0.25725
Pearson's r	0.85848	-0.79894
R-Square (COD)	0.73699	0.6383

From the above table, we find that the percentage effect of the independent variable wind speed - sea surface temperature on chlorophyll-a, the dependent variable, is equal to 0.737, 0.638, respectively, meaning that wind speed - sea surface temperature affects by (73.6%, 63.8%) on chlorophyll-a, respectively. And the square of the correlation coefficient R is used to find out the percentage change in the dependent variable and by which the variable can be predicted independently, see table 2.

Table (2). Summary

		Intercept		Slope	
		Value	Standard Error	Value	Standard Error
Chlorophyll-a	Wind speed	-0.1097	0.0092	0.03659	0.0014
	Sea surface Temperature	0.3463	0.0109	-0.0103	4.97E-4

Subsequently, the impact of wind speed and sea temperature on chlorophyll-a was examined by taking both factors into account (as an independent variable) on chlorophyll-a (as a dependent variable) and analyzing the data of the two variables during the period (January 2003 - April 2023) using a simple method for linear regression equation:

$y=a + b\,x$

Spread points between the two variables were plotted as follow:

To determine the significance of the model's quality, we used analysis of variance. Because we observed a linear relationship and a level of significance for F that is less than 0.05, which indicates that the independent and dependent variables are related and that the regression model is significant, we were able to reject the null hypothesis and accept the alternative. A significant figure whose outcomes are trustworthy is found in Tables 3, 4.

Table (3). Parameters

			Value	Standard Error	t-Value	Prob>|t|
Chlorophyll-a	Wind speed	Intercept	-0.10977	0.00919	-11.93848	3.86885E-26
		Slope	0.03659	0.0014	26.04061	3.90919E-72
	Sea surface Temperature	Intercept	0.34629	0.0109	31.75995	2.76827E-88
		Slope	-0.01026	4.965E-4	-20.66566	2.32116E-55

Chlorophyll: Slope is significantly different from zero (See ANOVA Table).

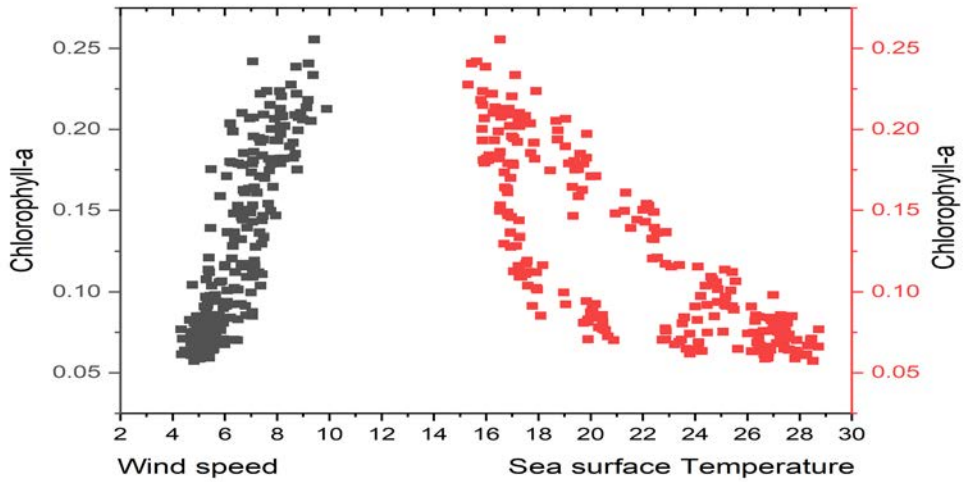

Figure (3). Scatterplot of red scatter sea surface temperature (C^0) - black scatter wind speed ($m.s^{-1}$) with chlorophyll-a ($mg.m^{-3}$).

Based on the ANOVA table 3. To test the significance of the regression we note that the value of F is equal to 678.1-427.06 respectively, with a probability of 0.0001 less than 0.05, which indicates the quality of the regression model and that it is statistically significant, and therefore the existence of a relationship between the two.

Table (4).ANOVA

			DF	Sum of Squares	Mean Square	F Value	Prob>F
Chlorophyll-a	Wind speed	Model	1	0.52417	0.52417	678.1132	<0.0001
		Error	242	0.18706	7.72982E-4		
		Total	243	0.71123			
	Sea surface Temperature	Model	1	0.45398	0.45398	427.06953	<0.0001
		Error	242	0.25725	0.00106		
		Total	243	0.71123			

Chlorophyll: At the 0.05 level, the slope is significantly different from zero.

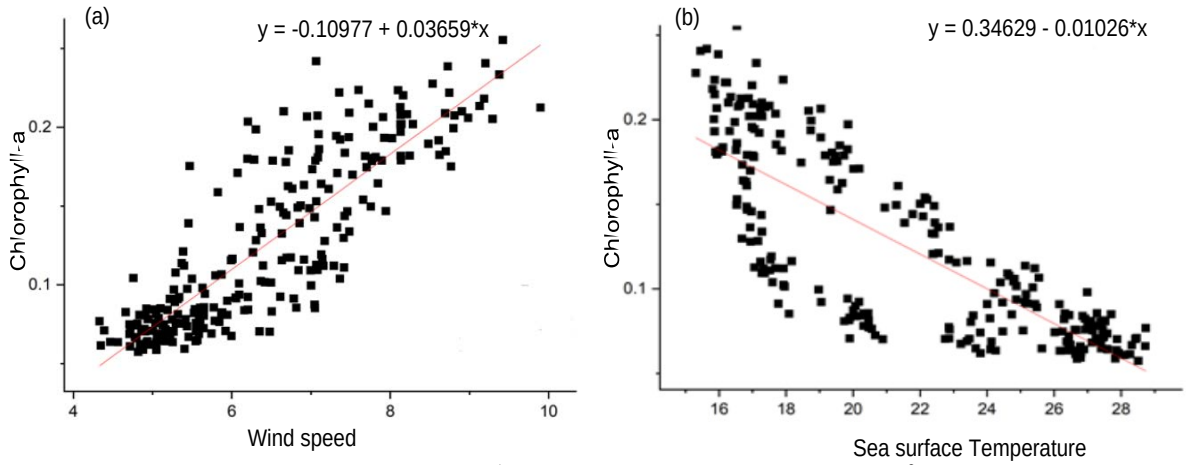

Figure (4). scatterplots for (a) wind speed ($m.s^{-1}$) and (b) sea surface temperature (C^0) , with the concentration of chlorophyll-a ($mg.m^{-3}$)

variables show figure 4. We notice that the points approach the line of the regression equation and that the residual residuals are distributed according to the normal distribution, which is a condition for applying the regression equation, as shown in the figure 5.

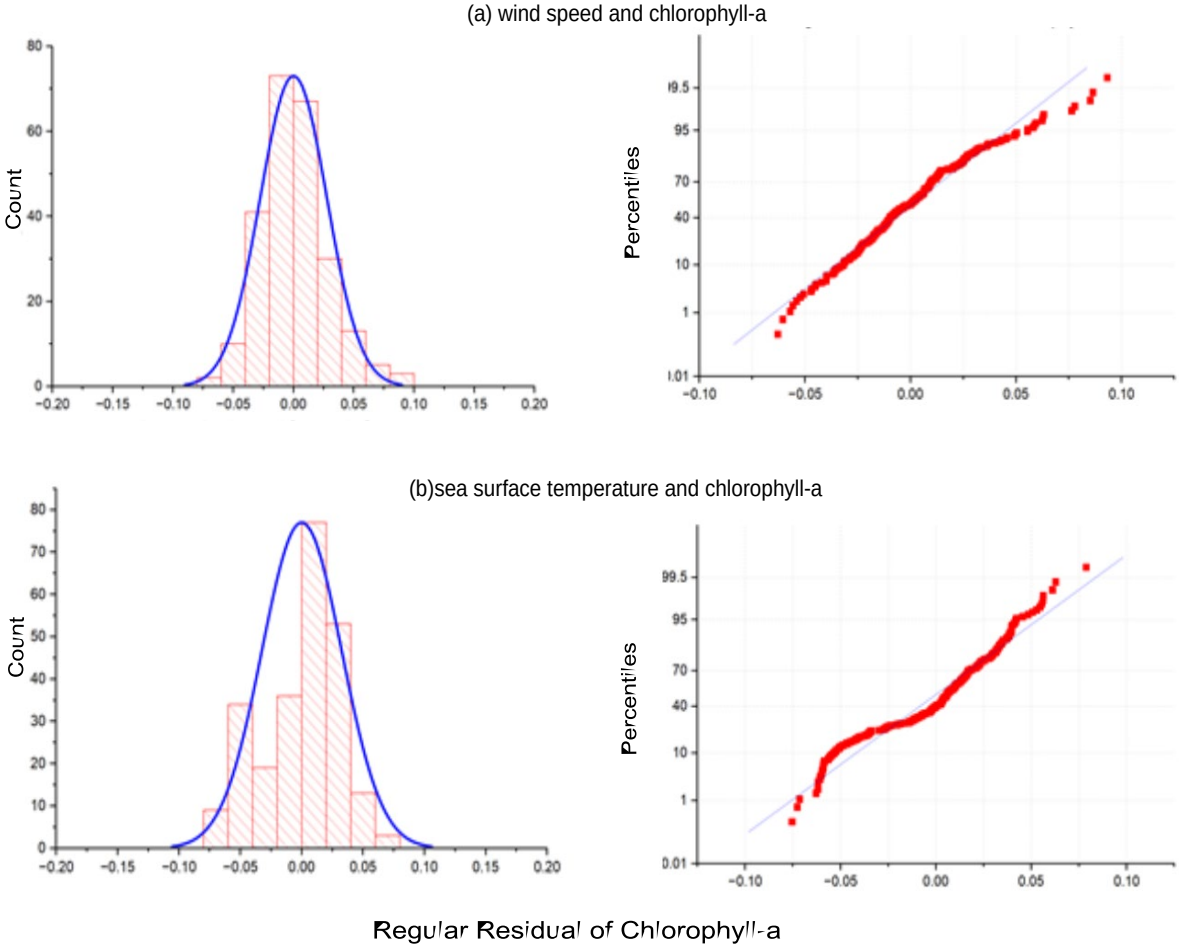

Figure (5). Normal plot of regression residual

As mentioned previously, the amounts of chlorophyll-a concentration in the Mediterranean are low, and this was evident in Figure 6 of the kernel density estimate analysis, which shows the chlorophyll –a concentration density with increasing or decreasing wind speed and temperature. The density of chlorophyll-a increases with increasing winds and reaches 1.08 when wind speed is 8 m/s^{-1} and amounts of chlorophyll-a are about 0.2 gm/m-^{3}, while the distribution of concentration density is large and reaches 1.7 when the chlorophyll-a is 0.1 gm/m^{-3}, where Its density in the sea against wind speed is 5.5 $m/s^{-1}$and the lowest density reaches 0.216, while the amounts of chlorophyll-a are about 0.29 gm/m^{-3} and the wind speed is about $10m/s^{-1}$, as shown in the frequency histogram for each of the winds and the concentration of chlorophyll-a in Figure 6.a. The nucleus density of chlorophyll-a concentration reaches 1.16 in the two cases of chlorophyll-a, reaching 0.2 and 0.05 gm/m^{-3} against temperatures 5.17 and 27.5C^{0}, respectively, explaining the frequency histogram in Fig. 6b for both density concentration chlorophyll –a with increasing or decreasing with sea surface temperature.

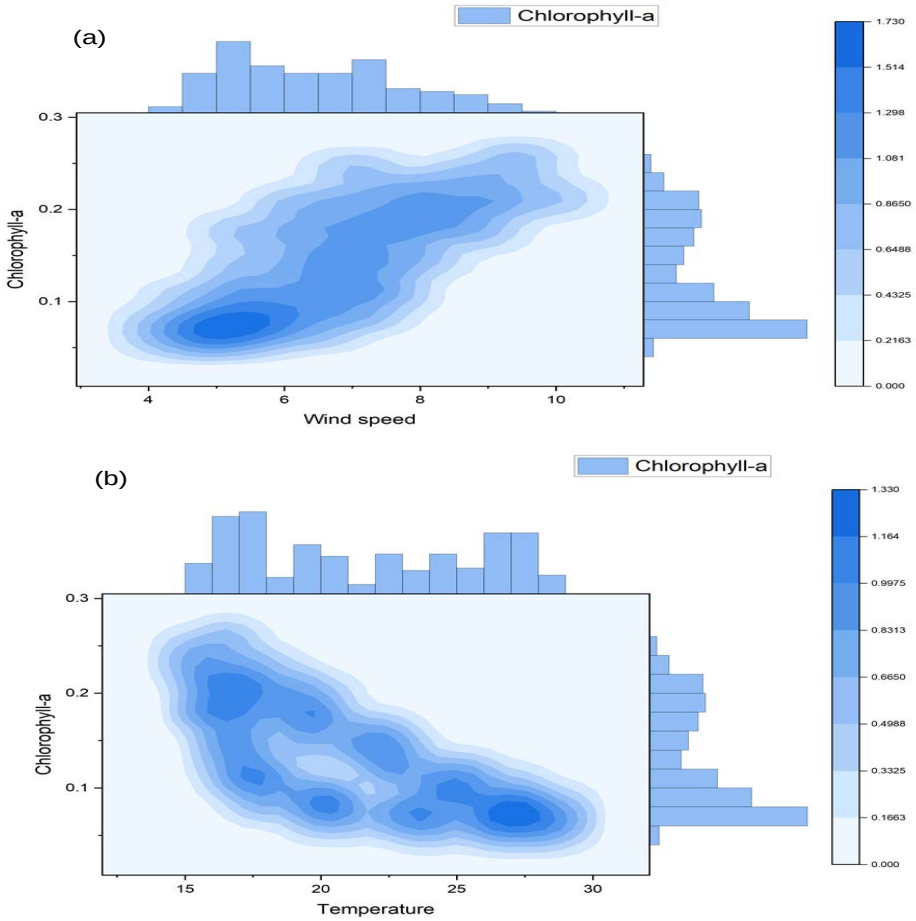

Figure (6). Kernel density estimate of the concentration of chlorophyll-a (gm/m^{-3}) with with (a) wind speed(m/s^{-1}), (b) sea surface temperature(C^0).

CONCLUSION

the world is currently bringing climate change in all land and ocean-related domains to light, and one of these changes is the effect of both sea surface temperature and wind speed on the concentration of chlorophyll-a, which is the main source of phytoplankton.

In this study, the relationship between wind speed and chlorophyll concentration is revealed. A is strong, as the wind speed increases, the concentration of chlorophyll-a increases and reaches 80.85, while the relationship is inverse between sea surface temperatures with the concentration of chlorophyll-a, as the higher the sea surface temperatures, the lower the concentration of chlorophyll-a in seawater and reaches The inverse relationship is about -0.798, and using statistical analysis and the use of Pearson correlation, we find that the percentage effect of wind speed and sea surface temperature on concentration chlorophyll-a, is affected by (73.6%, 63.8%) on the concentration of chlorophyll-a, respectively, and that there is a relationship between climate factors and chlorophyll-a concentration; the relationship between the sea's chlorophyll-a concentration's kernel density and its rise and fall with sea surface temperature and wind speed has been made evident, as the Mediterranean Sea typically has lower chlorophyll-a concentrations than other oceans.

ACKNOWLEDGEMENTS

Thanks to everyone who contributed to this work. We would especially like to express our gratitude to the anonymous reviewers who helped with revisions, and thanks to the website Giovanni of Satellite data used by NASA.

Duality of interest: The authors declare that they have/ have no duality of interest associated with this manuscript.

Author contributions: Example, A.B. developed the theoretical formalism, performed the analytic calculations and performed the numerical simulations. Both A.B and B.C. authors contributed to the final version of the manuscript. B.C. supervised the project.

Funding: A funding statement indicates whether or not the authors received funding (institutional, private and/or corporate financial support) for the work reported in their manuscript.

REFERENCES

Feng, J., Durant, J. M., Stige, L. C., Hessen, D. O., Hjermann, D. Ø., Zhu, L., Llope, M., & Stenseth, N. C. (2015). Contrasting correlation patterns between environmental factors and chlorophyll levels in the global ocean. *Global Biogeochemical Cycles, 29*(12), 2095-2107.

Gregg, W. W., Conkright, M. E., Ginoux, P., O'Reilly, J. E., & Casey, N. W. (2003). Ocean primary production and climate: Global decadal changes. *Geophysical Research Letters*, 30(15).

Hays, G. C., Richardson, A. J., & Robinson, C. (2005). Climate change and marine plankton. *Trends in ecology & evolution*, 20(6), 337-344.

Hopkins, J. E., Palmer, M. R., Poulton, A. J., Hickman, A. E., & Sharples, J. (2021). Control of a phytoplankton bloom by wind‐driven vertical mixing and light availability. *Limnology and Oceanography, 66*(5), 1926-1949.

Kahru, M., Gille, S., Murtugudde, R., Strutton, P., Manzano‐Sarabia, M., Wang, H., & Mitchell, B. (2010). Global correlations between winds and ocean chlorophyll. *Journal of Geophysical Research: Oceans, 115*(C12).

Katara, I., Illian, J., Pierce, G. J., Scott, B., & Wang, J. (2008). Atmospheric forcing on chlorophyll concentration in the Mediterranean. *Essential Fish Habitat Mapping in the Mediterranean*, 33-48.

Kotta, D., & Kitsiou, D. (2019). Chlorophyll in the eastern mediterranean sea: Correlations with environmental factors and trends. *Environments, 6*(8), 98.

Lin, L., Liu, D., Wang, Y., Lv, T., Zhao, Y., & Tan, W. (2023). Effect of wind on summer chlorophyll-a variability in the Yellow Sea. *Frontiers in Marine Science, 9*, 1104258.

Lionello, P., Malanotte-Rizzoli, P., Boscolo, R., Alpert, P., Artale, V., Li, L., Luterbacher, J, May, W, Trigo, R, Tsimplis, M. (2006). The Mediterranean climate: an overview of the main characteristics and issues (Vol. 4, pp. 1-26): Elsevier.

Turley, C., Bianchi, M., Christaki, U., Conan, P., Harris, J., Psarra, S., Ruddy, G., Stutt, E., Tselepides, A., & Van Wambeke, F. (2000). Relationship between primary producers and bacteria in an oligotrophic sea--the Mediterranean and biogeochemical implications. *Marine Ecology Progress Series, 193*, 11-18.

Valenti, D., Denaro, G., Ferreri, R., Genovese, S., Aronica, S., Mazzola, S., Bonanno, A., Basilone, G., & Spagnolo, B. (2017). Spatio-temporal dynamics of a planktonic system and chlorophyll distribution in a 2D spatial domain: matching model and data. *Scientific reports*, *7*(1), 220.

Wirasatriya, A., Maslukah, L., Satriadi, A., & Armanto, R. (2018). Different responses of chlorophyll-a concentration and Sea Surface Temperature (SST) on southeasterly wind blowing in the Sunda Strait. IOP Conference Series: Earth and Environmental Science,

Al-Mukhtar Journal of Basic Sciences 22 (1): 47-54, 2024
Doi: https://doi.org/10.54172/ymhfvs07

Research Article Open Access

Order Continuous Operators

Manal A. Elzidani, Hawa A. Eltaweel and Abdusalam A. Emsimir*

***Corresponding author:** a.msimer@edu.misuratau.edu.ly
Department of Mathematics, Faculty of Education, University of Misurata, Libya

Second Author: Department of Mathematics, Faculty of Education, University of Misurata, Libya

Third Author: Department of Mathematics, Faculty of Education, University of Misurata, Libya

Received:
25 September 2023

Accepted:
28 March 2024

Publish online:
30 April 2024

Abstract

The order continuous operators consider one of important topic in functional analysis and its applications, the affiliations among order continuous operators and the other classes of operators such as σ-order are continuous, order bounded, and singular operators, have been studied and investigated, we proved that if an order bounded operator $\mathcal{F}:\mathcal{U}\to\mathcal{V}$ concerning two Riesz space with $\mathcal{V}$ Dedekind complete is continuous and ordered, then $|\mathcal{F}|$ is order continuous, and this paper shows that if $\mathcal{U}$ is space that is countable, now $\mathcal{F}$ is not σ-order continuous, while $\mathcal{U}$ is uncountable, then $\mathcal{F}$ is necessarily σ-order continuous, by giving an example we showed that null ideal for the operator $\mathcal{F}$ is band when $\mathcal{F}$ is bounded ordered, further, it is ordered and continuous. Finally, we concluded the operator that is a positively and orderly continuous map on ordered dense with memorizing Riesz subspace of a Riesz space with its range is Dedekind complete, it has only unique ordered continuous expansion all of space.

Keywords: Riesz Spaces, Positive Operator, Order Continuous Operator, Order Bounded Operator.

INTRODUCTION

In linear algebra and functional analysis, the operator $\mathcal{F}:\mathcal{U}\to\mathcal{V}$ where $\mathcal{U}$ and $\mathcal{V}$ are Riesz spaces is defined as an order continuous operator whenever $u_\alpha \overset{0}{\to} 0$ in $\mathcal{U}$ gives $\mathcal{F}(u_\alpha)\overset{0}{\to}0$ inside$\mathcal{V}$; and σ-order continuous whenever $u_n \overset{0}{\to} 0$ in $\mathcal{U}$ implies $\mathcal{F}(u_n)\overset{0}{\to}0$ in $\mathcal{V}$. Many researchers studied this topic, and some of these previous studies have proven the theory of extending the positive order continuous operators(Veksler, 1960). Another study defined new classes of operators, which are so-called unbounded order continuous and further boundedly unbounded order continuous operators and gave extra settings under which uo-continuity is equivalent to order continuity of some operators on Riesz spaces (Bahramnezhad & Azar, 2018). The report investigated the relationships located between order to topology continuous operators and different types of operators for example b-weakly compact, order weakly compact and order continuous operators, and studied adjoint of order to norm continuous operators (Jalili et al., 2021). While recent study extends the properties of unbounded order continuous operators from $\mathcal{U}$ Riesz space into $\Re$ (Turan et al., 2022). Aydin and Gorokhova studied the concept of statistically continuous and bounded operators with statistically ordered convergent sequences on Riesz spaces (Aydin & Statistics, 2023). In this paper, some basic results from the theory of order continuous operators were studied with proofs as needed. First, this work introduces some of its types: σ-order continuous operators, order bounded operators, singular operators, and order continuous components of the positive operator, in addition, it shows some of

their properties as well as the relations between them, then it studied of describing the group of all continuously ordered operators and some their useful characterizations and some of its application.

Concepts and Theories:

Definition 1 from previous study (Abramovich & Aliprantis, 2002):
$\mathcal{F}: \mathcal{U} \to \mathcal{V}$ is called positive if $\mathcal{F}(u) \geq 0 \; \forall \, u \in \mathcal{U} \, ; u \geq 0$.
The beginning point within the theory of positive administrators may be a principal expansion theorem of Kantorovic (Kantorovitch, 1940), who proved that additive operator $\mathcal{F}: \mathcal{U}^+ \to \mathcal{V}^+$to be the constraint of a single positive operator from $\mathcal{U}$ into $\mathcal{V}$. The details follow.

Theorem 1 by Kantorovic (Kantorovitch, 1940)
If $\mathcal{F}: \mathcal{U}^+ \to \mathcal{V}^+$ is an additive operator, then $\mathcal{F}$ has a uniquely positive extension to the entire space $\mathcal{U}$, the unique extension (denoted by $\mathcal{F}$ again) is given by

$$\mathcal{F}(u) = \mathcal{F}(u^+) - \mathcal{F}(u^-) \quad \forall \; u \in X \; .$$

Definition 2 from previous study (Kreyszig, 1978):
The *disjoint complement* V^d is defined as follows:
$V^d = \{ u \in \mathcal{U} : u \perp v \; \forall \, v \in V \}$ Where V^{dd} means $(V^d)^d$.

Definition 3 from previous study (Aliprantis & Burkinshaw, 1985)*:*
If $\mathcal{U}$ Riesz space and $U \subset \mathcal{U}$, then U is named *solid* if $\forall \, u \in U, v \in \mathcal{U}$ and $|u| \leq |v|$ gives $v \in U$.
If *U* is solid sub space from $\mathcal{U}$, then *U* is named Ideal of space $\mathcal{U}$.

Definition 4 John (John, 1990)*:*
The ordered closed ideal is mentioned to be a *band.*

Definition 5 Aliprntis (Aliprantis & Burkinshaw, 1985):
If $\mathcal{B}$ is a band in Riesz space $\mathcal{U}$ and the following condition $\mathcal{U} = \mathcal{B} \oplus \mathcal{B}^d$ is met, then $\mathcal{B}$ is called a *projection band.*
The band does not have to be a projection band; we need to mention the following theorem which was proven by Riesz (Riesz, 2000).

Theorem 2 Aliprntis (Aliprantis & Burkinshaw, 1985):
If $\mathcal{B}$ is a vector which is a band in a Dedekind of complete Riesz space $\mathcal{U}$, formerly $\mathcal{U} = \mathcal{B} \oplus \mathcal{B}^d$ satisfied.

Definition 6 Ogasawara (Ogasawara, 1942). A net $\{ u_\alpha \}$ in a Riesz space is called the order convergent to u whenever there exists a net $\{ v_\alpha \}$ with the same indexed set satisfying $|u_\alpha - u| \leq v_\alpha \downarrow 0$ it is referred to as: $u_\alpha \overset{0}{\to} u$

Definition 7 Ogasawara (Ogasawara, 1942)*:* The operator $\mathcal{F}: \mathcal{U} \longrightarrow \mathcal{V}$ where $\mathcal{U}$ and $\mathcal{V}$ are two Riesz spaces is named to be
(a) Ordered continuous, if $u_\alpha \overset{0}{\to} 0$ inside $\mathcal{U}$ then $\mathcal{F}(u_\alpha) \overset{0}{\to} 0$ in $\mathcal{V}$.
(b) δ- ordered continuous, if $u_n \overset{0}{\to} 0$ inside $\mathcal{U}$ then $\mathcal{F}(u_{n)} \overset{0}{\to} 0$ in $\mathcal{V}$.
It is valuable to remember that a positive operator $\mathcal{F}: \mathcal{U} \to \mathcal{V}$ is ordered continuous $\Leftrightarrow$ $u_\alpha \downarrow 0$ in $\mathcal{U}$ gives $\mathcal{F}(u_\alpha) \downarrow 0$ in $\mathcal{V}$ (moreover $\Leftrightarrow$ $0 \leq u_\alpha \uparrow u$ in $\mathcal{U}$ gives $\mathcal{F}(u_\alpha) \uparrow \mathcal{F}(\mathrm{u})$ in $\mathcal{V}$).
the next example proves that δ- order continuous does not have to be an ordered continuous operator.

Example 1 Let $\mathcal{U}$ the vector space of all real functions that are Lebesgue integrable on the period $0 \leq u \leq 1$. It is clear that any two functions that are not equal at one point are considered two unequal functions, meaning of that $\mathcal{P} \geq \mathcal{Q}$ for all $0 \leq u \leq 1$, this is called the law of pointwise ordering of functions, $\mathcal{U}$ describes a Riesz space (for more details a function space). Further, see that $\mathcal{P}_\alpha \uparrow \mathcal{P}$ applied in $\mathcal{U} \Leftrightarrow \mathcal{P}_\alpha(u) \uparrow \mathcal{P}(u)$ satisfied of all $0 \leq u \leq 1$ in $\Re$.
If the operator $\mathcal{F}: \mathcal{U} \to \mathcal{R}$ is defined as follows

$$\mathcal{F}(\mathcal{P}) = \int_0^1 \mathcal{P}(u)du$$

It is clear that $\mathcal{F}$ is not an order continuous operator that is also positive, hence from the Lebesgue Dominated Convergence theory it is clear that $\mathcal{F}$ is δ- order continuous.
The following theorem shows that order continuous operators that are order bounded have a sum of useful characterizations.

Theorem 3 If $\mathcal{U}, \mathcal{V}$ are Riesz spaces where *Y* is Dedekind complete, and $\mathcal{F}: \mathcal{U} \longrightarrow \mathcal{V}$ is bounded ordered operator, then following arguments are equivalent:

a) The operator $\mathcal{F}$ is continuous.
b) If $u_\alpha \downarrow 0$ gives in $\mathcal{U}$, then $\mathcal{F}(u_\alpha) \overset{0}{\to} 0$ in $\mathcal{V}$.
c) If $u_\alpha \downarrow 0$ gives in $\mathcal{U}$, then $\inf\{|\mathcal{F}(u_\alpha)|\} = 0$ in $\mathcal{V}$.
d) $\mathcal{F}^+$ and $\mathcal{F}^-$ are together order continuous.
e) $|\mathcal{F}|$ is ordered continuous.

Proof: a) → b) and b) → c) are clear.
c) → d) to prove this paragraph, it is sufficient to prove that $\mathcal{F}^+$ is order continuous, suppose $u_\alpha \downarrow 0$ in $\mathcal{U}$, and $\mathcal{F}^+(u_\alpha) \downarrow s \geq 0$ in $\mathcal{V}$. It is need to prove that $s = 0$, Make some β fixed and let $u = u_\beta$.
Now $\forall\, v \in [o, u]$ and $\forall\, \alpha \geq \beta$ is:

$$0 \leq v - v \wedge u_\alpha = v \wedge u - v \wedge u_\alpha \leq u - u_\alpha$$

This means that:

$$\mathcal{F}(v) - \mathcal{F}(v - u_\alpha) = \mathcal{F}(v - v \wedge u_\alpha) \leq \mathcal{F}^+(u - u_\alpha) = \mathcal{F}^+(u) - \mathcal{F}^+(u_\alpha) \text{Therefore}$$

$$0 \leq s \leq \mathcal{F}^+(u_\alpha) \leq \mathcal{F}^+(u) + |\mathcal{F}(v \wedge u_\alpha)| - \mathcal{F}(v) \quad \ldots\ldots\ldots (\star)$$

applies $\forall\, \alpha \geq \beta$ and $\forall\, 0 \leq v \leq u$, since $\forall\, 0 \leq v \leq u$ gives $v \wedge u_\alpha \downarrow_{\alpha \geq \beta} 0$ this means that it fulfills the hypothesis $inf_{\alpha \geq \beta}\{|\mathcal{F}(v \wedge u_\alpha)|\} = 0$, referring to the inequality $(\star)$ note that $0 \leq s \leq \mathcal{F}^+(u) - \mathcal{F}(v)$ satisfies $\forall\, 0 \leq v \leq u$, from $\mathcal{F}^+(u) = \sup\{\mathcal{F}(v): 0 \leq v \leq u\}$, recent inequality leads to that $s = 0$,this is what is required,
d) → e) since $|\mathcal{F}| = \mathcal{F}^+ + \mathcal{F}^-$, this means that $|\mathcal{F}|$ is order continuous,
e) → a) this can be easily proven by applying the inequality $|\mathcal{F}(u)| \leq |\mathcal{F}|(|u|)$.
theorem 3 is true for σ-order continuous operators, and this can be proven in the same way as before.
The combination of all ordered continuous operators of $\ell_b(\mathcal{U}, \mathcal{V})$ is represented by the symbol $\ell_n(\mathcal{U}, \mathcal{V})$.
The symbol $\ell_n(\mathcal{U}, v)$ indicates that the order continuous operators are in addition normal operators, in another meaning:

$$\ell_n(\mathcal{U}, \mathcal{V}) = \{\mathcal{F} \in \ell_b(\mathcal{U}, \mathcal{V}); \mathcal{F}\ is\ order\ continuous\}.$$

The symbol $\ell_c(\mathcal{U}, \mathcal{V})$ symbolizes the collection of all ordered bounded operators from $\mathcal{U}$ into $\mathcal{V}$ which are σ-ordered continuous, in another meaning:

Obviously, $\ell_n(\mathcal{U}, \mathcal{V})$, $\ell_c(\mathcal{U}, v)$ $\ell_C(\mathcal{U}, \mathcal{V}) = \{\mathcal{F} \in \ell_b(\mathcal{U}, \mathcal{V}); \mathcal{F}\ is\ \sigma\text{–}\ order\ continuous\}$ are both two vectors subspaces of $\ell_b(\mathcal{U}, \mathcal{V})$ furthermore $\ell_n(\mathcal{U}, \mathcal{V}) \subseteq \ell_c(\mathcal{U}, \mathcal{V})$ satisfied. Once $\mathcal{V}$ is Dedekind complete. T. Ogasawara [14] proved that together $\ell_n(\mathcal{U}, \mathcal{V})$, $\ell_c(\mathcal{U}, \mathcal{V})$ are seen as bands of $\ell_b(\mathcal{U}, \mathcal{V})$, The next theorems and details follow.

Theorem 4 Ogasawara (Ogasawara, 1942)*:* If $\mathcal{U},\mathcal{V}$ are two Riesz spaces where $\mathcal{V}$ is Dedekind complete, this means that $\ell_n(\mathcal{U},\mathcal{V})$, $\ell_c(\mathcal{U},\mathcal{V})$ are together bands of $\ell_b(\mathcal{U},\mathcal{V})$.

Proof: It shall create that $\ell_n(\mathcal{U},\mathcal{V})$ is a band of $\ell_b(\mathcal{U},\mathcal{V})$. That $\ell_c(\mathcal{U},\mathcal{V})$ is a band can be demonstrated in a comparable way.

See firstly that if $|E|\le|\mathcal{F}|$ satiefies in $\ell_b(\mathcal{U},\mathcal{V})$ with $\mathcal{F}\in\ell_n(\mathcal{U},\mathcal{V})$, therefore from Theorem 3 gives that $E\in\ell_n(\mathcal{U},\mathcal{V})$, which is, $\ell_n(\mathcal{U},\mathcal{V})$ is an ideal of $\ell_b(\mathcal{U},\mathcal{V})$.

To prove that $\ell_n(\mathcal{U},\mathcal{V})$ is a band, let $0\le\mathcal{F}_\lambda(u)\uparrow\mathcal{F}(u)$ inside $\ell_b(\mathcal{U},\mathcal{V})$ with $\{\mathcal{F}_\lambda\}\subseteq\ell_n(\mathcal{U},\mathcal{V})$, and assume that $0\le u_\alpha\uparrow u$ in $\mathcal{U}$ At that time for λ fixed. We have

$$0\le\mathcal{F}(u-u_\alpha)\le\big(\mathcal{F}(u)-\mathcal{F}_\lambda(u)\big)+\mathcal{F}_\lambda(u-u_\alpha)$$

Since $u-u_\alpha\downarrow 0$ means that

$$0\le\inf\{\mathcal{F}(u-u_\alpha)\}\le(\mathcal{F}(u)-\mathcal{F}_\lambda(u))\ \forall\lambda.$$

This shows that $\mathcal{F}-\mathcal{F}_\alpha\downarrow 0\implies\inf(\mathcal{F}(u-u_\alpha))=0$ and then $\mathcal{F}(u_\alpha)\uparrow\mathcal{F}(u)$, In conclusion $\mathcal{F}\in\ell_n(\mathcal{U},\mathcal{V})$.

The symbol $\ell_s(\mathcal{U},\mathcal{V})$ denotes the ensemble of all order bounded operators from Riesz space $\mathcal{U}$into Riesz space $\mathcal{V}$, where $\mathcal{V}$ is Dedekind complete, which are disjoint from $\ell_c(\mathcal{U},\mathcal{V})$, in another meaning $\ell_s(\mathcal{U},\mathcal{V})=\ell_c^d(\mathcal{U},\mathcal{V})$

and its nonzero elements will be mentioned to as *singular operators.* Because $\ell_b(\mathcal{U},\mathcal{V})$ is a Dedekind complete Riesz space, this is given as a following from Theorem 2 that $\ell_c(\mathcal{U},\mathcal{V})$ is a projection band, this proves that $\ell_b(\mathcal{U},\mathcal{V})=\ell_c(\mathcal{U},\mathcal{V})\oplus\ell_s(\mathcal{U},\mathcal{V})$.

Especially, if $\mathcal{F}$ is order bounded operator from Riesz space $\mathcal{U}$ into Riesz space $\mathcal{V}$, then $\mathcal{F}$ has a unique decomposition $\mathcal{F}=\mathcal{F}_c+\mathcal{F}_s;\ \mathcal{F}_c\in\ell_c(\mathcal{U},\mathcal{V})$, $\mathcal{F}_s\in\ell_s(\mathcal{U},\mathcal{V})$. The operator $\mathcal{F}_s$ is known as singular component, and $\mathcal{F}_c$ is known as the σ-order continuous component of $\mathcal{F}$.

It may happen that $\ell_c(\mathcal{U},\mathcal{V})=\{0\}$.

Another basic imbalance is valuable in numerous considers and was presented by T. Ando, which is later called as *Ando s inequality.*

If $\mathcal{U}$ a Riesz space, $u,v\in\mathcal{U}$, and γ is a real number, then from identity $u-v=(1-\gamma)u+(\gamma u-v)$ we find that

$$u-v\le(1-\gamma)u+(\gamma u-v)^+$$

The σ-order continuous the following basic imbalance is valuable in numerous thinks about and was presented by

Theorem 5 supposes that $\mathcal{U}\ and\ \mathcal{V}$ are two Riesz spaces where $\mathcal{V}$ is Dedekind complete, and $\mathcal{F}:\mathcal{U}\longrightarrow\mathcal{V}$ is a positive operator, the following sentences are true $\forall\,u\in\mathcal{U}\,;u\ge 0$

1. $\mathcal{F}_c(u)=\inf\{\sup\mathcal{F}(u_n):0\le u_n\uparrow u\}$, and
2. $\mathcal{F}_n(u)=\inf\{\sup\mathcal{F}(u_\alpha):0\le u_\alpha\uparrow u\}$.

Proof*:* Frist, let's demonstrate the formula for $\mathcal{F}_n$

For each positive operator $L:\mathcal{U}\longrightarrow\mathcal{V}$ define $L^\circ:\mathcal{U}^+\longrightarrow\mathcal{V}^+$ by

$$L^\circ(u)=\inf\{\sup L(u_\alpha):0\le u_\alpha\uparrow u\}\ \forall u\in\mathcal{U}^+.$$

Obviously, $0\le L^\circ(u)\le L(u)\ \forall u\in\mathcal{U}^+$, and $L^\circ(u)=L(u)$ whenever $L\in\ell_n(\mathcal{U},\mathcal{V})$.

Furthermore, it is easy to see that L° is improver on $\mathcal{U}^+$, and then (use Theorem 1), covers to a positive operator from $\mathcal{U}$ into $\mathcal{V}$. On the other hand, it is easy to see that $L\longrightarrow L^\circ$ from $\ell_b^+(\mathcal{U},\mathcal{V})$ into $\ell_b^+(\mathcal{U},\mathcal{V})$, is likewise additive, $(L_1+L_2)^\circ=L_1^\circ+L_2^\circ$ satisfies, thus $L\longrightarrow L^\circ$ defines a positive Operator Form $\ell_b(\mathcal{U},\mathcal{V})$ into $\ell_b(\mathcal{U},\mathcal{V})$. From the inequality $0\le L^\circ\le L$ can be seen that $L\longrightarrow L^\circ$ is ordered continuous, $L_\alpha\downarrow 0$implies $L_\alpha^\circ\downarrow 0$.

Now let $\mathcal{F}:\mathcal{U}\longrightarrow\mathcal{V}$ be positive operator that is fixed. It is sufficient to demonstrat that $\mathcal{F}^\circ$ is ordered continuous. When this is proven, then $\mathcal{F}^\circ\le\mathcal{F}$ implies $\mathcal{F}^\circ=(\mathcal{F}^\circ)_n\le\mathcal{F}_n$, and since $\mathcal{F}_n\le\mathcal{F}^\circ$ holds trivially, we see that $\mathcal{F}^\circ=\mathcal{F}_n$. Finally, let $0\le v_\lambda\uparrow v$ in $\mathcal{V}$ it should be shown that $\mathcal{F}^\circ(v-v_\lambda)\downarrow 0$ in $\mathcal{V}$.

Fix the interval $\varepsilon\in(0,1)$, and suppose $\mathcal{F}_\lambda$ denote the operator defined by:

$$\mathcal{F}_A(u)=\sup\{\mathcal{F}(v):0\le v\le u\,,v\in A,u\in\mathcal{U}\}\ A\text{ ideal of }\mathcal{U}$$

that decides with $\mathcal{F}$ on the ideal created by $(\varepsilon v - v_\lambda)^+$, disappears on $(\varepsilon v - v_\lambda)^-$. Evidently, $\mathcal{F} \geq \mathcal{F}_\lambda \downarrow \geq 0$ and $\mathcal{F}_\lambda(v_\lambda - \varepsilon v)^+ = 0$ satisfied $\forall\, \lambda$.
Let $\mathcal{F}_\lambda \downarrow E$ in $\ell_b(\mathcal{U}, \mathcal{V})$. Since $R(v_\lambda - \varepsilon v)^+ = 0 \;\; \forall\, \lambda$ and $0 \leq (v_\lambda - \varepsilon v)^+ \uparrow (1-\varepsilon)v$, this means $E^\circ(v) = 0$.
From the Ando inequality

$$0 \leq (v - v_\lambda) \leq (1-\varepsilon)v + (\varepsilon v - v_\lambda)^+ \text{ , it follows that}$$

$$0 \leq \mathcal{F}^\circ(v - v_\lambda) \leq (1-\varepsilon)\mathcal{F}^\circ(v) + \mathcal{F}^\circ(\varepsilon v - v_\lambda)^+ \quad \ldots\ldots\ldots (1)$$

Now due to the reason $0 \leq u \leq (\varepsilon v - v_\lambda)^+$ gives $\mathcal{F}_\lambda(u) = \mathcal{F}(u)$, the following gives:

$$\mathcal{F}^\circ((\varepsilon v - v_\lambda)^+) = inf\,\{sup\,\mathcal{F}(u_\alpha): 0 \leq u_\alpha \uparrow (\varepsilon v - v_\lambda)^+\}$$
$$= inf\,\{sup\,\mathcal{F}_\lambda(u_\alpha): 0 \leq u_\alpha \uparrow (\varepsilon v - v_\lambda)^+\}$$
$$= \mathcal{F}_\lambda^\circ(\varepsilon v - v_\lambda)^+ \leq \mathcal{F}_\lambda^\circ(v)$$

By substituting into the equation (1) the following is obtained:

$$0 \leq \mathcal{F}^\circ(v - v_\lambda) \leq (1-\varepsilon)\mathcal{F}^\circ(v) + \mathcal{F}_\lambda^\circ(v) \quad \ldots\ldots\ldots (2)$$

Since $L \longrightarrow L^\circ$ is order continuous and $\mathcal{F}_\lambda \downarrow E$, this means that $\mathcal{F}_\lambda^\circ \downarrow E^\circ$, in other words, $\mathcal{F}_\lambda^\circ(v) \downarrow E^\circ(v) = 0$ applying inequality (2) we get

$$0 \leq \inf\{\mathcal{F}^\circ(v - v_\lambda)\} \leq (1-\varepsilon)\,\mathcal{F}^\circ(v)$$

satisfied for all $0 < \varepsilon < 1$, therefore $\mathcal{F}^\circ(v - v_\lambda) \downarrow 0$, as desired.
Let us assume that the order bounded operator $\mathcal{F}: \mathcal{U} \longrightarrow \mathcal{V}$ is between the two Riesz spaces $\mathcal{U}, \mathcal{V}$ where $\mathcal{V}$ is Dedekind completed. Then define the *null ideal* by $N_\mathcal{F}$ of $\mathcal{F}$ as follows:

$$N_\mathcal{F} = \{u \in \mathcal{U}: |\mathcal{F}|(|u|) = 0\}$$

It can be seen that $N_\mathcal{F}$ is ideal of $\mathcal{U}$.
The *carrier* of $\mathcal{F}$ is defined as the disjoint complement of $N_\mathcal{F}$, which is denoted by the symbol $C_\mathcal{F}$, meaning that:

$$C_\mathcal{F} = N_\mathcal{F}^d\{u \in \mathcal{U}: u \perp N_\mathcal{F}\}$$

obviously, $|\mathcal{F}|$ is positive on $C_\mathcal{F}$, $0 < u < C_\mathcal{F} \;\Leftrightarrow\; 0 < |\mathcal{F}|(u)$.
The following example shows that if the operator is order bounded and is order continuous, then its null ideal is a band, but the opposite is not true.

Example 2 assume that $\mathcal{U}$ is an infinite set, and that $\mathcal{U}_\infty = \mathcal{U} \cup \{\infty\}$ is the One-point compactification of $\mathcal{U}$ considered with the Discrete Topology, Therefore, a function $g: \mathcal{U} \longrightarrow \mathcal{R}$ belongs to $C(\mathcal{U}_\infty)$ $\Leftrightarrow$ there is at least one constant a (depending on g) so that $\forall\; \varepsilon > 0$, there is $|g(h) - a| < \varepsilon \;\; \forall$ values of u except a limited number of u, this mean that $g(\infty) = a$.
Now let's make a fixed countable subset $\{u_1, u_2, \ldots\}$ of $\mathcal{U}$, and then define the operator $\mathcal{F}: C(\mathcal{U}_\infty) \longrightarrow \mathcal{R}$ by

$$\mathcal{F}(g) = g(\infty) + \sum_1^\infty 2^{-n} g(u_n)$$

It is clear that $\mathcal{F}$ is a positive operator, also

$$N_\mathcal{F} = \{g \in C(\mathcal{U}_\infty): g(u_n) = 0\,, \forall\, n = 1,2, \ldots\}$$

because $g_\alpha \uparrow g$ satisfies in $C(\mathcal{U}_\infty)$ $\Leftrightarrow$ $g_\alpha(u) \uparrow g(u)$ satisfies in $\mathcal{R}$ $\;\forall\, u \in \mathcal{U}$, it gives that $N_\mathcal{F}$ is a band of $C(\mathcal{U}_\infty)$, however, we assertion that $\mathcal{F}$ is not order continuous.
To make sure in this, suppose the net $\{u_\alpha\} \subset C(\mathcal{U}_\infty)$ with α goes over the collection of all finite subsets of $\mathcal{U}$ Therefore, $0 \leq u_\alpha \uparrow \mathbf{1}$ satisfies in $C(\mathcal{U}_\infty)$ Although $\mathcal{F}(u_\alpha)$ not implies $\mathcal{F}(\mathbf{1})$.
Moreover, it is motivating to see that if $\mathcal{U}$ countable, thus $\mathcal{F}$ is not σ-order continuous, whereas if $\mathcal{U}$ is uncountable, then $\mathcal{F}$ must be σ-order continuous.
ideal A is said to be σ-*ideal* if the following is true $\{u_n\} \subseteq A\,, 0 \leq u_n \uparrow u \;\Rightarrow u \in A$.

Theorem 6: If $\mathcal{F}: \mathcal{U} \longrightarrow \mathcal{V}$ is order bounded operator between two Riesz spaces with $\mathcal{V}$ Dedekind complete, and $A_\mathcal{F}$ is the ideal generated by $\mathcal{F}$ in $\ell_b(\mathcal{U}, \mathcal{V})$, then $\mathcal{F}$ achieves the following:

1. the null ideal N_L is a band for any $L \in A_\mathcal{F}$ $\Leftrightarrow$ $\mathcal{F}$ is order continuous.
2. the null ideal N_L is a σ-ideal for any operator $L \in A_\mathcal{F}$ $\Leftrightarrow$ $\mathcal{F}$ is σ-order continuous.

Proof: To begin it's important only to prove (1) because the proof of (2) is similar. The "only if" part follows directly from Theorem 3 for the "if" part (in view of Theorem 3) we can suppose that $\mathcal{F} \geq 0$, let $0 \leq u_\alpha \uparrow u$ in $\mathcal{U}$ and $0 \leq \mathcal{F}(u_\alpha) \uparrow v \leq \mathcal{F}(u)$ in $\mathcal{V}$. The next to be shown $\mathcal{F}(u) = v$.
By the end, assume $0 < \varepsilon < 1\ \forall \alpha$, let $\mathcal{F}_\alpha$ be the operator given by relation (1) in Theorem 2 that approves with $\mathcal{F}$ on the ideal created by $(\varepsilon u - u_\alpha)^+$and vanishes on $(\varepsilon u - u_\alpha)^-$, it is clear that: $\mathcal{F} \geq \mathcal{F}_\alpha \uparrow \geq 0$,and $\mathcal{F}_\alpha(\varepsilon u - u_\alpha)^-$ for every α, let $\mathcal{F}_\alpha \downarrow L \geq 0$ in $\ell_b(\mathcal{U}, \mathcal{V})$ it is clear that $L \in A_\mathcal{F}$, and $L(\varepsilon u - u_\alpha)^- = 0$ satisfies $\forall\, \alpha$ and so $\{(\varepsilon u - u_\alpha)^-\} \subseteq N_L$ However, $0 \leq (\varepsilon u - u_\alpha)^- \uparrow (1 - \varepsilon)u$ in $\mathcal{U}$ and thus, because by our hypothesis N_L is a band, $u \in N_L$ In conclusion, $L(u) = 0$
Finally, the relation:

$$0 \leq \mathcal{F}(\varepsilon u - u_\alpha)^+ = \mathcal{F}_\alpha(\varepsilon u - u)^+ \leq \mathcal{F}_\alpha(u)$$

combined upon Ando is inequality $0 \leq u - u_\alpha \leq (1 - \varepsilon)u + (\varepsilon u - u_\alpha)^+$ implies $0 \leq \mathcal{F}(u) - v \leq \mathcal{F}(u - u_\alpha) \leq (1 - \varepsilon)\mathcal{F}(u) + \mathcal{F}(\varepsilon u - u_\alpha)^+ \leq (1 - \varepsilon)\mathcal{F}(u) + \mathcal{F}_\alpha(u)$
Considering that $\mathcal{F}_\alpha(u) \downarrow L(u) = 0$ the last inequality yields $0 \leq \mathcal{F}(u) - v \leq (1 - \varepsilon)\,\mathcal{F}(u)$ $\forall\, \varepsilon \in (0,1)$ Hence, $\mathcal{F}(u) = v$ holds.
To clarify the previous theorem, suppose the operator $\mathcal{F}: C(H_\infty) \to R$ is defined as in the previous example by

$$\mathcal{F}(g) = g(\infty) + \sum_1^\infty 2^{-n} g(h_n)$$

As it has been seen before,
$N_F = \{g \in C(H_\infty): g(h_n) = 0\ \forall\, n = 1,2, \ldots\}$, and this means that N_F is a band of $C(H_\infty)$. On the other hand, if $L: C(H_\infty) \to R$ is defined by

$$L(g) = g(\infty)$$

Then L is a positive operator satisfying $0 \leq L \leq \mathcal{F}$, it is clear that $N_L = \{g \in C(H_\infty): g(\infty) = 0\}$, it is clear that the net $\{h_\alpha\}$ of all characteristic functions of the finite subsets of H satisfies $\{h_n\} \subset N_L$ and $h_\alpha \uparrow \mathbf{1}$, as $\mathbf{1} \notin N_L$, not that N_L is not a band of $C(H_\infty)$, in accordance with Theorem 6 (1), let $\mathcal{U}$ and $\mathcal{V}$ be two Riesz spaces with $\mathcal{V}$ Dedekind complete, if $C_\mathcal{F} = \{0\}$, then $\mathcal{F} \in \ell_b(\mathcal{U}, \mathcal{V})$ is said to have *zero carrier*. It is clear to see that the zero administrators are arranged as persistent administrators with zero carriers. On the other hand, if $C_\mathcal{F} = \{0\}$, then $\mathcal{F} \perp \ell_b(\mathcal{U}, \mathcal{V})$. (To see this, write $\mathcal{F} = \mathcal{F}_n + \mathcal{F}_\sigma$, and note that $|\mathcal{F}| = |\mathcal{F}_n| + |\mathcal{F}_\sigma|$ So $N_\mathcal{F} \subseteq N_{\mathcal{F}_n}$, hence depending on the order denseness of $N_\mathcal{F}$ note that $N_{\mathcal{F}_n} = \mathcal{U}, \mathcal{F}_n = 0$ and so $\mathcal{F} = \mathcal{F}_\sigma \in \ell_b(\mathcal{U}, \mathcal{V})$, From $|\mathcal{F} + L| \leq |\mathcal{F}| + |L|$, it follows that $N_\mathcal{F} \cap N_L \subseteq N_{L+\mathcal{F}}$, and utilizing the truth that the crossing point of two arrange thick beliefs is an arrange thick perfect, note that the administrators of $\ell_b(\mathcal{U}, \mathcal{V})$ with zero carriers shape a perfect.
Another hypothesis tells us that this perfect is continuously arranged thick in $\ell_b(\mathcal{U}, \mathcal{V})$.

Theorem 7: Let $\mathcal{U}$ and $\mathcal{V}$ be two Riesz spaces with $\mathcal{V}$ Dedekind complete. Then the ideal $\mathcal{F} \in \ell_\sigma(\mathcal{U}, \mathcal{V}): C_r = \{0\}$ is order dense in $\ell_\sigma(\mathcal{U}, \mathcal{V})$.

Proof: since the set $\mathcal{F} \in \ell_\sigma(\mathcal{U}, \mathcal{V}): C_r = \{0\}$ is an ideal in $\ell_\sigma(\mathcal{U}, \mathcal{V})$, let $\mathcal{F} \in \ell_\sigma(\mathcal{U}, \mathcal{V})$ is the positive operator with zero carrier.
Since $\mathcal{F}$ is not order continuous, there exists (use Theorem 6) an operator $0 \leq L \leq \mathcal{F}$ where N_L is not a band, denote by B the band created by N_L, then let R be the operator firm by Theorem 6 where $R = L$ on $R = 0$ and مراجعة on B^d , it is clear that $N_L \subseteq N_R$, and $0 \leq R \leq L$. On the other hand, later $R = 0$ holds on $C_L = N_L^d = B^d$, we see that $N_L \oplus C_L \subseteq N_R$, and this (in the opinion of Theorem 2) shows that N_R is order dense in $\mathcal{U}$, this mean that R has zero carrier, finally note that $0 \leq R \leq \mathcal{F}$ holds.

From the previous theorem we know that $\ell_\sigma(\mathcal{U},\mathcal{V}) = \{0\}$ (means that $\ell_b(\mathcal{U},\mathcal{V}) = \ell_n(\mathcal{U},\mathcal{V})$) if and only if any nonzero operator between two Riesz spaces $\mathcal{U}$ and $\mathcal{V}$ has a nonzero carrier.
The following theorem explains some important relationships for order bounded operators.

Theorem 8 Alibrandi's and Burkinshaw (Aliprantis & Burkinshaw, 1983): For a pair of Riesz spaces $\mathcal{U}$ and $\mathcal{V}$ with $\mathcal{V}$ Dedekind complete, the following statements are equivalent:
1. Every order bounded operator from $\mathcal{U}$ into $\mathcal{V}$ is order continuous.
2. Every nonzero order bounded operator from $\mathcal{U}$ into $\mathcal{V}$ has a nonzero carrier.
3. The null ideal of every order bounded operator from $\mathcal{U}$ into $\mathcal{V}$ is a band.

The following result shows that when an operator is order continuous on a given ideal.

Theorem 9 Let $\mathcal{F}: \mathcal{U} \longrightarrow \mathcal{V}$ be a positive operator between two Riesz space with $\mathcal{V}$ Dedekind complete, and let U be an ideal of $\mathcal{U}$. Then the operator $\mathcal{F}$ is order (resp δ- order) continuous on U if and only if $\mathcal{F}_U$ is an order (resp δ-order) continuous operator.
Proof: first, the result of the "order continuous" case is proven. After that, the " σ-order continuous" case is proven in a similar way. the operator $\mathcal{F}_U$ is decided as follows:

$$\mathcal{F}_U(u) = \sup\{\mathcal{F}(v): v \in U \text{ and } 0 \le v \le u\};$$

whereas $\mathcal{F}_U = \mathcal{F}\ \forall\ u \in U$, it is clear that if $\mathcal{F}_U$ is an order continuous operator, then $\mathcal{F}$ must be order continuous on U .
to prove the opposite direction, let $\mathcal{F}$ is order continuous on U, and $0 \le u_\alpha \uparrow u$ in $\mathcal{U}$, let $\mathcal{F}_U(u_\alpha) \uparrow s \le \mathcal{F}_U(u)$. Now fix $v \in U \bigcap [0,u]$. Then $0 \le v \wedge u_\alpha \uparrow v$ holds in U, and so $\mathcal{F}(v \wedge u_\alpha) \uparrow \mathcal{F}(v)$ holds in $\mathcal{V}$. From

$$\mathcal{F}(v \wedge u_\alpha) = \mathcal{F}_A(v \wedge u_\alpha) \le s \le \mathcal{F}_A(u),$$

It follows that $\mathcal{F}(v) \le s \le \mathcal{F}_U(u)$ holds $\forall v \in U \bigcap [0,u]$ Hence,

$$\mathcal{F}_U(u) = \sup \mathcal{F}(U \bigcap [0,u]) \le s \le \mathcal{F}_A(u),$$

and so $\mathcal{F}_U = s$ holds, proving that $\mathcal{F}_U$ is an order continuous operator.

CONCLUSION

To Sum up, we concluded the positive order continuous operator $\mathcal{F}: H \longrightarrow \mathcal{V}$ where H is order dense majorizing Riesz subspace of Riesz space $\mathcal{U}$ and $\mathcal{V}$ is Dedekind complete, it has a unique order continuous extension on all Riesz space $\mathcal{U}$, it defined as

$$\mathcal{F}(u) = \sup\{\mathcal{F}(h): h \in H, 0 \le h \le u\}; u \in \mathcal{U}^+$$

The evidence of this result is as follows:
Since H majorizes $\mathcal{U}$ then:

located in $\mathcal{V}$ $\forall\ u \in \mathcal{U}^+$, now see: $E(u) = \sup\{\mathcal{F}(h): h \in H, 0 \le h \le u\}$
If $\{u_n\} \subseteq H$ when $0 \le u_\alpha \uparrow u$ then $\mathcal{F}(u_\alpha) \uparrow E(u_\alpha)$, and if $0 \le h \in H$ when $0 \le h \le u$, then $0 \le u_\alpha \wedge h \uparrow h$ satisfies in H, from the order continuity of $\mathcal{F}: H \to \mathcal{V}$ is:

$$\mathcal{F}(h) = sup\{\mathcal{F}(u_\alpha \wedge h)\} \le sup\{\mathcal{F}(u_\alpha)\} \le E(u)$$

This gives that $\mathcal{F}(u_\alpha) \uparrow E(u)$.

let $u, h \in \mathcal{U}^+$, choose nets $\{u_\alpha\}$ and $\{h_\beta\}$ of H^+ whereas $0 \le u_\alpha \uparrow u$ and $0 \le h_\beta \uparrow h$, this implies to that $0 \le u_\alpha + h_\beta \uparrow u + h$ holds in H^+, and so

$$.\mathcal{F}(u_\alpha) + \mathcal{F}(h_\beta) = \mathcal{F}(u_\alpha + h_\beta) \uparrow E(u+h)$$

from $\mathcal{F}(u_\alpha) \uparrow E(u)$ and $\mathcal{F}(h_\beta) \uparrow E(h) \implies E(u+h) = E(u) + E(h)$ holds, and $E: \mathcal{U}^+ \to \mathcal{V}^+$ is additive operator, returning to theorem 1, $\mathcal{F}$ extends uniquely to $E: \mathcal{U} \longrightarrow \mathcal{V}$, this means E is an extension of $\mathcal{F}$.

Duality of interest: The authors declare that they have no duality of interest associated with this manuscript.

Author contributions: Contribution is equal between authors.

Funding: No specific funding was received for this work.

REFERENCES

Abramovich, Y. A., & Aliprantis, C. D. (2002). *An invitation to operator theory* (Vol. 50). American Mathematical Society Providence, RI .

Aliprantis, C., & Burkinshaw, O. (1983). On positive order continuous operators. Indagationes Mathematicae (Proceedings ,(

Aliprantis, C., & Burkinshaw, O. J. P., New York. (1985). Positive Operators, Acad .

Aydin, A. J. H. J. o. M., & Statistics. (2023). Statistically order compact operators on Riesz spaces. 1-9 .

Bahramnezhad, A., & Azar, K. H. J. P. (2018). Unbounded order continuous operators on Riesz spaces. *22*, 837-843 .

Jalili, S. A., Azar, K. H., & Moghimi, M. B. F. J. P. (2021). Order-to-topology continuous operators. 1-10 .

John, B. C. J. N. I. (1990). A course in Functional Analysis, springer-verlag .

Kantorovitch, L. J. M. c. (1940). Linear operations in semi-ordered spaces. I. *7*(2), 209-284 .

Kreyszig, E. (1978). Introductory Functional Analysis with Applications. New York: Wiley&Sons. In: Inc.

Ogasawara, T. J. J. o. S. o. t. H. U., Series A. (1942). Theory of Vector Lattices. I (Japanese). *12*(1), 37-100 .

Riesz, F. J. J. o. P. D. A. P. (2000). Geometrical optical model of the image formation in Makyoh (magic-mirror) topography. *33*(23), 3033 .

Turan, B., Altin, B., & Gürkök, H. J. T. J. o. M. (2022). On unbounded order continuous operators. *46*(8), 3391-3399 .

Veksler, A. I. i. J. I. V. U. Z. M. (1960). On the homomorphism between the classes of regular operators in K-lineals and their completions. (1), 48-57 .

Al-Mukhtar Journal of Basic Sciences 22 (1): 55-63, 2024
Doi: https://doi.org/10.54172/x73s9v66

Research Article **Open Access**

The Inhibition Effect of Alcoholic Extract of *Capsicum Annuum* (Chili Pepper) on The Growth of Barely Grains' Associated Fungi Species

Fuzia E. Eltariki[1*], Mohamed M. Alsull[2]

***Correspondence authors:**
Fow_micro@yahoo.com
Department of Botany, Faculty of Science, Misurata University, Libya

Second Author:
m.alsoul@yahoo.com
Department of Botany, Faculty of Science, Misurata University, Libya

Received:
28 September 2023

Accepted:
17 April 2024

Publish online:
30 April 2024

Abstract

In this research, isolation and identification of some fungal species that were associated with barley grains (obtained from Misurata Agricultural Research Center) were carried out, to study the effect of their secretions on the germination and growth of barely seedlings. The ethanolic extract of Chili pepper was also tested for its biological control on the germination and growth of the chosen fungal species. 10 fungal species belonging to 4 different genera were isolated and identified from barley grains, among these, two species were selected (*Aspergillus niger* and *Rhizopus stolonifer*) for further investigation. Both of the two fungal filtrates showed an inhibitory effect on the germination and length of radicles of barley grains and seedlings, results also showed that ethanolic extract of *Capsicum annuum* (Chili pepper) had a varied inhibitory effect on spore germination of the selected fungal species, the reason for inhibition of fungi treated with *C. annuum* extract may be due to the presence of different chemicals have inhibitory effects on fungi.

Keywords: Barley Grains - Fungal Filtrates - Ethanolic Extract - Isolation - *Capsicum Annuum* - Germination.

Introduction

Barley is one of the most important and most widespread cereal crops in the world, in terms of adaptation, especially in dry areas. This spread of the barley crop is due to its increased tolerance to unsuitable environmental conditions. Many scientists believe that barley is the oldest grain known to man and cultivated, and fossils of its grains have been found in many countries of the world that have ancient civilizations (El-Hashash & El-Absy, 2019; Kant *et al*., 2016).

During harvest, transportation, or storage, barley grains are infected with many fungi belonging to the genera *Alternaria*, *Aspergillus*, *Rhizopus*, *Penicillium*, *Trichoderma* and other fungi (Fleurat-Lessard, 2017; Nishimwe *et al.*, 2020). These fungi cause significant economic losses because of their impact on the vitality of the grain and reducing its germination rate, which leads to a reduction in agricultural production. When using such grains in agriculture, as well as the ability of some species of the fungi *Penicillium* and *Aspergillus* to produce mycotoxins. The most prominent and dangerous of these toxins are aflatoxins, which are considered among the most dangerous food pollutants present due to their carcinogenic impacts on humans and animals (Mohapatra *et al*., 2017).

The use of fungicides has played a role in combating fungi for many years, but many problems have arisen in their use, such as environmental pollution, the emergence of resistant strains, and others. Among the control methods that are currently used successfully to combat pathogens are plant extracts as promising alternatives to chemical resistance methods, as many of them have been proven

to be effective in resisting fungal, as it is cheap and safe to use, and do not leave any toxic residue on plants, in addition to being easy to obtain due to its abundant availability in nature (Assress *et al*., 2021; Goswami *et al*., 2018).

This study aims to:

- Isolation and identification of some fungi species associated with barley grains.
- Investigating the effect of the isolated fungal filtrates, on grains' germination rate and seedling development
- Testing the inhibitory effect of alcoholic extract of *C. annuum* (Chili pepper), on the growth of the investigated fungi species.

MATERIALS AND METHODS

Samples Collection

Samples of barley grains were brought to the Faculty of Science / Botany Department and obtained from the Agricultural Research Center in Misrata (*Hordeum vulgare*), the barley Misurata cultivar 04.

Isolation and identification of fungi associated with barley grains

A random sample of barley grains was selected from the quantity that was brought to the lab, and using sterile forceps near the flame, part of which was planted in Petri dishes containing the (PDA), each dish has 5 grains and has equal proportions, barley grain were lightly pressed using a forceps, so that most of its surface become in direct contact and immersed in the agar.

After the planting, all the dishes were placed in the incubator at a temperature of 25 ° C, after 7 days of incubation, the dishes were extracted and the developing fungi were identified around the grains using a complex optical microscope and special scientific references (Gupta *et al*., 2020).

Identification of fungus to be studied ecologically and physiologically

The study selected various fungi from barley grains samples for environmental and physiological studies due to their presence in most samples and representing different grades and families **Figure (1)**.

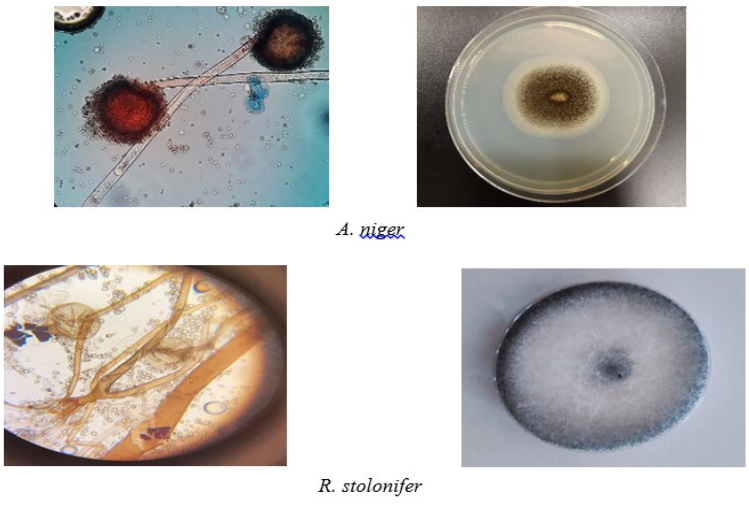

Figure:(1). Phenotypic (morphological and cultural), (Microscopical) characterization of some the isolates (*A. niger*, *R. stolonifer*) on PDA from barley grains.

Effect of fungi filterates on percentage of germination of barley grains and seedling growth:
Where 9 bottles containing each flask were equipped with 25 mL of PDB, Then, using the cutter, tablets were taken from the 9 mm PDA diameter containing *R. stolonifer, A. niger* for of 3-4 days, where each of the fungus was assigned 3 bottles. The three other vials were left without planting the fungus for comparison as in **Figure (2).**

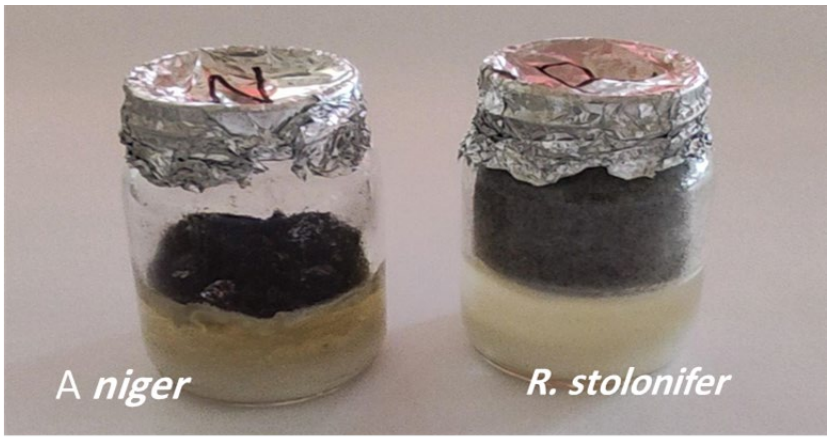

Figure:(2). Growth *A. niger, R. stolonifer* on PDB at 25 ° C After 10 days.

After the completion of the transplantation, all the bottles were placed in the incubator at 25 ° C, ten days later the vials were removed from the incubator and the leachate was separated from the growth using sterile filter paper.

to investigate the impact of these fungal filtrates on the germination and growth of barley grains and seedlings, several clean and sterilized petri dishes, with sterilized filter paper. Each containing 5 grains of barley sterilized with 1.0 % hydrogen peroxide solution, each petri dish was sprayed with 10 mL from the filtration. Each fungus was assigned three replicates, for comparison nine dishes containing the same number of grains were irrigated with sterile distilled water, which was not planted with fungi. After finishing the irrigation, all the dishes were placed in the incubator at 25°C. Ten days later, the grain-containing dishes were extracted from the incubator and the developing and non-developing grains were calculated in each dish. The percentage of germination was calculated according to the following equation:

$$\text{Percentage of germination (\%)} = \frac{\textit{Number of developing seeds}}{\textit{Total number of seeds}} \times 100$$

In addition, the length of the radicles and coleoptiles was measured on the tenth day by using a ruler, and observations were made on the pathological symptoms that appeared on each dish. Three dishes were allocated for each period (Al Fadl & Al Haidari, 2012).

Effect of Ethanolic Extracts of *C. annuum* (Chili pepper) on the Growth of Isolations Fungi from barley Grains
Ten (10) grams of dried *C. annuum* (Chili pepper) were thoroughly washed with distilled water, and dried, then crushed by ceramic mortar to form powder. 100 mL of ethanolic was added. 2 mL of this extract was added after sterilization into the media before the hardening. Tablets from the rim of the colony of *R. stolonifer* and *A. niger* grown for 3-4 days, were transferred into the center of each of these dishes, then incubated under 25°C, A week later, each bipolar diameter was measured for each fungal colony, each of these was implemented triplicates (Al-Jawhari, 2012). The inhibition ratio was estimated according to the following equation:

$$\text{Inhibition ratio\%} = \frac{\textit{The average of the comparison} - \textit{Average transaction diameter}}{\textit{The average of the comparison}} \times 100$$

RESULTS AND DISCUSSION

Isolation and identification of some fungi on barley grains:

This study showed that barley grains were contaminated with a lot of types and numbers of fungal pathogens depending on the area produced. From barley grains, about 142 colonies were obtained from the Misrata Agricultural Research Center. Table (1) shows the number of colonies obtained from barley grains.

This may be due to the fact that the Misrata Agricultural Research Center has a mild and humid climate during the time of the formation of the saplings, allowing the moisture-loving fungi and temperate fungi to have a longer period of growth and reproduction for several generations and thus producing a large number of germs.

For those fungi isolated from the area of the Agricultural Research Center Misrata, amounted to 10 species belonging to four genus, the *Aspergillus* species were the most common species and represented by four different species, as well as the *Rhizopus*, which had a total of 40 colonies (*A. niger and R. stolonifer*) were selected to conduct some tests on them.

Table (1): Genera and fungal species isolated on PDA from barley grains at 25 ° C, after 7 days.

Name of fungi	Numbers of colonies on parley grains (center)
Aspergillus sp.	10
Aspergillus sp_1	2
Aspergillus flavus	6
Rhizopus stolonifer	40
Aspergillus niger	10
Rhizopus sp.	5
Fusarium sp.	1
Fusarium oxysporum	21
Penicillium sp_1	35
Penicilliun chrysogenum	12
Total number of colonies	142
Total number of species	10
Total number of genera	4

Effect of fungi filterates on percentage of germination of barley grains and seedling growth

Barley grains are contaminated while they are in the field or when they are stored and put on the market with many fungi that are likely to be secreted in the grains as they develop excretions or toxins that may affect their vitality.

To clarify the role of secretions of some fungi on barley grain has run out of this experiment, which showed that the results of all the tested fungi impact on the proportion of germination and development of seedlings resulting from them, but varying degrees depending on the type of pollinated fungi, The effect of these fungal filtrates on the percentage of germination of barley grains and the

development of seedling, From Table (2) and Figures (3,4,5), we note that the most common filtrate on the percentage of grain germination is the leachate of *A. niger*, This filtarets reduced the percentage of germination in irrigated grains was 0% after 10 days compared to germination rate of 98% in irrigated grains with non-fungal medium (comparative) or distilled water, It was ranked second in terms of the effect of the fungal filterate *R. stolonifer,* which also reduced the percentage of germination in irrigated grains to 20% after 10 days of incubation.

As for the effect of filtrates fungi along the radicles and coleoptiles, the effect of *A. niger* was clear, some of the irrigated grains were formed after 10 days radicles were small and distorted brown the average length is 0.0 cm, while the coleoptiles were also short, the average length of 0.0 cm after 10 days of incubation, *R. stolonifer* filterate came in second place in terms of effect, as the irrigated grains were made up of the radicles and coleoptiles with a mean length of 0.5 and 1.5 cm respectively after 10 days compared to the irrigated grains with non-fungal medium (the comparison), the average length of the radicles and coleoptiles was 4.5 cm and 10.5 cm respectively during 10 days of incubation, This is consistent with the finding (Garuba *et al*., 2014).

This study was conducted to investigate the 7-day fungal effects filtrates of *A. niger* and *Penicillium Chrysogenum* isolated from corn seeds on germination ratio and seedling growth. Results showed that the seed germination ratio treated with fungal filtrates *A. niger* and *Penicillium Chrysogenum* (65.33%,79.67% respectively) were less than the control (100%).

It is obvious that the germination of barley grains and the development of their seedlings were more influenced by the filtrate of *A. niger*, this may be due to the fact that this fungus is known for its production of aflatoxins, which is likely to have been produced in the liquid medium in which it grew, reducing the germination rate of irrigated grains, This is consistent with the findings (Kabak *et al.*, 2006), which indicated that aflatoxin poisons may inhibit or reduce the germination ratio of grains and seeds of many crops and reduce the growth rate of their seedlings, and the effect of this leachate on the growth and development of the radicles and coleoptiles produced from irrigated grains(Abbas *et al*., 2009).

Results also indicated that, *R. stolonifer* has a deleterious effect on barley grains germination and seedling development, but the effect was mild on grain germination and evolution of the radicles and coleoptiles, where the cause of the lack of the effect of this leachate that it contains toxins or substances inhibiting growth, but it is of another type that differs in their chemical qualities from the toxins produced by *A. niger,* and some are likely to be a disincentive to produce naturally occurring Gibberellins produced by the embryo during germination leading to a shortening of the radicles and coleoptiles from the irrigated grains, This is consistent with the findings of the researchers (Finneseth, 2010; Mondéjar-López *et al*., 2022).

Table (2): Effect filtrates of tested fungi on the percentage of parley germination and growth of seedlings after 10 days.

Fungal filterates	Percentage of germination (Germination rate)	Length the radicles/cm	Length the coleoptiles/cm
A. niger	0 %	.00	.00
R. stolonifer	20 %	0.5	1.5
Control	98 %	4.5	10.5

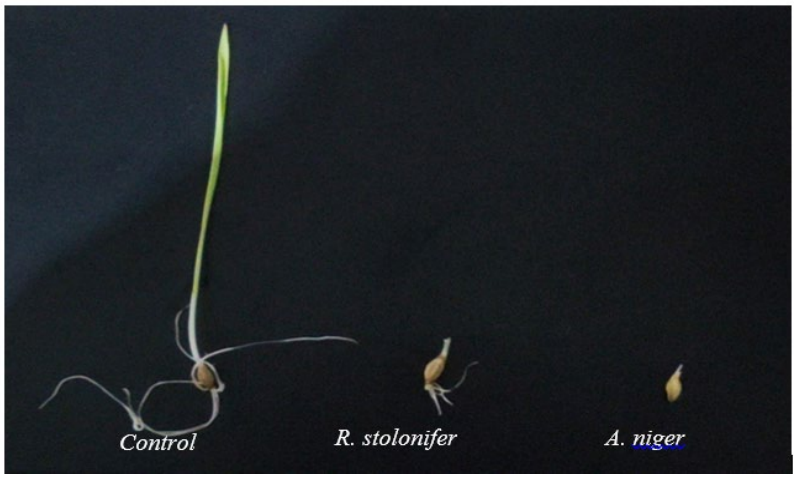

Figure:(3). Effect filtrates of tested fungi on the percentage of barley germination and growth of seedlings after 10 days.

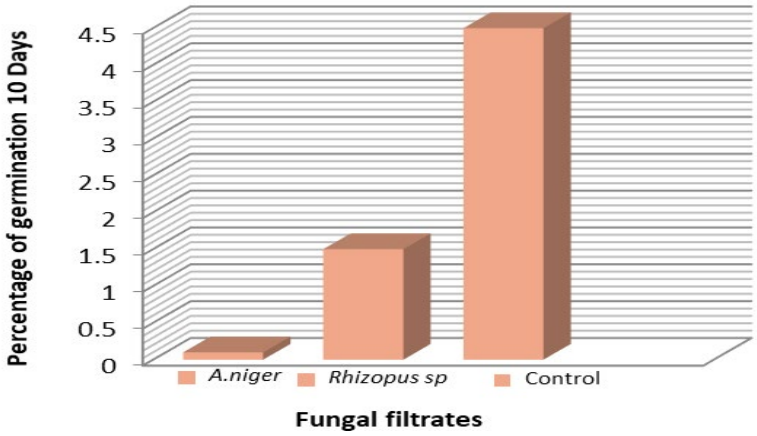

Figure:(4). Effect filtrates of tested fungi on the percentage of barley germination and growth of seedlings after 10 days.

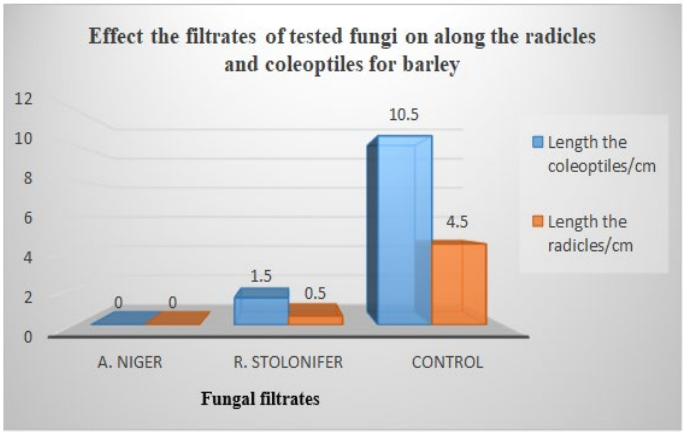

Figure:(5). Effect of the filtrates of tested fungi on along the radicles and coleoptiles for barley (10 days).

Effect of ethanolic extract of *C. annuum* (Chili pepper) on tested fungus associated with barley grains

The effect of ethanolic extract of *C. annuum* (Chili pepper) on the growth of irradiated fungi of parley grains is shown in tables (3-4). Ethanolic extract of *C. annuum* significantly inhibited the growth of tested fungi isolated from barley grains. (*R. stolonifer & A. niger*) where the diameter of the colony was 8.5 and 0.75 cm respectively compared to the treatment of the control 8.1 and 9 cm. The growth rate of *R. stolonifer* filling the dish with a note that no sporangium are created, (The ethanolic extract of *C. annuum* prevents the *R. stolonifer* to produce its spores), while the growth rate of *A. niger* when treated with the extract of *C. annuum* was 0.75 cm compared to the control of this fungus.

By observing the figures (6-7), the extract of the *C. annuum* is the superior effect, because it contains some active compounds such as saponins, phenols and alkaloids, It is known that these compounds have a disincentive effect for many pathogens (Agrios, 1985; Gülçin, 2005), This is consistent with what he found (Abdel Mohsen, 2011) In the testing of the efficiency of some plants, including *C. annuum* in the protection of the plant sun flower from the injury of fungus *Macrophomina Phaseolina* cause of rotting fever, with a reduction rate of fungal infection 53.1%. The reason for inhibition of fungi treated with chili extract is due to the presence of alkaloids Capsorubin, Dihgdro, Capsiain, Capsiacin, which may have an effect on these fungi, This is consistent with what he found (Tewari & Nayak, 1991) which found that the extract of this plant inhibits the growth of pathogenic fungi of rice, namely *Cochlibeolas migabeanus , Pyricularia oryzae , Rhizoctonia solani.* The reason for the inhibition of fungi treated with *C. annuum* extract may be due to the presence of different chemicals that have inhibitory effects on fungi, containing alkaloids and glycosides and the soap that melt easily in organic solvents and dissolved in water and which have an anti-fungal growth effect, This is consistent with what he found (Jiratko & Vesela, 1992), Which found that this extract inhibits the growth of *R. Solani*.

Table (3): The inhibitory effect of ethanolic *C. annuum* extract on *A. niger* at 25 ° C for one week.

Type of acetone extract	Average colony diameter (cm)	Percentage of inhibition%
C. annuum	0.75	90.3%
Control	8.1	0%

Table (4): The inhibitory effect of ethanolic *C. annuum* extract on *R. stolonifer* at 25 ° C for one week.

Type of acetone extract	Average colony diameter (cm) *	Percentage of inhibition%
C. annuum	8.5	5.5%
Control	9.0	0%

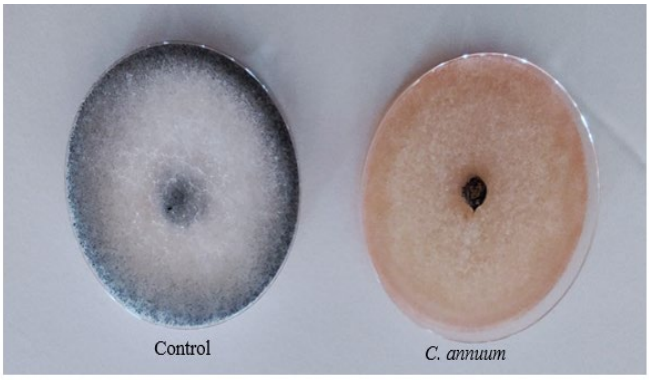

Figure:(6). Effect of ethanolic extract of *C. annuum* on growth *R. stolonifer* at 25 ° C for one week.

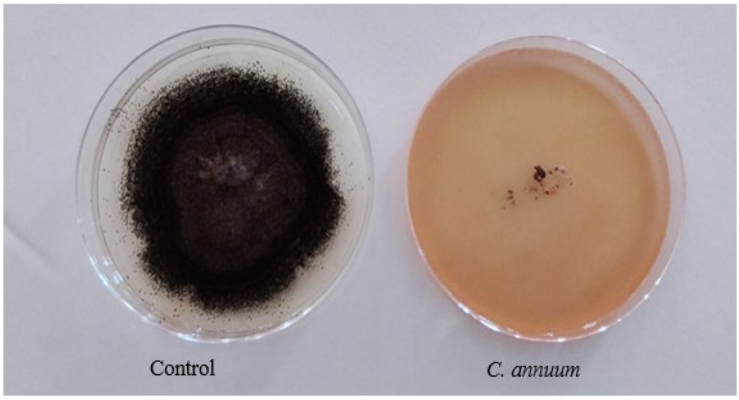

Figure:(7). Effect of ethanolic extract of *C. annuum* on growth *A. niger* at 25 ° C for one week.

CONCLUSION

The tested fungi and their secretions had an effect on the germination and the length of the radicles and coleoptiles for seedlings of barley grains. All the ethanolic extract tested of the *Capsicum annuum* (Chili pepper) showed a disincentive effect on the germination of the spores of the contaminated fungi for barley grains at varying rates.

Duality of interest: The authors declare that they have no duality of interest associated with this manuscript.

Author contributions: Contribution is equal between authors.

Funding: No specific funding was received for this work.

REFERENCES

Abbas, H., Wilkinson, J., Zablotowicz, R., Accinelli, C., Abel, C., Bruns, H., & Weaver, M. (2009). Ecology of Aspergillus flavus, regulation of aflatoxin production, and management strategies to reduce aflatoxin contamination of corn. *Toxin reviews*, *28*(2-3), 142-153.

Abdel Mohsen, H. A.-J. (2011). Test the efficiency of some plant powders in the protection of the sun flower plant from the infection of the fungus Macrophomia phaseolina (tassi) Goid, which causes the disease. *Faculty of Agriculture, University of Basra*, *3*(2).

Agrios, G. (1985). Plant pathology. Academic press Inc . New York N.Y. *Food Review*.

Al-Jawhari, I. F. (2012). The Effect of Acetonic Extracts on Some Plants on the Associated Mushrooms of Barley Seeds in Misurata City, Faculty of Education, Department of Life Sciences. *Journal of Agricultural Research*, *1*(2).

Al Fadl, F., & Al Haidari, F. (2012). Effect of leachates isolated from rice residues on wheat grain germination and growth of fusarium graminearum and Rhizoctonia solani Nurses and Trichoderma harzianum.Department of Plant Protection - Faculty of Agriculture - University of Kufa Iraq.

Assress, H. A., Selvarajan, R., Nyoni, H., Mamba, B. B., & Msagati, T. A. (2021). Antifungal azoles and azole resistance in the environment: current status and future perspectives—a review. *Reviews in Environmental Science and Bio/Technology*, 1-31.

El-Hashash, E. F., & El-Absy, K. M. (2019). Barley (Hordeum vulgare L.) breeding. *Advances in Plant Breeding Strategies: Cereals: Volume 5*, 1-45.

Finneseth, C. H. (2010). Evaluation and enhancement of seed lot quality in eastern gamagrass [Tripsacum dactyloides (L.) L.].

Fleurat-Lessard, F. (2017). Integrated management of the risks of stored grain spoilage by seedborne fungi and contamination by storage mould mycotoxins–An update. *Journal of Stored Products Research*, *71*, 22-40.

Garuba, T., Abdulrahaman, A., Olahan, G., Abdulkareem, K., & Amadi, J. (2014). Effects of fungal filtrates on seed germination and leaf anatomy of maize seedlings (Zea mays L., Poaceae). *Journal of Applied Sciences and Environmental Management*, *18*(4), 662-667.

Goswami, S. K., Singh, V., Chakdar, H., & Choudhary, P. (2018). Harmful effects of fungicides-Current status. *International Journal of Agriculture, Environment and Biotechnology*, *11*, 1011-1019.

Gülçin, İ. (2005). The antioxidant and radical scavenging activities of black pepper (Piper nigrum) seeds. *International journal of food sciences and nutrition*, *56*(7), 491-499.

Gupta, D. R., Surovy, M. Z., Mahmud, N. U., Chakraborty, M., Paul, S. K., Hossain, M. S., Bhattacharjee, P., Mehebub, M. S., Rani, K., & Yeasmin, R. (2020). Suitable methods for isolation, culture, storage and identification of wheat blast fungus Magnaporthe oryzae Triticum pathotype. *Phytopathology Research*, *2*(1), 1-13.

Jiratko, J., & Vesela, G. (1992). Effect of plant extracts on the growth of plant pathogenic fungi in vitro. *Ochrana Rostlin-UVTIZ (CSFR)*.

Kabak, B., Dobson, A. D., & Var, I. l. (2006). Strategies to prevent mycotoxin contamination of food and animal feed: a review. *Critical reviews in food science and nutrition*, *46*(8), 593-619.

Kant, L., Amrapali, S., & Babu, B. K. (2016). Barley. In *Genetic and Genomic Resources for Grain Cereals Improvement* (pp. 125-157). Elsevier.

Mohapatra, D., Kumar, S., Kotwaliwale, N., & Singh, K. K. (2017). Critical factors responsible for fungi growth in stored food grains and non-Chemical approaches for their control. *Industrial Crops and Products*, *108*, 162-182.

Mondéjar-López, M., Rubio-Moraga, A., López-Jimenez, A. J., Martínez, J. C. G., Ahrazem, O., Gómez-Gómez, L., & Niza, E. (2022). Chitosan nanoparticles loaded with garlic essential oil: A new alternative to tebuconazole as seed dressing agent. *Carbohydrate polymers*, *277*, 118815.

Nishimwe, K., Mandap, J. A. L., & Munkvold, G. P. (2020). Advances in understanding fungal contamination in cereals. *Advances in postharvest management of cereals and grains*, 31-66.

Tewari, S., & Nayak, M. (1991). Activity of four plant leaf extracts against three fungal pathogens of rice. *Tropical agriculture*, *68*(4), 373-375.

Al-Mukhtar Journal of Basic Sciences 22 (1): 64-74, 2024
Doi: https://doi.org/10.54172/0brvmk83

Research Article

Open Access

Performance Evaluation of Artificial Neural Networks for Estimating Reference Evapotranspiration in Shahat, Libya using limited climatic data

Mohamed A. Momen *, Osama A. Abdelatty

***Corresponding author:** Mohamed.abdelkarem@omu.edu.ly
Department of Soil and Water, Faculty of Agriculture, Omar Al-Mukhtar University, Libya

Second Author: Osama.abdelhamed@omu.edu.ly
Department of Soil and Water, Faculty of Agriculture, Omar Al-Mukhtar University, Libya

Received:
30 September 2023

Accepted:
28 March 2024

Publish online:
30 April 2024

Abstract

This study was conducted with the aim of evaluating the performance of artificial neural networks (ANNs) to estimate the reference evapotranspiration using limited climate data in Shahat region in Libya, compared to using the FAO Penman-Monteith equation (FPM), which requires temperature, wind speed, relative humidity and number of sunshine hours, which are rarely available in most meteorological stations in developing countries. In this study, we used the average temperature (T_{mean}) and the average relative humidity (RH_{mean}) obtained from Shahat meteorological station for the period from 1963 to 1999, and the extraterrestrial radiation (R_a), which can be calculated given the location and time of the day. These data are divided into two groups, from 1963 to 1988 and from 1989 to 1999 for the training and validation phases of the neural networks, respectively. This study concluded that using (T_{mean}), (RH_{mean}) and (R_a) gave the best agreement with the results calculated with the FAO Penman-Monteith equation, where the values of R^2 and RMSE are equal to 0.98 and 0.26, respectively.

Keywords: Reference Evapotranspiration, FAO Penman-Monteith Equation, Artificial Neural Networks

INTRODUCTION

Evapotranspiration (ET) is a term used to describe the sum of evaporation and plant transpiration from the land surface to the atmosphere. It is the second most important variable in the hydrological cycle after rainfall and has an important role as a controlling factor of runoff volume or river discharge, irrigation water requirement and soil moisture contents (Mohan & Arumugam, 1996). Therefore, an accurate estimate of the ET is crucial for studies on the hydrologic water balance, irrigation system design and management, crop production, water resources planning and management and environmental assessment (Irmak et al., 2003),(Temesgen et al., 2005),(Kumar et al., 2011).

ET can be experimentally determined directly by lysimeters or estimated by indirect methods such as the aerodynamic method, energy balance method and combined method. Due to the high cost of lysimeters, installation and maintenance, this instrument is not widely used. Therefore, most users prefer indirect methods based on meteorological data (Kim & Kim, 2008),(Dinpashoh, 2006).

The Penman-Monteith FAO 56 (FPM) model is recommended as the sole method for calculation of ETo and it has been reported to be able to provide consistent ETo values in many regions and climates (Allen et al., 2005),(Allen et al., 2006). The main shortcoming of the FPM method is, however, that it needs a large number of climatic data and variables which are unavailable in many regions, especially in developing countries like Libya.

According to (Kumar et al., 2002), evapotranspiration is a complex nonlinear phenomenon because it depends on the interaction of several climatic factors, including solar radiation, wind speed, air humidity and temperature, as well as the type and growth stage of crops. The choice of a method for estimating evapotranspiration depends on several factors. One of these factors is the availability of meteorological data, because complex methods that require a large number of variables are only applicable when all necessary data are available.

Over the past decade, intelligent computational models have been developed as alternative methods for estimating the ETo, such as the artificial neural networks (ANNs) technique (Landeras et al., 2008). ANNs are effective tools for modeling nonlinear processes, as they require few inputs and are able to map input-output relationships without any understanding of the physical process involved (Haykin, 1999),(Sudheer et al., 2003).

Several types of research have been conducted using ANNs to estimate evapotranspiration as a function of climatic elements (Kumar et al., 2002),(Sudheer et al., 2003),(Odhiambo et al., 2001),(Trajkovic et al., 2003),(Achite et al., 2022),(Genaidy, 2020),(Heramb et al., 2023),(Rajput et al., 2023),(Abdel-Fattah et al., 2023),(Tunalı et al., 2023),(Ekhmaj, 2012) and (Ekhmaj et al., 2013). These researches found satisfactory results, compared with those obtained from the FPM method.

This study was carried out to investigate the estimation of the reference evapotranspiration (ETo) by using ANNs technique as a function of limited climatic data such as temperature (T) and relative humidity (RH) and calculated extraterrestrial radiation (Ra), for the region of Shahat, Libya.

MATERIALS AND METHODS

Study area

The climatic data used in this study were obtained from Shahat weather station located of the longitude of 21° 51′E, the latitude of 32° 49′N, and a mean altitude is 621 meters above sea level. The Shahat region is characterized by a Mediterranean climate (hot, dry, summer, warm, rainy, winter), the rainiest month is January with a value of 121.1 mm, and the least rainy month of the year is July, with a precipitation of 0.5 mm, the total annual precipitation is 557.4 mm, and the coldest month of the year is the month January, with an average temperature of 9.5 ° C, while the hottest month is August, with an average temperature of 23.26 ° C, and the average temperature of 16.6 ° C.

The historical data series includes average monthly maximum (T_{max}), minimum (T_{min}) and mean air temperature (T_{mean})(° C), mean relative humidity (RH_{mean}) (%), and wind speed (U_2) ($m.s^{-1}$), which covered the period from 1945 to 1999. Because of the lack of a connected series of this data, the beginning was taken from 1963 and the missing data within this period has been processed. Table (1) shows the statistical parameters of meteorological variables at Shahat weather station. The map of the study area and the location of the meteorological station are shown in Figure (1).

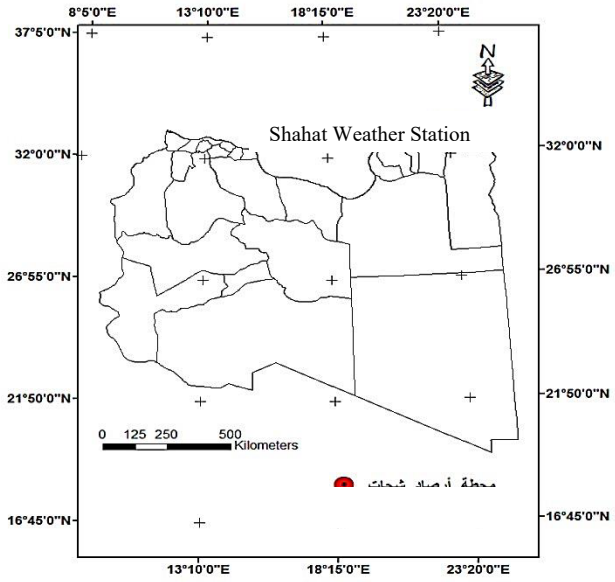

Figure:(1). location of the meteorological station

Table:(1). Statistical parameters of meteorological variables at Shahat weather station

Parameter	T_{max} (°C)	T_{min} (°C)	T_{mean} (°C)	RH_{mean} (%)	U_2 ($m.s^{-1}$)	Sun (hr)	FPM ($mm.d^{-1}$)
Mean	20.9	12.3	16.6	67.8	4.7	8.0	4.0
Standard Error	0.3	0.2	0.2	0.4	0.1	0.1	0.1
Standard Deviation	5.9	4.7	5.2	9.3	1.6	2.5	1.7
Range	22.1	17.9	19.8	50.0	8.0	11.1	6.7
Maximum	31.1	21.2	25.9	89.0	10.0	13.0	7.8
Minimum	9.0	3.3	6.2	39.0	2.1	1.9	1.1
Count	444	444	444	444	444	444	444

Reference Evapotranspiration (ETo)

The FPM equation was developed to describe ET of a reference grass crop, which is defined as the rate of evapotranspiration from a hypothetical crop with an assumed fixed height (12 cm), surface resistance (70 $s.m^{-1}$) and albedo (0.23), close resembling the evapotranspiration from an extensive surface of a disease-free green grass cover of uniform height, actively growing, completely shading the ground, and with adequate water and nutrient supply (Allen et al., 1998). The ETo was calculated using the standard equation (Eq1), recommended in the FAO 56 bulletin (Allen et al., 1998). This Equation takes the form:

$$ET_o = \frac{\left[0.408 \times \Delta(R_n - G) + \gamma\left(\frac{900}{T+273} U_2(e_s - e_a)\right)\right]}{\Delta + \gamma(1 + 0.34\, U_2)} \qquad (1)$$

Where:

ET_o : is the reference evapotranspiration [$mm.day^{-1}$];

R_n : is the net radiation at the crop surface [MJ m^{-2} day^{-1}];

G : is the soil heat flux density [MJ m^{-2} day^{-1}];

T : is the mean daily air temperature at 2 m height [°C];

U_2 : is the wind speed at 2 m height [m.s^{-1}];
e_s : is the saturation vapour pressure [kPa];
e_a : is the actual vapour pressure [kPa];
$e_s - e_a$: is the saturation vapour pressure deficit [kPa];
Δ : is the slope vapour pressure curve [kPa.°C^{-1}]; and
γ : is the psychrometric constant [kPa.°C^{-1}]

Due to the large amount of data needed for the calculation of ETo, the software REF-ET version 4.1, developed by (Allen, 2000) was used.

Artificial neural network (ANN)

An artificial neural network is a highly interconnected network of many simple processing units called neurons, which are analogous to the biological neurons in the human brain. Neurons having similar characteristics in an ANN are arranged in groups called layers. The neurons in one layer are connected to those in the adjacent layers, but not to those in the same layer. The strength of the connection between the two neurons in adjacent layers is represented by what is known as a 'connection strength' or 'weight'. An ANN normally consists of three layers which are an input layer, a hidden layer and an output layer (Bishop, 1995).

In a feed forward network, the weighted connections feed activations is only in the forward direction from an input layer to the output layer. In a recurrent network additional weighted connections are used to feed previous activations back into the network. The structure of a feed-forward ANN is shown in figure 2. In figure 2, the circles represent neurons; the lines joining the neurons represent weights; the inputs are represented by X's; Y represents the output; W_{ij} and W_{jk} represent the weights between input and hidden, hidden and output layers, respectively.

An important step in developing an ANN model is the training of its weight matrix. The weights are initialized randomly between a suitable range and then updated using a certain training mechanism (Minasny & McBratney, 2002) and (Jain & Kumar, 2006).

ANN is one of the non-parametric models that (do not need to any assumptions about the nature of the variables and their relationships with each other), discover nonlinear relations without the need of knowing the shape of this relationship. This is the reason for the power of ANN method. So the researchers focus on selecting the best network structure, best activation functions and best training algorithm which give the best results of the models. The implementation of such steps is very complicated. However, with the development of computers, it is easy to perform.

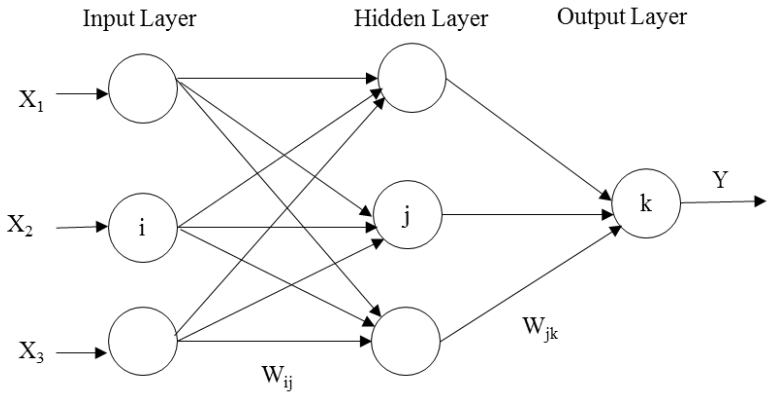

Figure: (2). The structure of a feed forward ANN (Oliveira et al., 2010)

Artificial Neural Net Work Development

In this study, the input variables to the ANN model include T_{mean}, RH_{mean} and extraterrestrial radiation R_a, while the output of the model produced predicted ETo. The extraterrestrial solar radiation is not measured data but is estimated for a certain day and location. One of the outputs of the REF-ET model version 4.1 is extraterrestrial radiation (R_a) (Allen, 2000).

The extraterrestrial radiation, for each day of the year and different latitudes can be estimated from the solar constant, the solar declination and the time of the year by:

$$R_a = \frac{24\,(60)}{\pi}\, G_{sc}\, d_r \left[\omega_s \sin(\varphi)\sin(\delta) + \cos(\varphi)\cos(\delta)\sin\left(\omega_s\right)\right] \qquad (2)$$

Where:
R_a: Extraterrestrial radiation [MJ m^{-2} day^{-1}],
G_{sc} : Solar constant = 0.0820 [MJ m^{-2} min^{-1}],
d_r : Inverse relative Earth-Sun,
ω_s : Sunset hour angle [rad],
φ : Latitude [rad],
δ : Solar declination [rad],

The data were divided into two groups. The first group 70% (311) is called the training set and 30% (133) is called validating datasets. Thus, the training data (from January 1963 to December 1988) were used to train the network and validating data (from January 1989 to December 1999) to validate the network.

The data used in this study were normalized for preventing and overcoming the problem associated with the extreme values. ANN models with 5 hidden layers have been tried for the present study. The output of the network is the values of predicted ETo. Training and validation of the networks are accomplished by ANNdotNET V 1.3 (Hrnjica, 2020). ANN models are trained using Feedforward network that uses a back propagation learning algorithm with Stochastic Gradient Decent (SGD) learner and 0.01 learning rate. The hyperbolic tangent (TanH) activation function was adopted.

The best ANN architecture for prediction of average FPM are selected on the basis of statistical parameters like root mean square error (RMSE), Coefficient of determination (R^2) and Nash-Sutcliffe (NSE).

Performance criteria:

The performance of the models was evaluated by a set of test data using root mean square error (RMSE), coefficient of determination (R^2) (Kennedy & Neville, 1986), and Nash-Sutcliffe efficiency (NSE) (Nash & Sutcliffe, 1970), between measured and predicted values. These statistics parameters are defined as follows:

$$RMSE = \sqrt{\frac{\sum_{i=1}^{n}(ET_{ANN} - ET_{FPM})^2}{\mathrm{n}}} \qquad (3)$$

$$R^2 = \frac{\left[\sum_{i=1}^{n}\left(ET_{ANN} - \overline{ET}_{ANN}\right)\left(ET_{FPM} - \overline{ET}_{FPM}\right)\right]^2}{\sum_{i=1}^{n}\left(ET_{ANN} - \overline{ET}_{ANN}\right)^2 \sum_{i=1}^{n}\left(ET_{FPM} - \overline{ET}_{FPM}\right)^2} \qquad (4)$$

$$\mathrm{NSE} = 1 - \frac{[\sum_{i=1}^{n}(ET_{FPM} - ET_{ANN})]^2}{\sum_{i=1}^{n}\left(ET_{FPM} - \overline{ET}_{FPM}\right)^2} \qquad (5)$$

Smaller values of RMSE and higher values of R^2 indicate higher model performance. The Nash-Sutcliffe (NSE) efficiency is used to evaluate the predictive power of the model and varies from -∞ to 1, with 1 being the perfect fit between the data estimated by the model and the measured data.

Where:
ET_{FPM} : FPM , (mm.day^{-1}),
ET_{ANN} : Predicted evapotranspiration, (mm.day^{-1}),
$\overline{ET}_{FPM}$: Average FPM, (mm.day^{-1}),
$\overline{ET}_{ANN}$: Average predicted evapotranspiration, (mm.day^{-1}),
n : Total number of samples.

A summary of the statistical description of the data used as inputs in the Neural Network model is presented in the table (2).

Table:(2). Statistical parameters of the climatic variables used for training and validation processes.

Statistical parameters	Climatic Variables		
	T_{mean} (°C)	RH_{mean} (%)	R_a (MJ m^{-2} day^{-1})
Training processes			
Maximum	25.2	89	41.46
Minimum	6.2	39	17.99
Mean	16.44	68.05	30.66
Standard Deviation	5.11	9.47	8.38
Count	311	311	311
Validation processes			
Maximum	25.9	83	41.46
Minimum	7.7	43	17.99
Mean	16.99	67.27	30.53
Standard Deviation	5.57	8.93	8.45
Count	133	133	133

RESULTS AND DISSCUSSION

Table (3) refers to the number of input, hidden and output nodes of each ANN model. Furthermore, Table (3) presents the statistical results of the optimum ANN models using different input combinations to estimate the FPM. In the training process, the ANN1 model, where only the mean temperature (T_{mean}) was used as an input to this model, the values of RMSE, R^2 and NSE were 0.84, 0.74 and 0.74 respectively. In the validation process, the performance metrics of the ANN1 model, were 0.74, 0.81 and 0.80 for RMSE, R^2 and NSE respectively.

Table:(3). Performance criteria of the ANN models during training and validation

Model	Input variables	Structure	Training			Validation		
			RMSE	R^2	NSE	RMSE	R^2	NSE
ANN1	T_{mean}	1-5-1	0.84	0.74	0.74	0.74	0.81	0.80
ANN2	T_{mean}, R_a	2-5-1	0.50	0.90	0.90	0.40	0.94	0.94
ANN3	RH_{mean}	1-5-1	0.94	0.68	0.68	0.96	0.68	0.66
AAN4	RH_{mean}, R_a	2-5-1	0.49	0.91	0.91	0.52	0.90	0.90
ANN5	T_{mean}, RH_{mean}	2-5-1	0.39	0.94	0.94	0.46	0.94	0.92
ANN6	T_{mean}, RH_{mean}, R_a	3-5-1	0.23	0.98	0.98	0.26	0.98	0.97

The scatter plot of predicted ETo values by the ANN1 model, compared with the FPM during the validation process, is presented in Figures (3). ANN2 model was performed better than ANN1. It can be observed that the presence of some of the input variables, such as extraterrestrial radiation (R_a) significantly affects the model's performances. Where RMSE, R^2 and NSE were 0.40, 0.94 and 0.94 respectively, i.e. a 16.05% increase in R^2. The scatter plot of predicted ETo values by the ANN2 model, compared with FPM is shown in Figure (4).

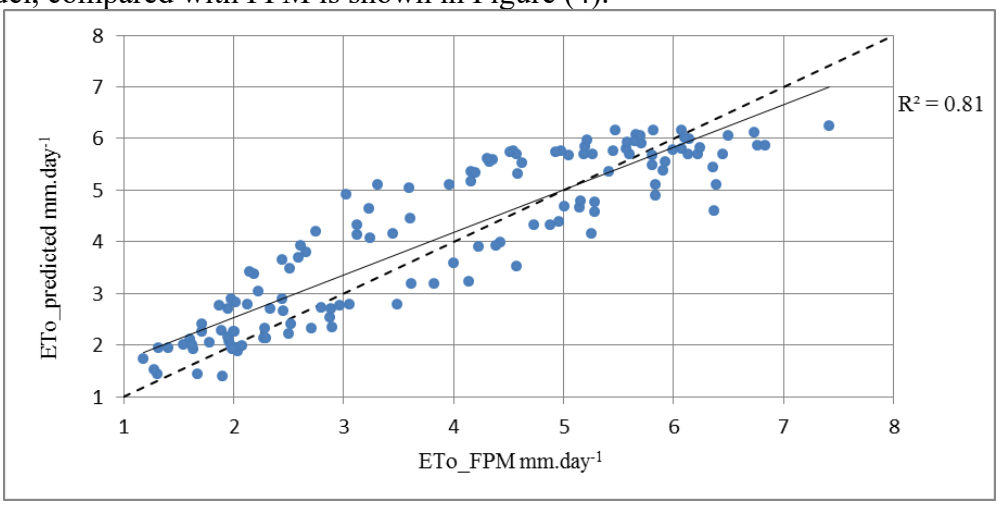

Figure: (3). scatter plot of predicted ETo values by the ANN1 model, compared with FPM during validation.

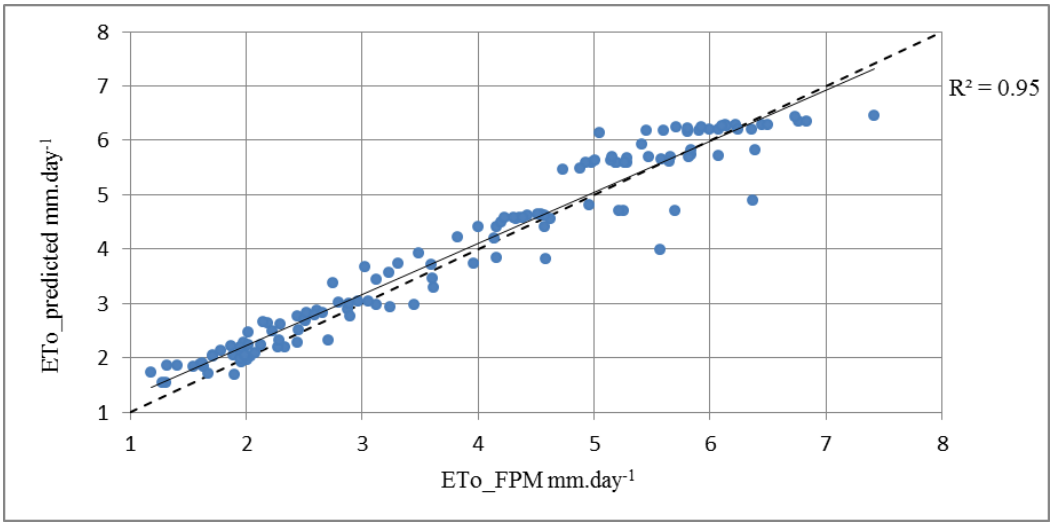

Figure: (4). scatter plot of predicted ETo values by the ANN2 model, compared with FPM during validation.

ANN3 model has the lowest performance compared with other combinations. In this model, only the mean relative humidity (RH_{mean}) was used. Figure (5) shows the scatter plot of this relationship. Figures from (6) to (8) show the scatter plot of predicted ETo values by the ANN4, ANN5 and ANN6 respectively compared with the FPM during the validation process. Where, (RH_{mean}+ R_a), (T_{mean}+ RH_{mean}) and (T_{mean}+ RH_{mean}+ R_a) were used for ANN4, ANN5 and ANN6 respectively.

Among all combinations of ANN models, the highest performance was with ANN6 model. Where the values of RMSE, R^2 and NSE were, 0.26, 0.98 and 0.97 respectively. These results correspond to the results of (Genaidy, 2020),(Heramb et al., 2023),(Rajput et al., 2023),(Abdel-Fattah et al., 2023),(Tunalı et al., 2023).

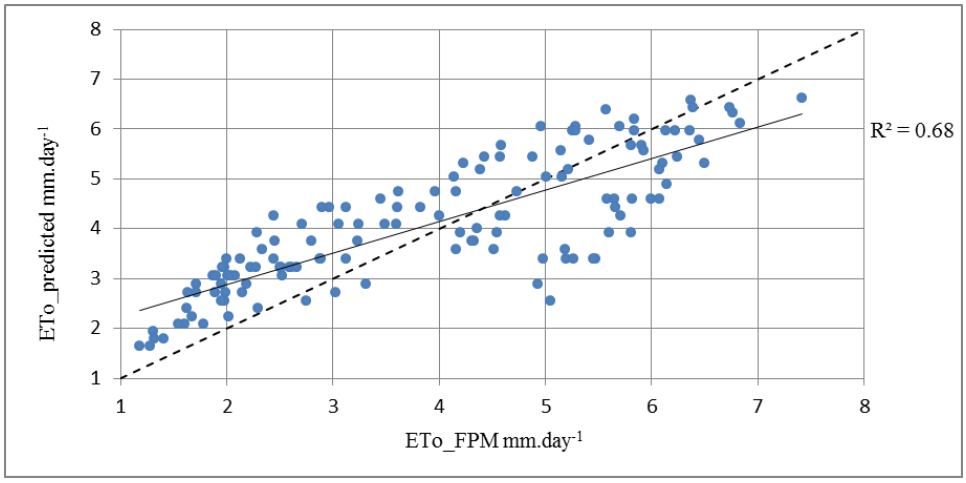

Figure: (5). scatter plot of predicted ETo values by the ANN3 model, compared with FPM during validation.

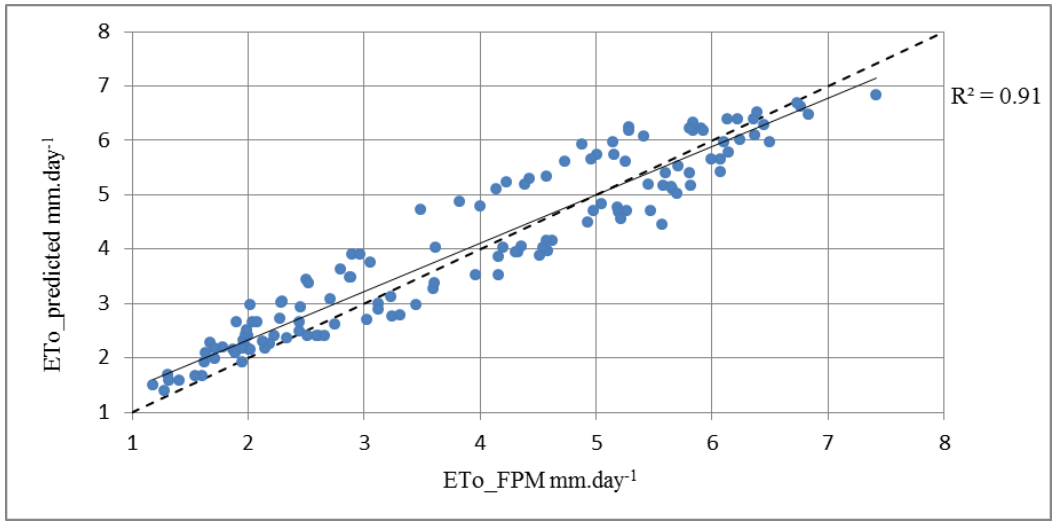

Figure: (6). scatter plot of predicted ETo values by the ANN4 model, compared with FPM during validation.

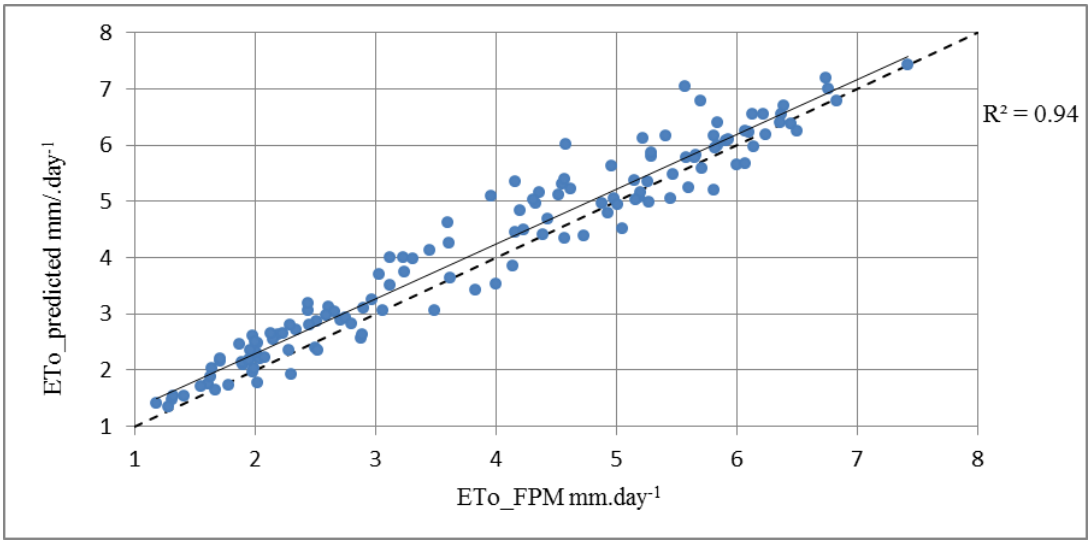

Figure: (7). scatter plot of predicted ETo values by the ANN5 model, compared with FPM during validation.

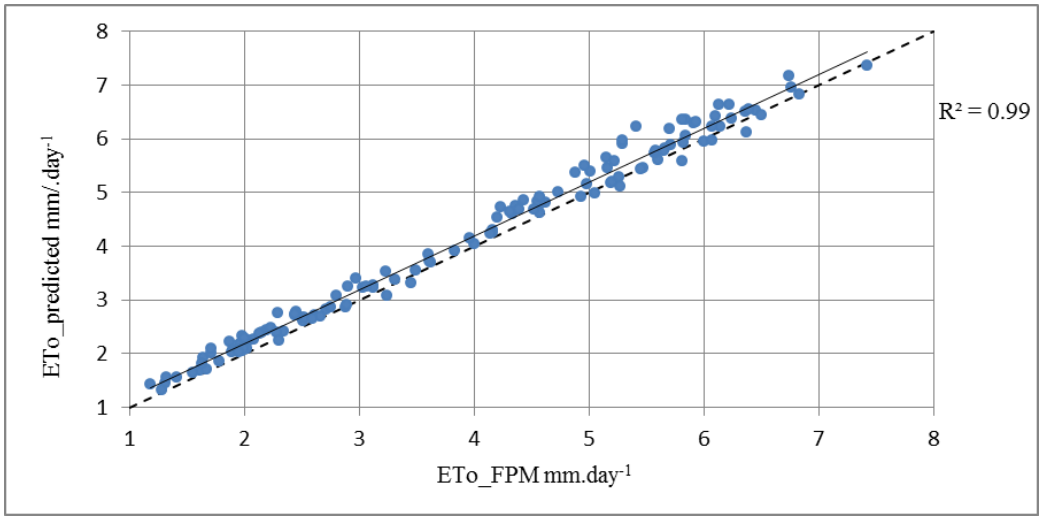

Figure: (8). scatter plot of predicted ETo values by the ANN6 model, compared with FPM during validation.

CONCLUSION

From the previous discussion it is clearly seen that depending on the number of climatic variables available to calculate the reference evapotranspiration (ETo) using artificial neural networks (ANNs), It can recommend using the mean temperature (T_{mean}) with the extraterrestrial radiation (R_a) or using the mean relative humidity (RH_{mean}) with the extraterrestrial radiation. The best result obtained was using the average temperature (T_{mean}), the average relative humidity (RH_{mean}), and the extraterrestrial radiation (R_a).

Duality of interest: The authors declare that they have no duality of interest associated with this manuscript.

Author contributions: All Authors contributed equally to this manuscript.

Funding: This manuscript did not receive any funding.

REFERENCES

Abdel-Fattah, M. K., Kotb Abd-Elmabod, S., Zhang, Z., & Merwad, A.-R. M. (2023). Exploring the Applicability of Regression Models and Artificial Neural Networks for Calculating Reference Evapotranspiration in Arid Regions. *Sustainability, 15*(21), 15494.

Achite, M., Jehanzaib, M., Sattari, M. T., Toubal, A. K., Elshaboury, N., Wałęga, A., Krakauer, N., Yoo, J.-Y., & Kim, T.-W. (2022). Modern techniques to modeling reference evapotranspiration in a semiarid area based on ANN and GEP models. *Water, 14*(8), 1210.

Allen, R. G. (2000). REF-ET: Reference Evapotranspiration calculation software for FAO and ASCE standarized equatioin Version 3.1.16 for Windows. University of Idaho Research and Extension Center, Kimberly, Idaho

Allen, R. G., Clemmens, A. J., Burt, C. M., Solomon, K., & O'Halloran, T. (2005). Prediction accuracy for projectwide evapotranspiration using crop coefficients and reference evapotranspiration. *Journal of Irrigation and Drainage Engineering, 131*(1), 24-36.

Allen, R. G., Pereira, L. S., Raes, D., & Smith, M. (1998). Crop evapotranspiration: guidelines for computing crop water requirements. FAO Irrigation and Drainage Paper no. 56, Rome, Italy.

Allen, R. G., Pruitt, W. O., Wright, J. L., Howell, T. A., Ventura, F., Snyder, R., Itenfisu, D., Steduto, P., Berengena, J., & Yrisarry, J. B. (2006). A recommendation on standardized surface resistance for hourly calculation of reference ETo by the FAO56 Penman-Monteith method. *Agricultural Water Management, 81*(1-2), 1-22.

Bishop, C. (1995). *Neural Networks for Pattern Recognition*. University Press.

Dinpashoh, Y. (2006). Study of reference crop evapotranspiration in IR of Iran. *Agricultural Water Management, 84*(1-2), 123-129.

Ekhmaj, A. I. (2012). Prediction of evapotranspiration using artificial neural networks model. Malaysia In: International Annual Symposium on Sustainability Science and Management. Terengganu,

Ekhmaj, A. I., Ben Zagta, M., Daw Ezlit, Y., & Shaghleb, A. M. (2013). Estimation of the Reference Evapotranspiration in Sirt Region Using an Artificial Neural Networks. *The Lybian Journal of Agriculture, 18*(1-2), 1-14.

Genaidy, M. (2020). Estimating of evapotranspiration using artificial neural network. *Misr Journal of Agricultural Engineering, 37*(1), 81-94.

Haykin, Simon. 1999. "Neural networks a comprehensive introduction." In.: Prentice Hall, New Jersey.

Heramb, P., Singh, P. K., Rao, K. R., & Subeesh, A. (2023). Modelling reference evapotranspiration using gene expression programming and artificial neural network at Pantnagar, India. *Information Processing in Agriculture, 10*(4), 547-563.

Hrnjica, B. (2020). ANNdotNET--deep learning tool on. NET Platform. *arXiv preprint arXiv:2009.11112*.

Irmak, S., Irmak, A., Allen, R., & Jones, J. (2003). Solar and net radiation-based equations to estimate reference evapotranspiration in humid climates. *Journal of Irrigation and Drainage Engineering, 129*(5), 336-347.

Jain, A., & Kumar, A. (2006). An evaluation of artificial neural network technique for the determination of infiltration model parameters. *Applied Soft Computing, 6*, 272-282.

Kennedy, J. B., & Neville, A. M. (1986). *Basic Statistical Methods for Engineers and Scientists* (3rd ed.).

Kim, S., & Kim, H. S. (2008). Neural networks and genetic algorithm approach for nonlinear evaporation and evapotranspiration modeling. *Journal of Hydrology, 351*(3-4), 299-317.

Kumar, M., Raghuwanshi, N., & Singh, R. (2011). Artificial neural networks approach in evapotranspiration modeling: a review. *Irrigation Science, 29*(1), 11-25.

Kumar, M., Raghuwanshi, N., Singh, R., Wallender, W., & Pruitt, W. (2002). Estimating evapotranspiration using artificial neural network. *Journal of Irrigation and Drainage Engineering, 128*(4), 224-233.

Landeras, G., Ortiz-Barredo, A., & López, J. J. (2008). Comparison of artificial neural network models and empirical and semi-empirical equations for daily reference evapotranspiration estimation in the Basque Country (Northern Spain). *Agricultural Water Management, 95*(5), 553-565.

Minasny, B., & McBratney, A. B. (2002). The Neuro-m Method for Fitting Neural Network Parametric Pedotransfer Functions. *Soil Science Society of America Journal, 66*, 352-361.

Mohan, S., & Arumugam, N. (1996). Relative importance of meteorological variables in evapotranspiration: Factor analysis approach. *Water Resources Management, 10*(1), 1-20.

Nash, J. E., & Sutcliffe, J. V. (1970). River flow forecasting through conceptual models part I—A discussion of principles. *Journal of Hydrology, 10*(3), 282-290.

Odhiambo, L. O., Yoder, R. E., Yoder, D. C., & Hines, J. W. (2001). Optimization of fuzzy evapotranspiration model through neural training with input–output examples. *Transactions of the ASAE, 44*(6), 1625.

Oliveira, A. L. I., Braga, P. L., Lima, R. M. F., & Cornélio, M. L. (2010, 2010/11/01/). GA-based method for feature selection and parameters optimization for machine learning regression applied to software effort estimation. *Information and Software Technology, 52*(11), 1155-1166. https://doi.org/https://doi.org/10.1016/j.infsof.2010.05.009

Rajput, J., Singh, M., Lal, K., Khanna, M., Sarangi, A., Mukherjee, J., & Singh, S. (2023). Performance evaluation of soft computing techniques for forecasting daily reference evapotranspiration. *Journal of Water and Climate Change, 14*(1), 350-368.

Sudheer, K., A. Gosain, & K. Ramasastri. (2003). Estimating Actual Evapotranspiration from Limited Climatic Data Using Neural Computing Technique. *Journal of Irrigation and Drainage Engineering, 129*(3), 214-218. https://doi.org/doi:10.1061/(ASCE)0733-9437(2003)129:3(214)

Temesgen, B., Eching, S., Davidoff, B., & Frame, K. (2005). Comparison of some reference evapotranspiration equations for California. *Journal of Irrigation and Drainage Engineering, 131*(1), 73-84.

Trajkovic, S., Todorovic, B., & Stankovic, M. (2003). Forecasting of reference evapotranspiration by artificial neural networks. *Journal of Irrigation and Drainage Engineering, 129*(6), 454-457.

Tunalı, U., Tüzel, I. H., Tüzel, Y., & Şenol, Y. (2023). Estimation of actual crop evapotranspiration using artificial neural networks in tomato grown in closed soilless culture system. *Agricultural Water Management, 284*, 108331.

Al-Mukhtar Journal of Basic Sciences 22 (1): 75-84, 2024
Doi: https://doi.org/10.54172/d09k0c70

Research Article **Open Access**

Morphological and Histological Description of Spiny Dogfish shark Liver, *Squalusacanthais*(Linnaeus,1758), Elasmobranchii, Squaliformes

Nagla A. Elfagi

***Corresponding author:**
elfaghi.n.a@sci.misuratau.edu.ly
Department of Zoology, Faculty of Science, Misurata University, Libya.

Received:
03 October 2023

Accepted:
24 February 2024

Publish online:
30 April 2024

Abstract

The current study describes the morphological and histological appearance of the liver of the spiny dogfish *Squalusacanthais*, which is classified as Class: Chondrichthyes, Subclass: Elasmobranchi. Morphologically, the liver was observed as large, and consists of two symmetrical lobes connected from the upper side, and the gallbladder was observed in the right lobe. Histologically, liver sections were prepared with H&E stain, and examined with a light microscope. Hepatic parenchyma was surrounded by a capsule of connective tissue and primarily composed of hepatocytes. The nuclei of these cells were observed at the terminal site, with lipid droplets in the cytoplasm. Central veins were observed, surrounded by connective tissue and lined with a squamous epithelial layer. Hepatocytes were, separated by numerous blood sinusoids with connective tissue. Blood arteries were observed, surrounded by thick muscular fiber walls and narrow lumens compared to veins. The portal vein was observed, along with the artery and bile duct, surrounded by a thick connective tissue. The bile duct was surrounded by a layer of muscular fibers, lined with a simple columnar epithelial layer with clear nuclei, and a connective tissue layer. Melanin-containing cells were observed, but no hepatic lobules or connective tissue were seen between them. Additionally, Hepato-pancreatic tissue was not identified.

Keywords: Histological Structure; Liver; Hepatocytes; *Squalusacanthais*; Chondrichthys; Elasmobranchs.

INTRODUCTION

Fish form the largest and most diverse group of vertebrates, teleosts representing more than 25,000 of all known fish species, Chondrichthyes, on the other hand, do not exceed 800 species (Bone & Moore, 2008). The spiny dogfish shark, *Squalusacanthias*, belongs to the class Chondrichthyes, subclass Elasmobranchii, and order Squaliformes. It is a carnivorous fish (Heckmann, 2001) that lives in saltwater in the northeast Atlantic Ocean and the Mediterranean Sea (Marine Biology Blog in Libya).

Morphological, anatomical, and histological studies of the digestive system of fish and its associated glands play an important role in understanding the mechanisms of food digestion and absorption (De Melo Germano et al., 2014). The liver is one of the most important glands associated with the

digestive system. It is a relatively large vital organ and has a similar basic function and structure in both Chondrichthyes and teleosts. The liver has many functions similar to those found in mammals, such as the production of vital chemicals for the process of digestion. The liver is highly sensitive to pollution with organic and inorganic compounds, as they can accumulate over time and cause life-threatening conditions due to the liver's ability to remove toxins and store harmful components. It is often used as a biological marker for environmental pollutants (Eppler et al., 2007). Additionally, the liver's functions include storing and producing energy, hormonal balance, and clotting, and it is the center of metabolism (De Melo et al., 2019). In fish, the liver produces bile and maintains metabolic balance, which includes processing and storing carbohydrates, proteins, fats, and vitamins. The liver also plays a major role in synthesizing plasma proteins such as albumin and fibrinogen, and liver tissues vary among species, but there are general features present in most species (Genten et al., 2009). Typically, it is reddish-brown in carnivorous animals, depending on the diet. The liver may be located in the anterior part of the abdominal cavity and adapts its size and shape to the available space between other visceral organs (Sales et al., 2017), or in some species, it may be elongated along the abdomen or attached to other intestines, or it may be a composite organ in the form of a hepato-pancreatic organ.

The liver tissues of fish differ from those of mammals in that hepatic cells rarely tend to form cords or distinctive lobules, and the typical portal triads are not clear (Mumford et al., 2007). The structural tissue of the liver is enclosed in a thin capsule of fibrous connective tissue and consists primarily of multi-surfaced hepatocytes with a visible cellular membrane usually with central nuclei. Glycogen deposits are often dissolved and fats are stored, resulting in a wide variety of liver tissues (Genten et al., 2009). The central veins can be randomly observed throughout the hepatic parenchyma, and structures with small gaps are apparent in hepatocytes due to the presence of fats. The presence of glycogen may indicate the fish's ability to synthesize or break down glycogen according to metabolic needs. The hepatic sinusoids are distributed among the hepatocytes that form a wide network. These sinuses are lined with blanket cells with dark nuclei and Kupffer cells that are star-shaped with large dark oval nuclei. In addition, a large amount of connective tissue is identified around blood vessels, and a network of blood vessels and bile ducts is found within the tissue components of the liver (Mokhtar, 2017).

There are limited studies on the liver tissues of elasmobranchs. A study conducted by (De Melo et al., 2019) indicated that the liver in the blue shark *Prionaceglauca* is the largest gland in the body, located in the abdominal cavity and is shaped like two elongated lobes, with the tip of the lower lobe tapered in a semicircular shape, while the right and left lobes of the liver are symmetrical. Elasmobranchs do not have a swim bladder, which requires them to constantly move to avoid drowning, which is why they have a high-fat content to float, as the liver acts as a hydrostatic organ.

Oguri (1978) in a study on dogfish, (Adams et al., 2015) in their study on the longfin mako shark (*Isuruspaucus*), and (Gajié et al., 2020) in their study on the catshark (*Scyliorhinuscanicula*) indicated that hepatocytes contain a large number of fat droplets and contain brown pigment granules called melano-macrophage centers MMC.

(Seyrafi et al., 2009) in their study on *Pangasiushypophthalmus*, as well as (Hibiya, 1982; Mumford *et al*., 2007; Coetzee, 2018) described the liver as being covered with a thin capsule consisting of a serous layer and connective tissue, part of which extends into the liver parenchyma. The liver lobules were not visible, and the liver parenchyma mainly consisted of multiple surface hepatocytes with central nuclei, with many hepatic sinusoids and cavities for fat storage. The hepatocytes of the

liver (spherical shaped) are irregularly distributed with sinusoids in between (Hibiya, 1982; Mumford et al., 2007).

The hepatic ducts that collect yellow bile from the liver were observed by (Borucinska et al., 2009) in their study on the liver of three species of fish. The portal triad, consisting of the hepatic vein, hepatic artery, and bile duct, has been described in teleost, but studies are limited to elasmobranchs (Akiyoshi& Inoue, 2004; Coetzee, 2018).

Due to the importance of comparative studies of fish in interpreting some phenomena and evolutionary relationships imposed by environmental, genetic, and life conditions on this vertebrata in general, this research was designed to study the morphological and histological structure of the liver in a type of fish belonging to the class of chondrichthyes.

MATERIALS AND METHODS

The current study was conducted on a type of chondrichthyes, specifically the spiny dogfish *S. acanthais* (Figure 1). The samples were collected from the fishing port in the area of Qasr Ahmed, and the area of Abu Qareen in the east of Misuratah, with a total of 4 samples. Morphometric measurements were conducted on the samples; the average lengths were (67.2 cm), and the average weights were (2.5 kg). The samples were then transferred to the animal science department laboratory at the Faculty of Science, Misrata University, in plastic polythene bags with ice to preserve them until the study was conducted. The fish were identified visually, and external morphometric measurements were taken. A longitudinal incision was made in the abdominal cavity using a scalpel from the beginning of the anus to the gill chamber, and then the liver was removed and placed in a dissecting dish to identify the main parts. Afterward, it was washed with a saline solution, cut into small pieces, and immediately transferred to 10% neutral formalin fixative to preserve it until the next step.

For histological studies, parts of the liver were taken and cut into small pieces, and placed in vials containing formalin w (10%). Each vial was labeled with the name of the fish used in the study and the specific part of the sample. The study samples were then sent to the tissue unit in the Misrata laboratory. The targeted study samples were processed in an ascending series of ethanol (70-100%), then soaked in xylene, embedded in paraffin wax, and then cut into tissue sections using the rotary microtome model Cut 5062 (an Argentic company SLEE Medical) with a thickness of 5 micrometers. The tissue sections were stained with hematoxylin and eosin (H&E) dyes, washed with water, dehydrated in an ascending series of ethanol, soaked in xylene, and mounted with DBX glue for examination under a light microscope (Bancroft & Stevens, 1977). The tissue sections were then photographed using a Motic BA 310 Digital microscope.

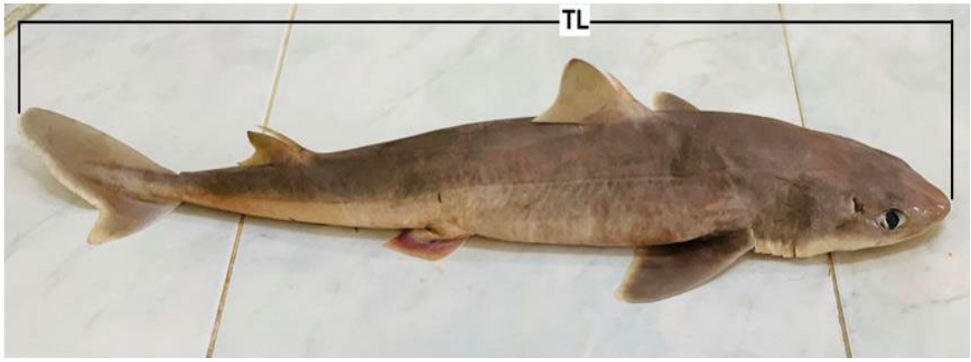

Figure: (1). The general appearance of the fish studied: *S acanthais*, Total length(TL).

RESULTS ANDDISCUSSION

The morphological examination showed that the liver of the *S. acanthais* fish occupies most of the abdominal cavity. It is large, takes a ventral position relative to the stomach and intestines, has a pinkish-yellowish color, and consists of two symmetrical lobes connected by an isthmus. Each lobe is elongated, broad at the top, tapered at the end. Additionally, the gallbladder was observed in the right lobe as shown in (Figure 2: A, B). These results are consistent with the findings reported by (De Melo et al., 2019) in their study of the liver of the *Prionaceglauca* shark, describing it as the largest gland in the body, located in the abdominal cavity, consisting of two symmetrical elongated lobes with a tapered lower end in a semi-circular shape, and with the gallbladder extended in the right lobe. In his study on the liver of the European Spotted Dogfish, (Oguri, 1978) described it as relatively small in size, which contradicts the current consensus that elasmobranchs typically have large livers. This was confirmed by (Genten et al., 2009; De Melo et al., 2019), who stated that the liver occupies more than 80% of the abdominal cavity. Like other chondrichthys, sharks do not have a swim bladder and must constantly move to avoid sinking. The average density of the liver is related to the fat content, and the high oil content of these fish allows them to float more easily in the water column, acting as a hydrostatic organ to help them maintain their position. The liver represents 20% of the total body weight (de Melo, et al. 2019), and its size and weight vary depending on the species, age, and season. According to (Brusle & Anadon, 1996), up to 90% of the liver can be made up of oil. There are also differences in liver structure between males and females, as well as between mature and immature fish. It has been observed that fat storage begins at the embryonic stage, where hepatocytes accumulate fat in the cytoplasm according to the growth of the embryo, as demonstrated by (De Melo et al., 2019) in their study on sharks.

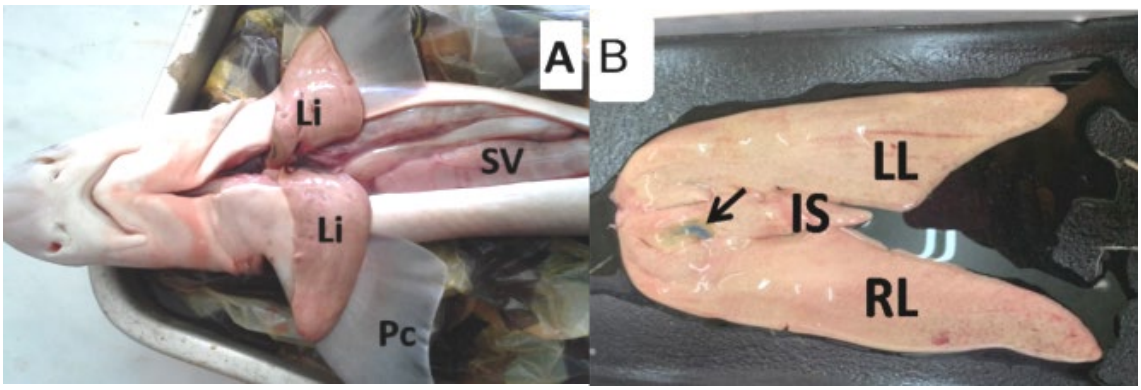

Figure: (2). The phenotype and location of the liver in Dogfish shows : A - liver lobes(Li), spiral valve (SV), pectoral fin (pc), B - right lobe of the liver (RL), left lobe of the liver(LL), gallbladder (arrow), isthmus (Is).

The histological appearance: The histological examination results in (Figure 3:A, B) show a section passing through the liver of Spiny dogfish *S.acanthais* composed of typical functional units associated with fish liver, including the basic structural tissue of the liver (parenchyma), blood vessels, and the biliary canal system, surrounded by a thin capsule of connective tissue. The hepatic parenchyma appears primarily as hepatocytes with a clear cellular membrane, rich in lipid droplets. Due to the large amount of fat in the liver, these hepatocytes vary in size and shape and do not have visible cytoplasm in H&E preparation, but they have an unstained appearance (white) (Figure 3). It seems that the organization of the liver parenchyma in elasmobranchs are less organized than in teleost. Additionally, some functional units such as biliary canals were less prominent. The high content of fat in the liver may have led to an evolutionary change in elasmobranch hepatic parenchyma, where hepatocytes were observed to be organized in separate clusters, separated by a thin layer of

connective tissue that likely provides support to the parenchyma. The high fat content may lead to a less stable organ structure without supportive connective tissue (Coetzee, 2022). The blood vessels consist of spherical arteries, large veins, and small blood sinuses. The arteries have a significantly thicker muscular layer and connective tissue layer surrounding the vessel compared to the larger veins. It is also difficult to distinguish the central veins and portal veins. The section shows the presence of the central vein surrounded by connective tissue and containing blood cells, as observed in (Figure 3& 4), and the numerous blood sinuses that drain into the central veins are visible due to the single file of red blood cells visible in these capillaries. The figure (Figure 3: A, B) also indicates the leakage of blood cells from blood vessels that appear as blood clots, although the liver does not provide the histological structure of the typical hexagonal liver of mammals, and liver lobules or the connective tissue separating them were not observed. Also, Hepato-pancreatic tissue, often identified in some fish species, was not identified.

The results of this study are consistent with the study conducted by (Seyrafi et al., 2009) in their study of *P.hypophthalmus* and Coetzee (2022) in their study on three species of Elasmobranches, *Sphyrnalewini, Carcharhinubrevipinna,* and *Aetobatus narinari*, where they described the liver as covered with a thin capsule composed of the serous layer, and liver lobules were not clearly seen, And the hepatic parenchyma is primarily composed of multi-surfaced hepatocytes usually with central nuclei, and there were many liver sinusoids and gaps for storing fat, and macrophages cells, but (Seyrafi et al., 2009) pointed out the presence of pancreatic-secreting tissues in the liver, which was not consistent with the current study and Coetzee's study. (2022) where they did not observe the presence of pancreatic tissues within the hepatic parenchyma.

In (Figures 3: C, D), the external capsule appears composed of connective tissue lined with squamous epithelial cells that surround the parenchyma of the liver. Also, the different hepatocytes appeared to differ in shape and size, surrounded by a visible cellular membrane, and the nuclei of these cells were observed at the peripheral site of the cytoplasm and not central because they contained droplets of fat. This is consistent with what (De Melo et al., 2019) pointed out in their study of the liver in the shark *P. glauca* and (Coetzee, 2022) in his study of three species of elasmobranches fish *S. Lewin, C. brevipinna*, and *A. narinari*, where they mentioned that hepatocytes appear in different sizes of fat gaps that are introduced into the cells, leading to a shift in their nuclei from the center to the periphery. Given that the liver contains a tremendous amount of fat in all the sections examined, the liver tissue appears like adipose tissue.

Also, the results showed the presence of macrophages that play a role in engulfing foreign bodies and removing bacterial causes of inflammation and disease that enter the bloodstream. This is consistent with what (Seyrafi, et al., 2009); Coetzee, 2022) have pointed out, and may be present due to environmental hepatic toxins from human pollution (Gajić et al., 2020). The presence of these cells in hepatic parenchyma is consistent with what was found in the study by (Adams et al., 2015; Gajić et al., 2020) on different species of elasmobranches. Additionally, histological examination revealed the presence of melanomacrophage centers, which contain melanin granules, and these structures appeared mostly spherical and stained dark brown in H&E.

These results were consistent with the findings of (Oguri, 1978) in his study of the liver of European spotted dogfish, where he noted that hepatocytes contain a large number of fat droplets, as well as brown pigment granules called melanin granules, which are usually irregularly distributed in liver parenchyma and serve as evidence of environmental stress. They are also an indicator of water quality and oxygen content, as well as a sign of chemical pollution in the environment where fish live (Agius and Roberts, 2003). Some studies on elasmobranch species have also reported the pres-

ence of MMCs, such as the study conducted by (Gajić et al., 2020) on the shark (*Scyliorhinuscanicula*). Also, in a study conducted by (Borucinska et al., 2009) on three species of elasmobranchs, the mako shark, the thresher shark, and the blue shark, the authors reported the presence of MMC in the liver, testes, kidneys, and spleen. According to (Adams et al., 2015), MMC was found in the liver of the shark *Isuruspaucus*, it has detoxification and recycling functions in the liver, as it breaks down endogenous and exogenous materials and then becomes metabolic dumps (Mooney, 2012).

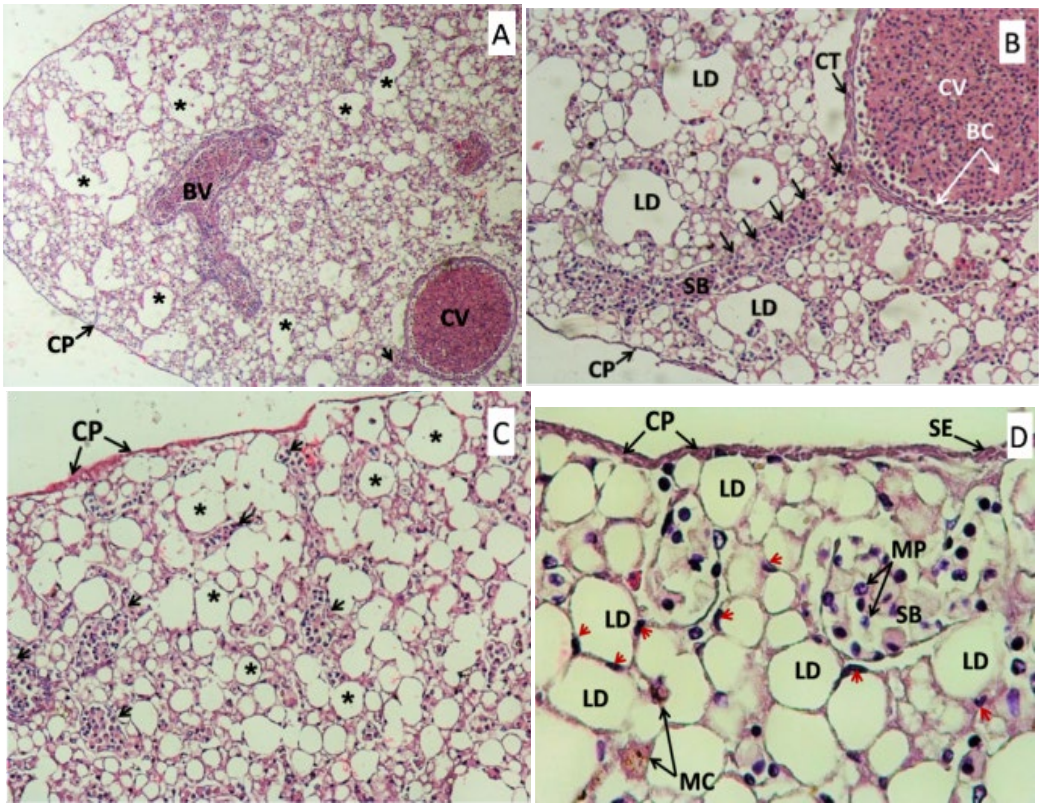

Figure: (3). Histological sections through the liver in a dogfish (*S.acanthias*)
A-Capsule (CP), central vein (CV), blood vessel (BV), hepatocytes containing fat droplets (*), blood leak (Arrowhead in black) 40X, H&E.
B- Capsule (CP), central vein (CV), connective tissue surrounding the central vein (CT), blood cells (BC), hepatocytes containing fat droplets (LD), blood sinusoid (SB), blood leak (arrows) 100X, H&E.
C-Capsule (CP), blood sinusoids (Arrowhead), hepatocytes containing fat droplets (*) 100X, H&E.
D-Capsule (CP), squamous epithelial cells (SE), blood sinusoids (SB), hepatocytes containing fat droplets (LD), hepatocyte nuclei (Arrowhead in red), macrophage cells (MP), melanocyte centers (MC) 400X, H&E.

The portal triads were identified in some tissue areas, where the portal vein and its blood cells, the blood artery, and the bile duct are collected, as the connective tissue appears thick and blue around the bile ducts and veins (Figure 4:A, B, C, D). The bile duct appears surrounded by a layer of muscle fibers and lined with a simple columnar epithelial layer, with clear nuclei that appear dark in color, and a layer of connective tissue near the portal vein, as in (Figure 4: B). However, it cannot be compared to the typical portal triad found in mammalian livers, and this is consistent with what was mentioned by (Genten et al., 2009; Mumford et al., 2007), and Coetzee (2022) in their study on several species of Chondrichthyes.

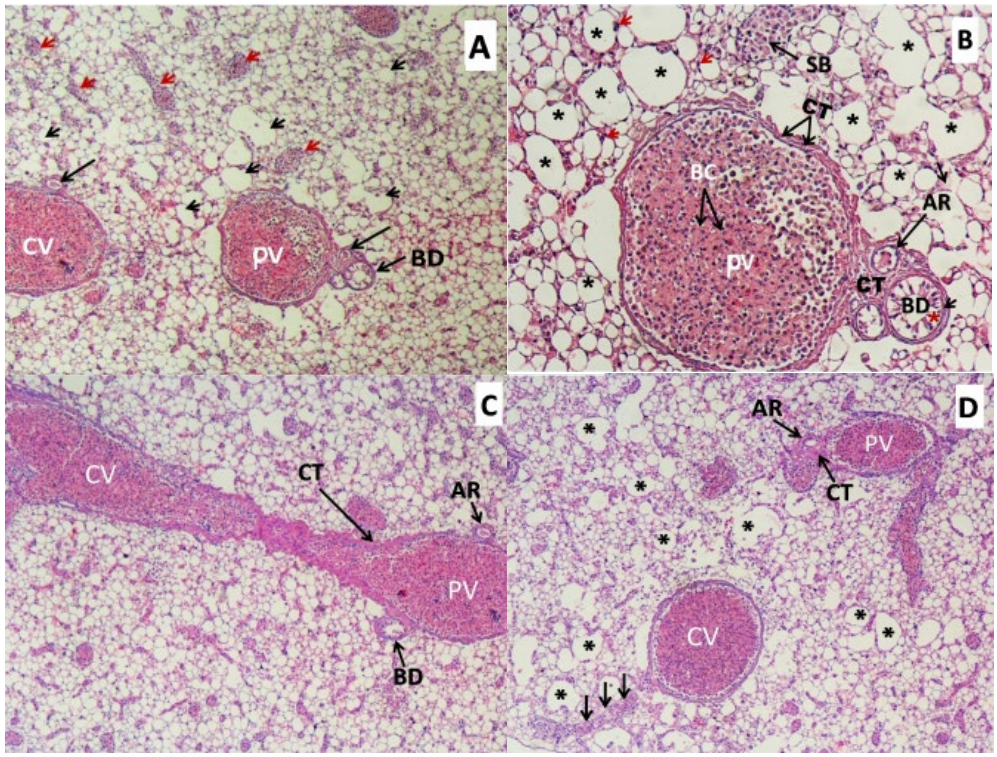

Figure: (4). A- Central vein (CV), portal vein (PV), bile duct (BD), blood artery (long arrow), blood sinusoids (Arrowhead in red), hepatocytes with fat droplets (Arrowhead in black) 40X, H&E. **B**-Hepatocytes showing fat (*in black), hepatocyte nuclei (Arrowhead in red), blood sinusoids (SB), portal vein (PV), red blood cells (BC), artery (P), bile duct(BD), connective tissue (CT), columnar epithelial cells (* in red) 100 X, H&E. **C**- Central vein (CV), portal vein (PV), bile duct (BD), blood artery (P), connective tissue (CT) 40X, H&E. **D**- Portal vein (PV), blood artery (P), connective tissue (CT), hepatocytes containing fat droplets (*), central vein (CV), blood leak (Arrowhead in black) 40X, H&E

In mammals, the accumulation of fat within hepatocytes is considered a disorder known as hepatic steatosis. When there is excess fat for a prolonged period, hepatocytes may become damaged and inflamed. In sharks, however, this condition is a healthy and necessary adaptation to help them float, as well as to serve as a glycogen store for conversion to glucose and energy, because they are animals with large energy expenditure. Another function of fat in the liver is its importance during embryonic development, where females use this fat to maintain and nourish their young (De Melo, et al., 2019). Although the accumulation of fat in the shark liver is considered fairly normal, it is also listed here as a change that should be considered in toxicological studies, since the fat content (cytotoxicity) can increase due to exposure to toxic substances since the liver is the main organ of detoxification and is important for the metabolism of fats, proteins, carbohydrates, bile secretion, excretion of toxic substances and a large blood supply, it can play an important role in the extent of exposure to toxic substances (Hibiya, 1982; Van Dyk et al., 2007; Mohamed, 2009; Yancheva et al., 2015; &De Melo et al., 2019). The liver is the main organ for the biological accumulation of substances due to the presence of enzymes that metabolize toxins, which often harm the organ (Mumford et al., 2007; &Borucinska et al., 2009). Elasmobranch species mainly use proteins and fats as part of their energy reserves (Remme et al., 2005). The main component of the liver is squalene, a fatty acid that is also used in the production of cosmetic products (Remme et al., 2005; & Cardeñosa, 2019). Therefore, fat accumulation can be considered somewhat normal, but exposure to toxins can also increase levels above normal, resulting in changes in fat or hepatic steatosis, as suggested in (Adams et al., 2015) study on longfinmako fish.

CONCLUSION

The liver of spiny dogfish, is large, occupying most of the abdominal cavity, and its tissue structure differs from the typical mammalian liver, with the absence of hepatic lobules and typical portal triads being unclear. Hepatocytes appear with varying sizes and contain a huge amount of fat, resembling adipose tissue. In mammalian livers, fat accumulation is considered hepatic steatosis, while in shark livers, it is a healthy and necessary condition. Since Elasmobranchs do not have a swim bladder, the liver acts as a hydrostatic organ to help them float. Pancreatic tissue is absent.

ACKNOWLEDGEMENT

The researchers express their thanks and appreciation to sister Ibtisam Mohammed for helping to bring the samples.

ETHICS

Authors should address any ethical issues that may arise after the publication of this manuscript.

Duality of interest: The authors declare that they have no duality of interest associated with this manuscript.

Author contributions: Contribution is equal between authors.

Funding: No specific funding was received for this work.

REFERENCES

Adams, D., Borucinska, J., Maillet, K., Whitburn, K. & Sander, T. (2015). Mortality due to a retained circle hook in a longfin mako shark /*surs paucus* (Guitart-Mandav). *Journal of Fish Disease*, 38(7): 621-628.

Agius, C., & Roberts, R. J. (2003). Melano-macrophage centres and their role in fish pathology. *Journal of fish diseases*, *26*(9), 499-509.

Akiyoshi, H., & Inoue, A.(2004). Comparative histological study of teleost livers in relation to phylogeny. Zoological Science, 21(8): 841-850.

Bancroft, J. D., & Stevens, A. (1977). Theory and practice of histochemical techniques. *Churchilli Vingstone, New York pi*, *16*, 164-195.

Bone, Q., & Moore, R. (2008). *Biology of Fishes* (3rd ed.). Taylor and Francis. https://doi.org/10.1201/9781134186310

Borucinska, J.D., Kotra, K., Shackett, M.& Barker,T. (2009). Melanomacrophages in three species of free-ranging sharks from the northwestern Atlantic, the blue shark *Prionacae glauca* (L), the shorttih mako, *Isurus oxyrhinchus* Rafinesque, and the thresher, *Alopias vulpinus* (Bonnaterre), *Journal of Fish Diseases*, 32(10): 883-891.

Brusle, J., & Anadon, G. G. (1996). The structure and function of fish liver. Fish Morphology. *Edited by Munshi, JSD and Dutta, HM Science Publishers Inc*.

Cardeñosa, D. (2019). Genetic Identification of threatened shark species in pet food and beauty care. Conservation Genetics, 20: 1383-1387.

Coetzee, H. J. (2018). The effect of organochlorine pesticides aldrin and methoxychlor on the health status of *Clarias gariepinus* by means of a histology-based approach. M.Sc. Dissertation. Department of Zoology. University of Johannesburg. South Africa.

Coetzee, H. J. (2022). *A histological study of selected target organs of three elasmo- branch species from the coast of KwaZu- lu-Natal, South Africa* (Doctoral dissertation, University of Johannesburg

de Melo Germano, R., Stabille, S. R., de Britto Mari, R., Pereira, J. N. B., Faglioni, J. R. S., & de Miranda Neto, M. H. (2014). Morphological charact- eristics of the P terodoras granulosus digestive tube (V alenciennes, 1821) (O steichthyes, D oradidae). *Acta Zoologica*, *95*(2), 166-175.

De Melo, L. F., Cabrera, M. L., Rodrigues, A. C. B., Turquetti, A. D. O. M., Ruivo, L. P., Bruno, C. E. M., & Rici, R. E. G. (2019). Morphological Description of Blue Shark Liver, Prionace glauca (Linnaeus, 1758), Elasmobranchii, Carcharhiniformes. *Int. J. Adv. Eng. Res. Sci*, *6*, 286-290.

Eppler, E., Caelers, A., Shved, N., Hwang, G., Rahman, A. M., Maclean, N., ... & Reinecke, M. (2007). Insulin-like growth factor I (IGF-I) in a growthen- hanced transgenic (GH-overexpressing) bony fish, the tilapia (*Oreochromis niloticus*): indication for a higher impact of autocrine/paracrine than of endocrine IGF-I. *Transgenic research*, *16*(4), 479-489.

Gajic A, AliC A,Kahric A, Bilalovic N, Supié J & Besirovic H. (2020). Melanomacro- phage centeres and diseases occurring in lesser- spotted catsharks, Scyliorhinus canicula (L.), from the southern Adriatic Sea -importance for monitoring. *Acta Adriatica*, 61(2): 175-184.

Genten, F., Terwinghe, E., & Danguy, A. (2009). *Atlas of fish histology*. CRC Press.

Heckmann, R.(2001). Roundworms and their cousins: commen fish invaders. *Journal of Aquacultural of Magaz*. 33-44.

Hibiya, T. (1982). An atlas of fish histology: Normal and pathological features. Kondasha Ltd. Tokyo.

Mohamed, F. A. S. (2009). Histopathological studies on *Tilapia zillii* and *Solea vulgaris* from Lake Qarun, Egypt. *World Journal of Fish and Marine Sciences*, 1(1): 29-39.

Mokhtar, D. M. (2017). *Fish histology: from cells to organs*. Apple Academic Press.

Mooney, A.(2012). An assessment of the health status and edibility fish from three impoundments in the North West Province. South Africa. M.Sc. Dissertation. Department of Zoology. University of Johannesburg. South Africa.

Mumford, S., Heidel, J., Smith, C., Morrison, J., MacConnell, B., & Blazer, V. (2007). Fish histology and histopathology. *US Fish and Wildlife National Conservation Training Center, Amerika Serikat*.

Oguri, M. (1978). Histochemical observations on the interrenal gland and liver of european spotted dogfish. *Bull. Jap. Soc. Sci. Fisheries*, *44*, 703-9.

Remme, J.F., Stokes, I.S. & Larssen, W.E. (2005). Bioactive lipids in deep-sea sharks. *Research Council of Norway. Report* A0510.

Sales, C. F., Silva, R. F., Amaral, M. G., Domingos, F. F., Ribeiro, R. I., Thomé, R. G., & Santos, H. B. (2017). Comparative histology in the liver and spleen of three species of freshwater teleost. *Neotropical Ichthyology*, *15*

Seyrafi, R. E. Z. A., Najafi, G., Rahmati-Holasoo, H., Hajimohammadi, B., & Shamsadin, A. S. (2009). Histological study of hepatopancreas in iridescent shark catfish *Pangasius hypophthalmus* . *Journal of Animal and Veterinary Advances*, *8*(7), 1305-1307.

Van Dyk, J. C. , Pieterse, G. M. & Van Vuren, J.H.J. (2007). Histological changes in the liver of Oreochromis mossambicus (Cichlidae) after exposure to cadmium and zinc. Ecotoxicology and Environmental Safety, 66(3): 432-440.

Yancheva, V., Velcheva, L., Stoyanova, S. & Georgieva, E. (2015). Histological biomarkers in fish as a tool in ecological risk assessment and monitoring program s: A Review. Applied Ecology and Environmental Research, 14(1): 47-75.

Al-Mukhtar Journal of Basic Sciences 22 (1): 85-91, 2024
Doi: https://doi.org/10.54172/1cg6wn36

Research Article **Open Access**

On Menger Spaces in Generalized Topology

Assakta K. Bashier

***Corresponding author:** alsaktamohammed@bwu.edu. Department of Mathematics, Faculty of Science, Bani Waleed University, Libya.

Received:
16 November 2023

Accepted:
25 February 2024

Publish online:
30 April 2024

Abstract

We introduce new types of covering properties in generalized topology, namely; λ-Menger and λ-uniformly Menger spaces, and investigate their fundamental properties. To achieve this, we replace open sets in the definition of the standard Manger spaces with λ-open sets of generalized topological spaces. The results show that the λ-Menger property is stronger than the Menger property. Additionally, λ-Menger spaces are preserved when forming subspaces and countable unions. We also characterize λ-uniformly Menger spaces and study their relationship with λ-Menger spaces. Examples are given to further illustrate our results.

Keywords: Generalized topological space; λ-Menger space; λ-uniform space

INTRODUCTION

In this paper, we investigate the Menger covering property of generalized topological spaces. We introduce the concepts of λ-Menger spaces and λ-uniformly Menger spaces and investigate some of their characteristics. Generalized topological spaces, in the sense of A. Csàszàr, was introduced in (Csàszàr, 2002). A collection λ of subsets of a set X is called a generalized topology (GT) if it satisfies the following:
(1) $\emptyset \in \lambda$,
(2) λ is closed under arbitrary unions.
The elements of λ are generalized open sets (λ-open sets) and their complements are λ-closed sets. In generalized topology, the condition that the whole space is a λ-open set is dropped. A generalized topological space (GTS) is a pair (X, λ), where X is a non-empty set and λ is a generalized topology on X. If $X \in \lambda$, then (X, λ) is called a strong GTS (λ-space). Every topological space is a λ-space but the converse is not true (Csàszàr, 2002). In topology, several types of generalized open sets were introduced. For example, semi-open sets (Levine, 1963), α-open sets (Njàstad, 1965), Pre-open sets (Mashhour et al., 1982), and β-open sets (Abd El-Monsef et al., 1983). However, the concept of λ-open sets contains all these classes of open sets (Csàszàr, 2002). Various topological notions were examined in the context of generalized topology, for instance, generalized homotopy (Bashier, 2022), generalized separation axioms (Makai et al., 2016), and λ-compactness (Sarsak, 2013). In this work, we investigate the Menger property and its uniform version in the setting of generalized topology by using covers whose members are λ-open sets.

The Menger property is one of the classical selection principles which was first introduced by K. Menger (Menger, 1924). A topological space (X,τ) is called Menger (or has Menger property) if for each sequence $(\mathcal{U}_n : n \in \mathbb{N})$ of open covers of X, there is a sequence $(\mathcal{V}_n : n \in \mathbb{N})$ such that $\mathcal{V}_n$ is a finite subset of $\mathcal{U}_n$ for each n and $\bigcup_{n\in N}\mathcal{V}_n$ is an open cover of X. Further details on selection principles can be found in (Kočinac, 2020) and (Scheepers, 1996) and references therein.

There are generalizations of the concept of Menger spaces in the literature, for example, uniformly Menger (Kočinac, 2003), Semi-Menger (Sabah et al., 2016), α-Menger (Kočinac, 2019), Pre-Menger (Tyagi et al., 2021), and β-Menger (Kule, 2022). Our new generalized structures, the λ-Menger and the λ-uniformly Menger spaces, extend and complement previous work.

PRELIMINARIES

Through this article, a λ-space (X,λ) (or just X) means a strong GTS. The entourages of the diagonal are used in our approach to uniform spaces, the reader is referred to [(Engelking, 1989), Chapter 8] for unexplained notation or terminology.

Definition 2.1 (Csàszàr, 2007) Let (X,λ) be a GTS. A base for a GT λ, denoted by $\mathcal{B}$, is a collection of subsets of X with $\emptyset \in \mathcal{B}$ such that $\lambda = \{\bigcup_{i\in I} B_i : B_i \in \mathcal{B}\}$.

Definition 2.2 (Csàszàr, 2002) Let (X,λ_1) and (Y,λ_2) be two GTS's. A function $f : (X,\lambda_1) \to (Y,\lambda_2)$ is called (λ_1,λ_2)-continuous if $m \in \lambda_2$ implies $f^{-1}(m) \in \lambda_1$.

Definition 2.3 (Sarsak, 2013) Let A be a nonempty subset of (X,λ). The generalized subspace is a pair (A,λ_A), where $\lambda_A = \{U \cap A : U \in \lambda\}$ is the GT on A.

Observe that, if (X,λ) is a λ-space, then (A,λ_A) is a λ_A-space [(Sarsak, 2013), Remark

2.12].

Definition 2.4 (Sarsak, 2013) A λ-space (X,λ) is called λ-compact (λ-Lindelöf, respectively) if any cover of X by λ-open sets has a finite (countable, respectively) subcover.

Definition 2.5 (Dey et al., 2022) Let X be a non-empty set. A non-empty family $\mathbb{U}_\lambda$ of subsets of $X \times X$ is called a λ-uniformity on X if:

(1) $U \in \mathbb{U}_\lambda$ then $\Delta \subseteq U$, where $\Delta = \{(x,x) : x \in X\}$ is the diagonal on $X \times X$.
(2) $U \in \mathbb{U}_\lambda$ and $V \supseteq U$ then $V \in \mathbb{U}_\lambda$.
(3) $U \in \mathbb{U}_\lambda$ then there exists some $V \in \mathbb{U}_\lambda$ such that $V \circ V \subseteq U$.

The pair $(X,\mathbb{U}_\lambda)$ is called a λ-uniform space.
Recall that, given $U \in \mathbb{U}_\lambda$, $x \in X$ and $A \subset X$, then $U[x] = \{y \in X : (x,y) \in U\}$ and $U[A] = \bigcup_{x\in A} U[x]$ (Engelking, 1989).

Theorem 2.1 [(Dey et al., 2022), Theorem 2.10] Let $(X,\mathbb{U}_\lambda)$ be a λ-uniform space, and let $\tau(\mathbb{U}_\lambda)$ be a collection of subsets of X defined as: A subset $G \in \tau(\mathbb{U}_\lambda)$ if and only if for every $x \in G$, there exists some $U_x \in \mathbb{U}_\lambda$ such that $U_x[x] \subseteq G$.Then $\tau(\mathbb{U}_\lambda)$ is a strong GT on X.

The GT $\lambda = \tau(\mathbb{U}_\lambda)$ is called the generalized topology on X induced by the λ-uniformity$\mathbb{U}_\lambda$.

λ -MENGER SPACES

Before we start the main results, we recall the definition of generalized covers. A λ-open cover of (X,λ) is a collection $\mathcal{U}$ of subsets of X such that the elements of $\mathcal{U}$ are λ-open sets and $X \subseteq \bigcup \mathcal{U}$ (Thomas & John, 2012). A λ-open subcover of $\mathcal{U}$ is a sub-collection $\mathcal{V} \subset \mathcal{U}$ which itself

is a λ-open cover (Thomas & John, 2012).

Definition 3.1. A λ-space (X,λ) is called a λ-Menger space (or has the λ-Menger property) if for any sequence $(\mathcal{U}_n : n \in \mathbb{N})$ of λ-open covers of X, there is a sequence $(\mathcal{V}_n : n \in \mathbb{N})$ such that for each $n \in \mathbb{N}$, $\mathcal{V}_n$ is a finite subset of $\mathcal{U}_n$ and $X \subseteq \bigcup_{n\in\mathbb{N}} \mathcal{V}_n$.

Example 3.1. Let $\mathbb{R}$ be the set of real numbers. Consider the standard strong GTS $(\mathbb{R},\lambda_s)$ introduced in (Csàszàr, 2007), where λ_s has a base set given by
$\mathcal{B} = \{(-\infty, s) : s \in \mathbb{R}\} \cup \{(t,\infty) : t \in \mathbb{R}\}$
We claim that $(\mathbb{R},\lambda)$ is a λ_s-Menger space. To prove this, observe that the λ_s-open sets take one of the following forms: $\emptyset$, $\mathbb{R}$, $(-\infty,s)$, (t,∞), $(-\infty,s)\cup(t,\infty)$ where $s \le t$ and $s,t \in \mathbb{R}$. Using the fact that any open interval can be written as the union of an increasing sequence of compact sets, let

$$(-\infty, s) = \bigcup_{n\in\mathbb{N}} [s-n, s-1/n],$$

$$(t,\infty) = \bigcup_{n\in\mathbb{N}} [t+1/n, t+n].$$

Therefore, for any sequence $(\mathcal{U}_n : n \in \mathbb{N})$ of λ_s-open covers of $\mathbb{R}$ and for each $n \in \mathbb{N}$, there is a finite sub-collection $\mathcal{V}_n \subseteq \mathcal{U}_n$, which covers the compact intervals $[s-n, s-1/n] \cup [t+1/n, t+n]$.
It easily follows that $\bigcup_{n\in N} \mathcal{V}_n$ is a λ_s-open cover of $\mathbb{R}$.

Example 3.2. Let $\mathbb{R}$ be the set of real numbers and $\lambda = \{G \subseteq \mathbb{R} : 0 \in G\} \cup \{\emptyset\}$. Then $(\mathbb{R},\lambda)$ is a λ-space. The set $\{\{0,x\} : x \in \mathbb{R}\}$ is a λ-open cover of $\mathbb{R}$ which does not contain a countable subcover. Therefore, $(\mathbb{R},\lambda)$ is not λ-Lindelöf, and hence, it is not λ-Menger.

Remark 3.1. Evidently, every λ-compact space is λ-Menger, and every λ-Menger space is λ-Lindelöf. The converse is not true for both cases.

Example 3.3. There is a λ-Menger space that is not λ-compact. Consider the λ-Menger space in Example 3.1. The set $\{(-\infty, n) : n \in \mathbb{N}\}$ is a λ_s-open cover of $\mathbb{R}$ that does not have a finite λ_s-subcover. Hence $(\mathbb{R},\lambda_s)$ is not λ_s-compact.

Example 3.4. There is a λ-Lindelöf space that is not λ-Menger. Let (X,λ) be a λ-space where $X = [0,1) \subset \mathbb{R}$, and λ has as a base given by
$\mathcal{B} = \{[0,r) : r \in [0,1)\} \cup \{[r,1) : r \in [0,1)\}$.
The λ-open sets take one of the following forms: $\emptyset$, X, $[0,r)$, $[r,1)$, $[0,r)\cup[s,1)$ where $r,s \in [0,1)$ and $r \le s$. Using similar arguments as in [(Engelking, 1989), Example 3.8.14], we can easily see that every λ-open cover of X by basis elements has a countable subcover; hence, X is a λ-Lindelöf space. On the other hand, X is not λ-Menger. To prove this, let $a,b \in X$ such that $a < b$. Let $(\mathcal{U}_n : n \in \mathbb{N})$ be a sequence of λ-open covers of X consisting of intervals $[a,b)$, where each cover $\mathcal{U}_{n+1}$ is obtained by dividing each interval in $\mathcal{U}_n$ into smaller ones. For each $n \in \mathbb{N}$, choose a finite $\mathcal{V}_n \subset \mathcal{U}_n$. Since $\mathcal{V}_n$ is finite, pick one element $[a_n,b_n) \in \mathcal{U}_n$ such that $[a_n,b_n) \notin \mathcal{V}_n$. Then, there is one point x in the intersection of the intervals $[a_n,b_n)$ such that $x \notin \mathcal{V}_n$ for each n. Therefore, $\bigcup_{n\in\mathbb{N}} \mathcal{V}_n$ is not a λ-open cover of X.

Remark 3.2. If λ is not a strong GT on X, then (X,λ) is λ-compact and therefore it is λ-Menger.

Lemma 3.1. If (X,λ) is a finite GTS, then X is λ-Menger.

Proof. Every finite GTS (X,λ) is λ-compact [(Thomas & John, 2012), Theorem 3.5], hence, it is λ-Menger. □

Let the collection of all semi-open (Levine, 1963) (Pre-open (Mashhour et al., 1982), α-open (Njàstad, 1965), β-open (Abd El-Monsef et al., 1983), respectively) subsets of a topological space (X,τ) be denoted by $SO(X)$ ($PO(X)$, $\alpha O(X)$, $\beta O(X)$, respectively). If $\lambda = SO(X)$ ($PO(X)$, $\alpha O(X)$, $\beta O(X)$, respectively), then (X,λ) is a λ-space (Csàszàr, 2002). Evidently, we have:

Proposition 3.1. If (X,τ) is a topological space and $\lambda = SO(X)$ (resp. $PO(X)$, $\alpha(X)$, $\beta(X)$), then the following are equivalent:
(1) (X,λ) is λ-Menger.
(2) (X,τ) is semi-Menger (Sabah et al., 2016) (pre-Menger (Tyagi et al., 2021), α-Menger (Kočinac, 2019), β-Menger (Kule, 2022), respectively).

Theorem 3.1. Let λ_1 and λ_2 be two strong GT's on a set X with $\lambda_1 \subset \lambda_2$. If (X,λ_2) is λ_2-Menger, then (X,λ_1) is λ_1-Menger.

Proof. Let (X,λ_1) and (X,λ_2) be two GTS's such that $\lambda_1 \subset \lambda_2$. Suppose that (X,λ_2) is λ_2-Menger. Since $\lambda_1 \subset \lambda_2$, then any sequence $(\mathcal{U}_n : n \in \mathbb{N})$ of λ_2-open covers of (X,λ_2) will also cover (X,λ_1). Applying the λ_2-Menger property of (X,λ_2), we can find a sequence $\mathcal{V}_n \subset \mathcal{U}_n$ of finite subsets whose union covers (X,λ_1). Hence, (X,λ_1) is λ_1-Menger. □

Proposition 3.2. Let (X,τ) be a topological space. Every λ-Menger space is Menger.

Proof. For any topological space (X,τ), let λ stands for any of the families $\alpha O(X)$, $PO(X)$, $SO(X)$, or $\beta(X)$. We have that
$\tau \subset \alpha O(X) \subset PO(X) \subset \beta O(X)$,
and
$\tau \subset \alpha O(X) \subset SO(X) \subset \beta O(X)$.
It follows by Theorem 3.1 that if (X,λ) is a λ-Menger space, then (X,τ) is a Menger space. □

Theorem 3.2. Let X_n be a subset of a λ-space (X,λ), where $n \in \mathbb{N}$. If $X = \bigcup_{n\in\mathbb{N}} X_n$ and X_n is a λ_{X_n}-Menger space for each n, then (X,λ) is a λ-Menger space.

Proof. Let $X_n \subseteq X$ with $X = \bigcup_{n\in\mathbb{N}} X_n$. Assume that the generalized subspace (X_n,λ_{X_n}) is λ_{X_n}-Menger for each $n \in \mathbb{N}$. Now, let $(\mathcal{U}_n : n \in \mathbb{N})$ be a sequence of λ-open covers of X. Since $X = \bigcup_{n\in\mathbb{N}} X_n$, then $\mathcal{U}_n$ will also be a sequence of λ-open covers of X_n for each n. But X_n is λ_{X_n}-Menger, so for each $n \in \mathbb{N}$, there exists a finite sub-collection $(\mathcal{V}_m^n : m \in \mathbb{N})$ of $(\mathcal{U}_n : n \in \mathbb{N})$ covering each X_n with $\bigcup_{m\in\mathbb{N}} \mathcal{V}_m^n$ covers X_n. Set $\mathcal{V}_n = \bigcup_{m\in\mathbb{N}} \{\mathcal{V}_m^n : m, n \in \mathbb{N}\}$. Then for each $n \in \mathbb{N}$, $\mathcal{V}_n$ is a finite subset of $\mathcal{U}_n$ such that $\bigcup_{n\in\mathbb{N}} \mathcal{V}_n$ is a λ-open cover of (X,λ). □

Theorem 3.3. Let (A,λ_A) be a generalized subspace of a λ-space (X,λ). If X is a λ-Menger space, then A is a λ-Menger space provided that A is λ-closed and λ-open in X.

Proof. Let (A,λ_A) be a λ-open and λ-closed generalized subspace of a λ-Menger space (X,λ). Let $(\mathcal{U}_n : n \in \mathbb{N})$ be a sequence of λ-open covers of (A,λ_A). By Definition 2.3, every λ_A-open set of the

λ-open and λ-closed A of X is the intersection of a λ-open set of X with A. Therefore, for each $n \in \mathbb{N}$ and for each $U \in \mathcal{U}_n$, there exists a λ-open set $M(U,n)$ in X such that $U = A \cap M(U,n)$. Let $\mathcal{M}_n = \{M(U,n): U \in \mathcal{U}_n\} \cup \{X \backslash A\}$, $n \in \mathbb{N}$. Thus, $(\mathcal{M}_n : n \in N)$ is a sequence of λ-open covers of X. Applying the λ-Menger property of X, there exists a finite subset $\mathcal{W}_n$ of $\mathcal{M}_n$ for each $n \in \mathbb{N}$ such that $\bigcup_{n\in\mathbb{N}} \mathcal{W}_n$covers X by λ-open sets. Let $\mathcal{V}_n = \{U: M(U,n) \in W_n\}$ for each n. The sequence $(\mathcal{V}_n : n \in \mathbb{N})$ witnesses for $(\mathcal{U}_n : n \in \mathbb{N})$ that (A, λ_A) is a λ-Menger space. □

Theorem 3.3 generalizes several results in the literature. For example, in a topological space (X, τ), if we take $\lambda = PO(X)$ then we get Theorems 3.5 of (Tyagi et al., 2021). If $\lambda = \beta O(X)$, we get Proposition 4.3 of (Kule, 2022). If $\lambda = \alpha O(X)$, we get Proposition 2.4 of (Kočinac, 2019).

λ-UNIFORMLY MENGER SPACES

Definition 4.1. A λ-uniform space $(X, \mathbb{U}_\lambda)$ is said to be λ-totally bounded if for each $U \in \mathbb{U}_\lambda$, there exists a finite subset A of X such that $U[A] = X$.

Definition 4.2. Let $(X, \mathbb{U}_\lambda)$ be a λ-uniform space. We say that X is λ-uniformly Menger space (or has the λ-uniform Menger property) if for any sequence $(U_n : n \in \mathbb{N})$ of elements of $\mathbb{U}_\lambda$, there exists a sequence $(A_n : n \in \mathbb{N})$ of finite subsets of X such that $X = \bigcup_{n\in N} U_n[A_n]$.

Theorem 4.1. Let $(X, \mathbb{U}_\lambda)$ be a λ-uniform space. Then X is λ-uniformly Menger if and only if for each sequence $(U_n : n \in \mathbb{N})$ in $\mathbb{U}_\lambda$, there exists a sequence $(V_n : n \in \mathbb{N})$ of finite subsets of X such that for each $n \in \mathbb{N}$ and for each $V \in V_n$, we have $V \times V \subseteq U_n$ and $\bigcup_{n\in N} V_n$ is a λ-open cover of X.

Proof: Let $(U_n : n \in \mathbb{N})$be a sequence in $\mathbb{U}_\lambda$. Suppose that X is λ-uniformly Menger. By definition, there is a sequence $(A_n : n \in \mathbb{N})$ of finite subsets of X such that $X = \bigcup_{n\in\mathbb{N}} U_n[A_n]$. For each $n \in \mathbb{N}$ and for each $A \in A_n$, set $V_1 = U_n[A_1]$, $V_2 = U_n[A_2]$, … , $V_n = U_n[A_n]$. Then $(V_n : n \in \mathbb{N})$ is a sequence of finite subsets of X such that $X \subseteq \bigcup_{n\in N} V_n$. Also, $V \subset U_n[A]$ for each $V \in V_n$and for some $A \in A_n$, therefore $V \times V \subseteq U_n$.
On the other hand, let $(U_n : n \in \mathbb{N})$ be a sequence in $\mathbb{U}_\lambda$. Let $(V_n : n \in \mathbb{N})$ be a sequence of finite subsets of X that satisfies the conditions of the second part of the theorem. For each $n \in \mathbb{N}$ and for each $\in V_n$, choose a point x_V^n in V_n such that $x \in U_n[x_V^n]$ for each $x \in X$. Define a sequence $(A_n : n \in \mathbb{N})$ as $A_n = \{x_V^n : x_V^n \in V_n\}$. Then each A_n is a finite subset of X such that $X = \bigcup_{n\in N} U_n[A_n]$. Hence, X is λ-uniformly Menger. □

Proposition 4.1. Let $\mathbb{U}_\lambda$and $\mathbb{V}_\lambda$ be two λ-uniformities on a set X such that $\mathbb{U}_\lambda \subseteq \mathbb{V}_\lambda$. If $(X, \mathbb{V}_\lambda)$ is λ-uniformly Menger, then $(X, \mathbb{U}_\lambda)$ is also λ-uniformly Menger.

Theorem 4.2. Let (X, λ) be a λ-space, where $\lambda = \tau(\mathbb{U}_\lambda)$ the GT is induced by the λ-uniformity $\mathbb{U}_\lambda$. If (X, λ) is a λ-compact space, then $(X, \mathbb{U}_\lambda)$ is λ-totally bounded space.

Theorem 4.3. Let (X, λ) be a λ-space, where $\lambda = \tau(\mathbb{U}_\lambda)$ is the GT induced by the λ-uniformity $\mathbb{U}_\lambda$. If (X, λ) is a λ-Menger space, then $(X, \mathbb{U}_\lambda)$ is a λ-uniformly Menger space.
Proof. Let $(U_n : n \in \mathbb{N})$ be a sequence in $\mathbb{U}_\lambda$. The λ-uniformity $\mathbb{U}_\lambda$ generates a GT $\lambda = \tau(\mathbb{U}_\lambda)$, where $G \in \lambda$ if and only if for every $x \in X$, there is some $U_x \in \mathbb{U}_\lambda$ such that $U_x[x] \subseteq G$ [5, Theorem 2.10]. Suppose that (X, λ) is a λ-Menger space, where $\lambda = \tau(\mathbb{U}_\lambda)$ is the GT induced by the λ-uniformity $\mathbb{U}_\lambda$. Then, by Definition 3.1, for each sequence $(\mathcal{U}_n : \mathrm{n} \in \mathbb{N})$ of λ-open covers of X, there exists a sequence of finite subsets $\mathcal{V}_n$ of $\mathcal{U}_n$such that $\mathrm{X} \subseteq \bigcup_{n\in\mathbb{N}} \mathcal{V}_n$. Let $V \in \mathcal{V}_n$. Since V is a λ-open set,

there is some $U_x \subset U_n \in \mathbb{U}_\lambda$ such that $U_x[x] \subseteq V$. Choose a point $x_V \in V$ and let $A_n = \{x_V : V \in \mathcal{V}_n\}$. Then for each n and for each $V \in \mathcal{V}_n$ we have $V \subset U_n[x_V]$ and therefore, by Theorem 4.1, the sequence $(A_n : n \in \mathbb{N})$ witnesses for $(U_n : n \in \mathbb{N})$ that X is a λ- uniformly Menger space. □

Remark 4.1. The converse of Theorem 4.3 is not true. Consider the following example.

Example 4.1. cf. [(Kočinac, 2003), Note 3] There is a λ-uniform space $(X, \mathbb{C}_\lambda)$ which is λ-uniformly Menger, but the λ-space $(X, \tau(\mathbb{C}_\lambda))$ is not λ-Menger. To prove this, recall that every λ-Menger space is λ-Lindelöf (Remark 3.1). Let (X, λ) be a λ-Tychonoff space (Makai et al., 2016), which is not λ-Lindelöf. Hence, X is not λ-Menger.

On the other hand, consider $(\mathbb{R}, \lambda_s)$ as defined in Example 3.1. It is shown that $(\mathbb{R}, \lambda_s)$ is a λ_s-Tychonoff space (Makai et al., 2016). Let $C_{\lambda,\lambda_s}(X) = \{f : (X, \lambda) \to (\mathbb{R}, \lambda_s)\}$ be the set of all (λ, λ_s)-continuous and bounded functions. The authors (Gupta & Sarma, 2015) introduced a topology τ on $C_{\lambda,\lambda_s}(X)$, which has a sub-base given by the set $S_{\lambda,\lambda_s} = \{(U, V) : U \in \lambda, V \in \lambda_s\}$,

where

$(U, V) = \{f \in C_{\lambda,\lambda_s}(X) : f(U) \subseteq V\}$.

Now, using $(C_{\lambda,\lambda_s}(X), \tau)$ in arguments similar to Example 8.1.19 and Example 8.3.4 in (Engelking, 1989), we can construct a λ-uniformity $\mathbb{C}_\lambda$ on X, which generates the original GT on X. Moreover, $(X, \mathbb{C}_\lambda)$ is λ-totally bounded and thus, λ-uniformly Menger.

CONCLUSION

The present paper deals with the initiation and study of the Menger covering property in the context of generalized topological spaces. Firstly, we defined in Definition 3.1 the notion of λ-Menger, studied some of its properties and provided several examples that illustrate some aspects of λ-Menger spaces. Secondly, we defined the notion of a λ-uniformly Menger space in Definition 4.2, gave a characterization of λ-uniformly Menger spaces in terms of λ-open covers, and examined its relationship with λ-Menger spaces.

Duality of interest: The author declares that they have no duality of interest associated with this manuscript.

Funding: No specific funding was received for this work.

REFERENCES

Abd El-Monsef, M. E., El-Deeb , S. N., & Mahmoud, R. A. (1983). β-open sets and β-continuous mappings. *Bull. Fac. Sci. Assiut Univ., 12*(1), 77-90.

Bashier, A. K. (2022). Generalized homotopy in generalized topological spaces. *The Libyan Journal of Science, 25*(1), 25-28.

Csàszàr, A. (2002). Generalized topology, generalized continuity. *Acta Math. Hungar., 96*(4), 351-357.

Csàszàr, A. (2007). Normal generalized topologies. *Acta Math. Hungar., 115*(4), 309-313.

Dey, D., Mandal, D., & Mukherjee, M. N. (2022). Uniformity on generalized topological spaces. *Arab J. Math. Sci., 28*(2), 184-190.

Engelking, R. (1989). *General Topology* (2nd ed.). Berlin: Heldermann Verlag.

Gupta, A., & Sarma, R. D. (2015). Function space topologies for generalized topological spaces. *Journal of Advanced Research in Pure Mathematics, 7*(4), 103-112.

Kočinac, L. D. (2003). Selection principles in uniform spaces. *Note Mat., 22*(2), 127-139.

Kočinac, L. D. (2019). Generalized open sets and selection properties. *Filomat, 33*(5), 1485-1493.

Kočinac, L. D. (2020). Variations of classical selection principles: An overview. *Quaest. Math., 43*(8), 1121–1153.

Kule, M. (2022). β-Menger and β-Hurewicz spaces. *Hacet. J. Math. Stat., 51*(1), 1-7.

Levine, N. (1963). Semi-open sets and semi-continuity in topological spaces. *Amer. Math. Monthly, 70*(1), 36-41.

Makai, E., Peyghan , E., & Samadi, B. (2016). Weak and strong structures and the T 3.5 property for generalized topological spaces. *Acta Math. Hungar., 150*(1), 1-35.

Mashhour, A. S., Abd El-Monsef, M. E., & El-Deeb, S. N. (1982). On precontinuous and week precontinuous mappings. *Proc. Math. Phys. Soc. Egypt, 53*, 47-53.

Menger, K. (1924). Einige überdeckungssätze der punktmengenlehre. *Stzungsberischte Abt. 3a, Mathematik, Astronomie,Physik, Meteorologie und Mechanik (Wiener Akademie, Wien), 133*(1), 421-444.

Njàstad, O. (1965). On some classes of nearly open sets. *Pacific J. Math., 15*(3), 961-970.

Sabah, A., Khan, M. u., & Kočinac, L. D. (2016). Covering properties defined by semi-open sets. *J. Nonlinear Sci. Appl., 9*(6), 4388-4398.

Sarsak, M. S. (2013). On μ-compact sets in μ-spaces. *Quest. Ans. Gen. Topol, 31*(1), 49-57.

Scheepers, M. (1996). Combinatorics of open covers I: Ramsey theory. *Topology Appl., 69*(1), 31-62.

Thomas , J., & John, S. J. (2012). μ-compactness in generalized topological spaces. *J. Adv. Stud. Topol., 3*(3), 18-22.

Tyagi , B. K., Singh, S., & Bhardwaj, M. (2021). Covering properties defined by preopen sets. *Asian-Eur. J. Math., 14*(3), 2150035.

Al-Mukhtar Journal of Basic Sciences 22 (1): 92-102, 2024
Doi: https://doi.org/10.54172/7vcp1e92

Research Article **Open Access**

A Brief Comparison of Google Cloud and iCloud Services

Faiza A. M. Mansour [1*], Najat A. Atbaiga [2]

***Corresponding author:**
firstfaiza.18@su.edu.ly
Department of Compute Science, Sirte University, Libya

Second Author:
najatatbaiga@su.edu.ly
Department of Compute Science, Sirte University, Libya

Received:
25 January2024

Accepted:
12 April 2024

Publish online:
30 April 2024

Abstract

The provision of computing resources on demand via the Web with pay-per-use billing is known as cloud computing. Small organizations find cloud computing a very competitive and attractive solution due to its pay-per-use model. Cloud computing delivers many services through the Internet. Services include databases, platforms, data storage, and networking resources hosted at remote data centers. The scalability, flexibility, and cost-effectiveness of cloud computing contributed to its rising popularity. There are several significant players in the cloud computing market, including Google Cloud, Amazon Web Services, Microsoft Azure, etc., each offering a wide range of services and advantages. Considering various factors such as security, cost, reliability, and functionality, choosing the best option presented among different cloud service providers is a challenging task. This paper introduces an overview of cloud computing, its architecture, characteristics, and briefly describes Google Cloud and iCloud services. The main objective of this work is to compare the services provided by the selected cloud platforms. The findings indicated several robust services offered by both Google Cloud and iCloud. The user's requirements are the basis for the selection process.

Keywords: Cloud Computing, Google Cloud, iCloud, Cloud Service Provider (CSP), Comparison.

INTRODUCTION

Applications and data storage have changed significantly as a consequence of cloud computing. Nowadays, practically everything is hosted on a "Cloud" as opposed to executing applications and storing data locally on a computer. The term "cloud computing" refers to a method of delivering IT resources on demand via the Internet with a pay-as-you-go pricing scheme (Goudar, 2012). A service provider and a subscriber are the two different types of people who are involved in this system. Users can deploy applications and access files from any device that has Internet connectivity by using cloud computing (Rafat Ara, 2020). Google's Gmail is an example of a cloud-computing provider. The use of cloud computing has various benefits, including accessibility from anywhere at any time, reduced investment in infrastructure, and faster processing time with better geographic coverage (P. Ravi Kumar, 2017).

Service providers are actually the IT staff of the company, a third party, or a combination of both of them. On the other hand, the term "subscriber," can refer to any person who uses a service provider's offerings (Isaac Odun Ayo, 2018). The term "Cloud Service Providers" (CSPs) (e.g., Google Cloud, Microsoft Azure, Amazon Web Service (AWS)) refers to vendors that provide their custom-

ers with access to cloud computing resources and services that are dynamically used according to client demand (Aaqib Rashid, 2019). Customers can access online services using a web browser over the Internet in several kinds of fields, such as business, education, and governance, whereas information and software are stored on data center-based cloud servers (Singh, 2022). As defined by cloud service models, these services can be grouped into three categories. These categories mainly include Platform as a Service (PaaS), Infrastructure as a Service (IaaS), and Software as a Service (SaaS) (Karan Gulia, 2021). Many companies, like Google, Microsoft, Apple, and Amazon have introduced cloud services to the user. They offered a variety of storage options depending on the client's needs and business requirements (Pallavi Wankhede, 2020). A variety of services, including computing, storage, networking, and databases are available through the Google Cloud platform (Sumit Kumar, 2019). iCloud is capable of offering features such as synching browser data between iOS devices, locating your phone, Apple’s mail service, contacts service, calendar service, news service, and App Data, and storing information about website passwords (Hera Arif, 2019).

The structure of this paper starts with a brief introduction to cloud computing. Then some of the previous studies related to the selected service providers are highlighted in section 2. Section 3 explains some significant characteristics of cloud computing. Cloud computing architecture is presented in section 4. Section 5 introduces a brief definition of Google Cloud and iCloud services. The comparison of the providers is displayed in section 6. The discussion is presented in section 7. Section 8 concludes this work.

Related Work

Numerous studies and comparisons of cloud service providers have been conducted and published. A summary of these studies is presented in this section. Studies address the primary factors that a company has to take into account before selecting a cloud service provider, as well as the primary reasons for selecting a cloud service provider. (Moss, 2014) To address the fundamental interoperability issues, Cyberdesign Works developed Sanscode, a cross-platform cloud computing solution. The authors pointed out that Sanscode, which supports a lot of iCloud's capabilities and provides a few extra features, might offer a workable alternative solution. The strategy used by Apple's iCloud was examined and compared with Sanscode. (M.Akila, 2018) Conducted a comparison among iCloud, One Drive, Google Drive, Amazon, and Dropbox. They compared and reviewed the advantages, file features, ease of use, accessibility on mobile devices, support, security, file content, cost, ranking, plans, and supported OS system. The result of the comparison was mentioned that the consumers could choose the best cloud service that suited their requirements. (Sethi, 2019) Investigated the iCloud service model and the built-in security features. Service models were explained to the security risks and the security measures, based on that the iCloud system may provide effective service gains. (Iqura Khan, 2019) Presented a comparison between Google Cloud, Amazon Web Services, and Microsoft Azure from the user's point of view. Parameters such as Storage as a Service, virtual machine types, and availability zones were used to compare various CSPs. The conclusion is that the selected CSPs offer a wide range of distinctive virtual machines and storage as a service, also according to the client’s demand to select one of them. (Hera Arif, 2019) Addressed that cloud service providers in terms of services offered as well as the features of the iCloud and Google Cloud. The final point was concluded that both Google Cloud and iCloud provide a variety of services, and the choice would be based on the needs of the user. (Tripathi, 2020) Analyzed some of the cloud computing market leaders GCP, AWS, and Azure's characteristics, including computation, performance, and storage space management. The features of AWS, GCP, and Azure were evaluated and summarized to assist customers in selecting the features that would meet their needs. (Muhammad Ayoub Kamal, 2020) Compared the service, benefits, and prices of AWS, GCP, and Microsoft Azure CSPs and emphasized key service characteristics including computing, infrastruc-

ture, and storage. The study's conclusion was that, although AWS dominates the cloud market in terms of market share and many of its service features, GCP and Microsoft Azure are only marginally superior to AWS regarding pricing and security.

The Cloud Computing Characteristics

Cloud computing offers very low cost, great performance, vast scalability, and reliability as compared to dedicated storage systems. With the help of cloud computing, users may access their data from anywhere globally and work together in groups and with other users. Cloud computing platforms have several interesting criteria that make them acceptable for upcoming IT services and applications. *The National Institute of Standards and Technology (NIST)* has identified some essential features for cloud computing systems (Aaqib Rashid, 2019) (Tripathi, 2020).

- ***Rapid elasticity*:** Provides scalable services. Users can request authorization in this way if they need additional cloud storage.
- ***Pay as per usage*:** If not completely free, CSP services are very reasonably priced. Pay-as-you-go billing reduces maintenance costs because infrastructure is not required to be purchased. (Rafat Ara, 2020).
- ***Measured Services*:** The pay-per-use model used by cloud service providers enables monitoring, regulation, and optimization of resources and services that users utilize. For instance, how they use electricity, water, or gas, consumers can use these services (Tripathi, 2020).
- ***Broad Network Access*:** Through a variety of hardware (such as laptops, mobile phones, and PDAs), customers can access cloud resources constantly and from any location (i.e., ubiquitously) (Mohammad Ilyas Malik, 2018).
- ***Resource Pooling*:** The cloud is a collection of physical and virtual computing resources. In the sense that the consumer has no influence over or awareness of their location, these resources are not location-dependent.
- ***On-demand self-service*:** Cloud-computing services, including storage, server time, network access, and CUP time, etc., can be automatically distributed according to consumer needs without requiring human interaction (Isaac Odun Ayo, 2018).
- ***Customization*:** A cloud is a reconfigurable environment that may be modified based on user demand in terms of apps and infrastructure (Aaqib Rashid, 2019).
- ***Security*:** This is a crucial issue of cloud computing. Data will not be lost even if a server has failed due to providing a snapshot of the saved data. The data is stored on storage devices according to that it will be impossible for anyone to access or hack (Rafat Ara, 2020).

Cloud Computing Architecture

Cloud architecture describes how technological components interact to build a cloud, in which resources pooled and shared utilizing virtualization technology (Aman Yevge, 2022). A cloud platform and the applications that operate on are powered by a virtualized architecture that consists mostly of all the technologies, including hardware and software. Cloud architecture consists of four key parts (Kaur, 2018) as shown in Figure1:

- Front-end platform describes the client or device used to access the cloud.
- Back-end platform includes service and storage.
- A cloud-based delivery system enables information to be delivered between the Front-end and the Back-end.
- A network to connect cloud clients, storage, and servers.

Front-end architecture includes all technologies that allow clients of the organization to communicate with the applications stored in the cloud. Front–end architecture can be a web browser or local networks of common web apps. As an example, in the case of Gmail, The front-end architec-

ture is the web application that gives the users access to the services that the Gmail architecture offers. Front-end architecture can be divided into three parts:

1. **Front-end software architecture**: this refers to the software that enables users to execute cloud-computing applications on their computers.
2. **User interface**: this is a collection of all the features and a description of how users can use them to perform operations in the cloud.
3. **Client device/ network**: refers to client-side hardware such as PCs, smartphones. These devices do not require a lot of computing power as most of the complex tasks are processed on the cloud.

Back-end architecture is the component of cloud computing that supplies the support to run the front-end architecture. It contains components such as hardware and storage and is typically located in a remote server form. Cloud service providers, such as Microsoft Azure and AWS, are in control of the back-end architecture.

The essential components of backend Cloud architecture. (Rafat Ara, 2020)

1. **Application**: includes the server side of the application that is provided to the end user. The resources in the backend are coordinated with the various consumer needs through this layer.
2. **Service**: any operation that is performed on the cloud computing system. Web services, application development environments, and storage are all provided.
3. **Cloud runtime**: where the service runs. It is comparable to an operating system in the cloud that uses virtual machines to enable several runtimes to be operated together on the same server.
4. **Storage**: where all the data requested to run the cloud software resides. It consists of several hard devices in server bays that have been divided by management software.
5. **Infrastructure:** the engine running all cloud software services. It contains a CPU, GPU, and all other components needed for the system to operate efficiently. A lot of cloud service providers also offer accelerators such as Google stencil processing unit, which is accessible to Google Cloud platform customers to conduct AI tasks.
6. **Cloud security**: the main part of cloud software architecture that is increasingly being set to the test more and more given the increase. Some of the methods used to secure cloud architecture include:
    - Offering protection at every layer.
    - Creating resilient design and avoiding redundancy.
    - Including elasticity and scalability.
    - Considering deployment-appropriate storage.
    - Concentrating on notifications and alerts
    - Producing standardization, automation, and centralization.

    This security architecture enables the system to function even when there is a Cyberattack.
7. **Management**: The management component is responsible for setting up coordination and managing backend components such as storage services, runtime cloud infrastructure, applications, and security issues.

Delivery system is the third key component of cloud architecture, it allows the information to be delivered between the frontend and the backend and includes Infrastructure as a Service (IaaS), Platform as a Service (PaaS), and Software as a Service (SaaS).

Cloud deployment models

Though the fundamentals are always the same, cloud architectures are heavily dependent on deployment models selected from the system. There are four basic deployment models in cloud computing. They are described briefly below: (Ouda, 2020):

1. **The public cloud:** the capacity of one divided server hosting multiple distinct partitions, each of which is open for usage and without firewalls separating various cloud instances (Prof. Hiral B. Patel, 2021).
2. **A private cloud:** a divided public cloud that is firewall-protected to prevent non-company personnel from accessing (Critical systems). (Akshat Rajpurohit, 2018).
3. **Multi-cloud**: Multiple different public cloud services obtained from various suppliers are included in multi-cloud architecture (P. Ravi Kumar, 2017).
4. **Hybrid cloud:** In a hybrid cloud environment, a company combines both private and public clouds to achieve the same purpose (Prof. Hiral B. Patel, 2021).

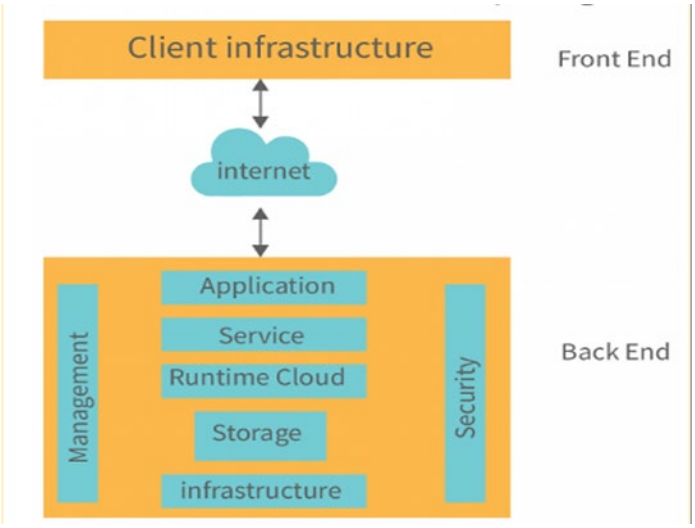

Figure: (1). Cloud Computing Architecture diagram (Rafat Ara, 2020)

Cloud Computing Service Providers

The concept of Cloud Computing came into the spotlight in the year 1950 with access via thin/static clients and the utilization of mainframe computers. After that, in 1961, John McCarthy suggested that computing services would be offered similarly to utilities, such as gas, electricity, water, and telephone, and that services would be readily available on demand (Kaur T., 2019). In 1970, the concept of virtualization improved the shared access mainframe technology (Hajjdiab, 2017). Twenty years later, in 1999, Salesforce.com was one of the first companies that used the idea of delivering enterprise applications through a simple website (Hera Arif, 2019). The public became more familiar with the idea of cloud storage because of the quick adoption of Amazon's web store in 2002 and Google Docs in 2006 (O'Regan, 2016). Cloud computing experienced a significant boom in the late 2000s, with 2009 seeing the introduction of Web 2.0 and browser-based apps such as Google Apps, Windows Azure, and many other well-known companies jumping on board in the years that followed (O'Regan, 2016) (Jianwen Wendy Chen, 2017). Apple introduced iCloud, whereas Google played a significant role and launched the Google Cloud Platform (GCP). Additionally, numerous vendors have started cloud computing research projects. The physical infrastructure for cloud computing, including computers, cooling systems, and hard drives, is hosted in several data centers owned and run by CSPs across the world. Google Cloud and iCloud are examples of these providers.

Google Cloud Services

In April 2008, the Google cloud platform launched as a cloud service (Pranay Dutta, 2019). Google delivers services like processing, storage, and networking through its Google Cloud service. Services including Infrastructure-as-a-Service, Platform-as-a-Service, and Software-as-a-Service are available through Google Cloud (Trivedi, 2014). Among Google's products are Google Search and YouTube. Cloud computing services provided by Google are divided into four primary categories. *The first category* is related to Computing. Google's compute engine allows customers to use IaaS or PaaS based on their requirements. Storage falls under *the second category*. Users' data can be stored in a non-SQL and schema-less database using Google Cloud Storage. In addition, users can process complex SQL queries using Google Cloud SQL which is connected with MySQL (Alreshidi, 2019). Big data is the focus of *the third category*. Google uses Big Query for fast and easy analysis of big data, which is highly scalable. The support applications that Google offers fall under *the fourth category* (Hera Arif, 2019). Google has developed several applications that allow customers to view the same files on various platforms. This includes Gmail, Google Suite, and Calendar (Riti, October 24, 2018). Google Cloud integrates several applications and provides numerous services to cloud users. Google has become one of the most significant service providers due to this integration since it allows cloud users to finish their tasks easily (Youssef, 2012). It also saves time and money since developing and maintaining software to provide all of these applications and services is an expensive process and time-consuming. The main benefits of using Google Cloud are automatic data synchronization between devices, and the automatic Backup of the user's data. Google Drive needs a little bit of setup if the user already has a Google account and easily saves attachments from their Gmail directly to Drive with only a few clicks (M.Akila, 2018). As well as there are also significant challenges which are having one-way (256-bit AES) encryption and sharing storage space with Gmail, so if your inbox is overflowing, you will get less cloud storage space.

iCloud Services

Apple first announced iCloud as a free cloud computing, synchronization, and storage service in October 2011 (Moss, 2014). From the data point of view, the primary services of iCloud are online storage, file sharing, synchronization between different platforms and devices, and iOS device backup. Backups can be created on any Apple device that uses iCloud service, and a device can also be restored using the previously created backup (Coulston, 2018). iCloud services can be used to back up various applications offered to Apple users. These apps include Calendar, Mail, contacts, reminders, notes, iTunes, App Store, iBooks, Music, Safari, and App Store. This can effectively help users with multiple devices to maintain synchronization with all. Some features of iCloud are Find My iPhone and iPad, photo sharing, reminder services, iCloud drive for data storage, notes, keychain, and web data (Maheshwari, 2016). Another feature that iCloud offers; is the iCloud Keychain, which can help store private data like passwords and credit card numbers; that can be used across numerous devices (Coulston, 2018). Since iCloud Drive only provides 5 GB of free storage, users may need to subscribe to a higher capacity plan if they want more space (Rafat Ara, 2020). The use of iCloud services highlighted some advantages; iCloud is rapidly becoming the standard cloud service among iOS developers. Automatic synchronizing of data among devices, iCloud is more secure due to the multi-factor authentication and encryption mechanism, and tightly integrated (M.Akila, 2018). 256-bit AES encryption is used to secure the most data stored on iCloud**.** This includes backups, calendars, contacts, photos, reminders, short memos, and many more, all stored with effective encryption. For many app developers, iCloud is a cloud for iOS and Mac OS devices and applications. This is considered as the main limitation of iCloud since it is incompatible with other mobile platforms such as Windows Mobile and Google's Android (Moss, 2014). This indicates that data cannot be stored or shared between the different Smartphone systems. Another limi-

tation is that iCloud cannot act as a download target for iOS browsers and Apple does not offer iCloud Drive apps for Android or Windows Phones (M.Akila, 2018).

Comparing of Google Cloud and iCloud Services

Small enterprises and IT companies are adopting cloud services at an extremely fast rate due to their advantages and reasonable costs. Both share a lot of similar features in common, including productivity apps, file backups, cloud sync, file sharing, etc. However, when it comes to being used on various platforms, things change. Table 1 highlighted some criteria parameters to be compared between Google Cloud & iCloud:

Table: (1). Comparison table between Google Cloud and iCloud services (Moss, 2014) (M.Akila, 2018) (Hera Arif, 2019) (Pallavi Wankhede, 2020).

Criteria parameters	Google Cloud	iCloud
Owner	Google	Apple
Launch year	2008	2011
Operating system support	Windows Mac IOS Android	Apple ecosystem Mac IOS
Platform availability	Available as a web app or for installation on a wide range of platforms.	Works perfectly on Apple devices, but the features of the app would be constrained for Windows users.
Storage plans	Offers: 15GB free 100GB for 1.99$ 200GB for 2.99 $ 2TB for 9.99 $	Offers: 5GB: Free 50GB for 1$ 100GB: $1.99 200GB: $2.99 2TB: $9.99
Security features	All data uploaded or created in Docs are encrypted in transit and at rest with AES-256 bit encryption and it has only one-way encryption.	Employs advanced data protection which is end-to-end encrypted, and uses two-way encryption for both files that are saved and in transit using 256-bit AES Standard encryption. It constantly encrypts and never exchanges keys.
File sharing & collaboration features	Enables you to share files and folders with other people by sending links to view or download the files. Furthermore, as long as they have Google Drive, other users can exchange files regardless of their device or operating system.	Allows to share videos, images, and more with people you choose and offers almost the same capabilities, and to achieve that, it uses other apps like HipChat, Pager Duty, and iCalendar.
Synchronization & Sync speed	Regardless of platform or file format, automated synchronization and outstanding performance.	iCloud is the greatest option for automated file synchronization if you have an Apple device. iCloud fails when compared to other platforms.
Availability zones/ Cloud locations	World wide	World wide
Backup	Backup your data automatically with a few clicks once you have a Google account.	Any Apple device that uses the iCloud service can create backups that already exists and may also be utilized to restore a device.
Database Services	Cloud SQL Cloud spanner NoSQL database Cloud Bigtable	SQLkit databases SQLite databases
Content	Email, calendar, contacts, documents	Contacts, Email calendar, documents
Ease of use and accessibility	Supports	Supports
Networking service	Cloud Virtual Network; VPC Virtual Private Cloud Cloud load balancing Cloud DNS Cloud CDN Cloud interconnect	iCloud private relay
File size limit	Varies	Varies
Virtual machine types	Standard machines High-memory machines High-CPU machines Mega-memory machines	Apple devise can run other operating systems by installing UTM app "virtual machine hosted for iOS"
Emphasis	Collaboration	Apple users

DISCUSSION

Google Cloud and iCloud offer a set of features and the decision is on a case-by-case basis. Backing Up and synchronization of data is automatically in Google Cloud regardless of platform, as well as iCloud only if you have an Apple device. On Apple devices, iCloud performs well but not on pc. However, iCloud struggles with running other operating systems as a virtual machine, but it is possible by installing the UTM app. The only problem with the UTM app is not listed on the app store, and the only way to install it is to provide a developer certificate. Virtual machines can be hosted on Google's infrastructure, with just a few steps in the Google cloud console to create an instance. Moreover, the Google Cloud Platform produces a free tier that provides limited access to GCP services and resources. Both iCloud and Google Cloud use the Advanced Encryption Standard (AES) algorithm. Google Cloud has only one-way encryption using 256-bit AES while iCloud uses 256-bit AES with end-to-end encryption. The two-factor authentication in iCloud means any information in your account can only accessed with your devices and no third party. iCloud private relay in iCloud hides your IP address and your internet traffic by using two different proxies that protect your privacy. The problems with iCloud private relay which only works with Safari, may make things slower and have some issues with some sites.

Google Cloud VPCs help users to increase the IP space without any workload, which gives them more flexibility and growth options according to their needs. Google Drive is accessible on iOS and Android and is also known as a PWA "a Progressive Web App". PWA utilizes the resources of the browser and needs less storage than the actual software. For Android to be supported in iCloud there should be various third-party apps. Those apps provide contact and calendar sync options when it comes to previewing and playing files. iCloud is unreliable when trying to play or preview a video file, and does not support as many file types. Most likely, Google Drive will be downloaded. In price, almost both are offering the same monthly plan, you have just got to choose which plan meets your requirements. iCloud offers 5GB of free storage but Google Cloud provides 15GB free for users. The upgrading in iCloud starts with 50GB for 1$ and Google Cloud starts with 100GB for about 2$. Although iCloud wins the point for being more secure, Google Cloud earns the greatest option which is running efficiently across all platforms.

CONCLUSION

Cloud service providers such as Google Cloud and iCloud are vendors that provide services to end-users. To determine which one best suits the demands of the user, we compared some features of Google Cloud and iCloud. This paper presented an introductory background to cloud computing, highlighted some related work, architecture, characteristics, and explored two popular cloud services. It also introduced a comparison between the selected cloud service providers based on some selected parameters summarized in the table. Every service provider has many features that are the same with different terminologies. The services that the customer needs to utilize are the ones that will be determined to be the most appropriate. Each service has a price, and the more distinguished the service, the higher the cost. Comparing the two most widely used cloud platforms and exploring the various services offered by each cloud provider are the primary goals of this work. Both Google Cloud and iCloud provide reliable cloud computing services with their unique strengths. Google Cloud specializes in cross-platform accessibility and collaborative tools. On the other hand, iCloud is the preferred option for higher security. However, overall to conclude, both platforms have achieved success in some features and the selection between them is as per the requirements of the user.

Duality of interest: The authors declare that they have no duality of interest associated with this

manuscript.

Author contributions: Contribution is equal between authors.

Funding: No specific funding was received for this work.

REFERENCES

Aaqib Rashid, A. C. (2019, Feb). Cloud Computing Characteristics and Services: A Brief Review. *International Journal of Computer Sciences and Engineering*, pp. 421-426.

Akshat Rajpurohit, A. J. (2018). A Review on Cloud Computing and its Security Issues. (pp. 28-32). National Conference on Smart Computation and Technology in Conjunction with The Smart City Convergence.

Alreshidi, E. (2019). Comparative Review of Well-Known Cloud Service Providers (CSPS). pp. 165-170.

Aman Yevge, P. G. (2022, Feb. 8). Review Paper on Cloud Service Provider – AWS, Azure, GCP.

Coulston, L. (2018). *Understanding and Using iCloud.* Blurb, ISBN-13: 978-1388776602.

Goudar, S. K. (2012, December). Cloud Computing – Research Issues, Challenges, Architecture, Platforms, and Applications: A Survey. *International Journal of Future Computer and Communication*, pp. 356-360.

Hajjdiab, S. M. (2017, November 7-9). Comparison between Amazon S3 and Google Cloud Drive. *Association for Computing Machinery, ACM*, pp. 250-255.

Kaur, T. (2019, June). Cloud Computing: A Study of the Cloud Computing Services. *International Journal for Research in Applied Science & Engineering Technology (IJRASET)*, pp. 1933-1938.

Hera Arif, H. H. (2019). A Comparison between Google Cloud Service and iCloud. *2019 IEEE 4th International Conference on Computer and Communication Systems*, (pp. 337-340).

Iqura Khan, B. D. (2019). Study of Various Cloud Service Providers: A Comparative Analysis. 5th International Conference on: "Next Generation Computing Technologies" NGCT 2019.

Isaac Odun Ayo, A. M. (2018). Cloud Computing Architecture: A Critical Analysis. *IEEE*.

Jianwen Wendy Chen, Y. Z. (2017). *Handbook of Research on End-to-End Cloud Computing Architecture Design (Advances in Systems Analysis, Software Engineering, and High Performance Computing)*. IGI Global, ISBN-10: 1522507590.

Karan Gulia, S. K. (2021, July). A Review Paper on Cloud Computing. *IJISET - International Journal of Innovative Science, Engineering & Technology*, pp. 422-427.

Kaur, M. R. (2018, June). Cloud Computing: Architecture and Services. *RESEARCH REVIEW International Journal of Multidisciplinary*, pp. 20-23.

M.Akila, D. (2018). A Comprehensive Survey Regarding Performance Evaluation of Services Among Cloud Providers. *International Journal of Pure and Applied Mathematics*, pp. 16113-16118.

Maheshwari, S. A. (2016). iCloud and Its Security Issues in Relation with Find My iPhone. *International Journal of Computer Science and Information Security (IJCSIS),*, pp. 275-280.

Mohammad Ilyas Malik, S. H. (2018). Cloud Computing-Technologies. *International Journal of Advanced Research in Computer Science*, pp. 379-384.

Moss, C. (2014). Integrating Cloud Computing and Mobile Applications:A Comparative Study Based on Icloud and Sanscode. *Journal of Cloud Computing*, pp. 1-9.

Muhammad Ayoub Kamal, H. W. (2020, January). Highlight the Features of AWS, GCP and Microsoft Azure that Have an Impact when Choosing a Cloud Service Provider. *International Journal of Recent Technology and Engineering (IJRTE)*, pp. 4124-4132.

O'Regan, G. (2016). *Introduction to the History of Computing: A Computing History Primer*. Springer ,ISBN-10: 9783319331379.

Ouda, G. K. (2020). Cloud computing service providers: A comparative study. *Samarra Journal of Pure and Applied Science*, pp. 76-89.

P. Ravi Kumar, P. H. (2017). Exploring Security Issues and Solutions in Cloud Computing Services – A Survey. pp. 3-31.

Pallavi Wankhede, M. T. (2020, April 02). Comparative study of cloud platforms - Microsoft Azure, Google Cloud Platform and Amazon EC2. *International Journal of Research in Engineering and Applied Sciences*, pp. 60-64.

Pranay Dutta, P. D. (2019, April). Comparative Study of Cloud Services Offered by Amazon, Microsoft & Google. *International Journal of Trend in Scientific Research and Development (IJTSRD)*, pp. 981-985.

Prof. Hiral B. Patel, P. N. (2021, March 2). Cloud Computing Deployment Models: A Comparative Study. *International Journal of Innovative Research in Computer Science & Technology (IJIRCST)*, pp. 45-50.

Rafat Ara, M. A. (2020, June). Cloud Computing: Architecture, Services, Deployment Models, Storage, Benefits and Challenges. *International Journal of Trend in Scientific Research and Development (IJTSRD)*, pp. 837-842.

Riti, P. (October 24, 2018). *Pro DevOps with Google Cloud Platform: With Docker, Jenkins, and Kubernetes*. Apress, ASIN: B07FL76Z13.

Sethi, D. V. (2019, June). A Study on Security Service Model in iCloud Environment. *International Journal of Research in Engineering*, pp. 370-373.

Singh, G. (2022, November). Cloud Computing Characteristics and Services: A Brief Review. *International Journal of Research Publication and Reviews*, pp. 1827-1832.

Sumit Kumar, S. K. (2019). A Comparative Study of Various Cloud Service Platforms. *Journal of Advanced Database Management & Systems*, pp. 7-12.

Tripathi, D. M. (2020). Cloud Computing: Comparison and Analysis of Cloud Service Providers—AWS, Microsoft and Google. *Proceedings of the SMART–2020, IEEE Conference ID: 50582* (pp. 281-285). India: 9th International Conference on System Modeling & Advancement in Research Trends.

Trivedi, R. S. (2014, April 01). Literature review: Cloud Computing –Security Issues, Solution and Technologies. *International Journal of Engineering Research*, pp. 221-225.

Youssef, A. E. (2012, July). Exploring Cloud Computing Services and Applications. *Journal of Emerging Trends in Computing and Information Sciences*, pp. 838-847.